SHOCK WAVE-BOUNDARY LAYER INTERACTION WITH TANGENTIAL INJECTION

By

ESSAM M. MITWALLY

Bachelor of Science
Faculty of Engineering, Cairo University
Cairo, Egypt, UAR
1958

Master of Science
Oklahoma State University
Stillwater, Oklahoma
1961

Submitted to the Faculty of the Graduate School of
the Oklahoma State University
in partial fulfillment of the requirements
for the degree of
DOCTOR OF PHILOSOPHY
August, 1965

SHOCK WAVE-BOUNDARY LAYER INTERACTION

WITH TANGENTIAL INJECTION

Thesis Approved:

Jerald D. Parker
Thesis Adviser

Kenneth S. Bell

Robert G. McIntyre

Dean of the Graduate School

ACKNOWLEDGEMENT

The author wishes to acknowledge the governments of the United Arab Republic and the United States for their financial aid in the form of a scholarship, which enabled the author to proceed in his program of study.

The members of the author's advisory committee, Dr. J. D. Parker, Dr. J. H. Boggs, Dr. K. J. Bell and Dr. R. McIntire, deserve a special word of gratitude for their valuable comments. The thesis adviser, Dr. Parker, deserves additional recognition for assistance and counsel. Professor F. Sherman of the University of California, Berkeley, deserves a note of appreciation for the valuable suggestions and discussions rendered the author.

The author would like to thank Dr. E. C. Fitch, Jr. and Mr. C. R. Gerlach for urging the author to proceed with the present work by providing a very comfortable atmosphere at the Mechanical Engineering Laboratory.

The author expresses deep appreciation to Mrs. Judith Johnson for the wonderful job she has done in preparing the manuscript and for the time she has put forth while others were in need of her attention.

Finally, the author wishes to express his deepest appreciation for his family and friends who had faith, hope, charity and encouragement for him. This thesis is dedicated to them.

TABLE OF CONTENTS

TABLE OF CONTENTS (CONT.)

LIST OF FIGURES

LIST OF FIGURES (CONT.)

PREFACE

The phenomenon of shock waves occurs in many situations. An object flying at supersonic speed produces shock waves in the fluid around it. The shock waves occur when the fluid is disturbed by any discontinuity in geometry of the flying object. An example of such geometrical change could be the air intake ports of a rocket or a supersonic plane. A shock wave may also occur inside a rocket motor when the products of combustion flow past a discontinuity in the flow field. The shock wave causes a static pressure rise and a loss in stagnation pressure which reduces the overall efficiency of the rocket motor. The shock wave also strikes the boundary layer which forms near the wall and causes it to separate adding more losses to the flow process.

In short, the phenomenon of the shock wave causes a loss, in general. (It is claimed that in the case of the experimental supersonic bomber XB-70 a shock wave takes place near the air intake ports, thus raising the pressure under the body which shifts the center of pressure to the designed location when the plane speed goes from subsonic to supersonic. The strength of the shock wave could then be controlled to give any desired pressure rise by varying the shock angle at such ports. This is one example where shock waves could be used benificially.)

Many researchers have investigated this phenomenon, (as will appear in chapter I). Some have investigated the effect of the shock wave on the boundary layer, especially when separation takes place. Others

tried injecting different fluids at an angle to the heated surface, but the cooling fluids were dispersed when hit by the shock wave.

The present study was thought of because of the aforementioned difficulties. However, the investigation of the effect of cooling is not the prime concern of this study.

The situation which is investigated here could represent a real case. The geometry involved was limited to a case of a laminar boundary layer forming on an insulated flat plate. At a distance from the leading edge, there is an injection slot, Figure (1). The injected fluid is not assumed to mix with the flowing gas (air). The effect of injection on boundary layer separation is investigated from the point of view that the injection increases the momentum associated with the flowing fluid particles in the boundary layer. This helps in overcoming the "pressure hill" caused by the incident shock wave.

Some assumptions were made regarding the behavior of the physical properties of the flowing gas and the injected fluid. These assumptions may not be valid in some cases; however, their use was to facilitate the mathematical work and it is felt that this would not change the trend of the results.

CHAPTER I

INTRODUCTION

In the usual formulation of the Prandtl boundary layer theory the static pressure distribution along the surface is given by the inviscid flow over the surface in the absence of the boundary layer. In supersonic flow, however, the static pressure distribution is not a given datum of the problem, but is determined by the interaction between the external inviscid flow and the viscous layer near the surface.

Within the boundary layer in supersonic flow, separation can be provoked in a variety of ways, for instance, by an oblique shock wave incident upon the boundary layer or by a step in the wall. In some cases, separation takes place well upstream of the agency provoking it.

Feldmann and Rott (4) first observed this phenomenon in the supersonic region over an airfoil at transonic speeds. All the main features of the flow pattern are strikingly delineated in the Schlieren studies of Liepmann (5). Following earlier work in this type of problem by Oswatitsch (6) and Wieghardt and Lees (7) gave a theoretical explanation of the extensive region of upstream influence of adiabatic flow, and showed that the over pressure on the surface decays exponentially with distance upstream of the separation point.

In spite of the long-time interest in the boundary layer-shock wave interaction problem, a satisfactory theoretical analysis does not yet exist. Some theoretical studies employ a modified Karman-Pohlhausen

method, without much success (8,9); others utilize a two-moment method, but are forced to patch together the pre-separation and post-separation regions by means of various ad hoc techniques (10,11); still others utilize a plausible, but semi-empirical mixing or mass entrainment rate between the inviscid and viscous flows (3,12). The situation is particularly unsatisfactory for flows with heat transfer. Recently, Lees and Reeves (1) constructed a theory which, they claim, is capable of including the entire flow within a single framework, without introducing semi-empirical features. The present study assumes that boundary layer approximations are valid over the entire viscous flow region. This assumption is, in fact, valid up to the point of separation.

The prime concern of this study is separation. It is asserted, and shown, that the injection of a different fluid alongside the wall would, in addition to cooling the wall, delay separation. The effect of cooling the surface, in itself, delays separation. This was proven by Bray et al (2) who utilized a modified Crocco-Lees mixing theory (3). But the main concern here is to show that the injection as a supplier of extra kinetic energy to the flow in the boundary layer, delays separation. Therefore, this study is limited to the case of adiabatic flow over a flat plate.

Once one assumes the validity of the boundary layer theory, integral or moment methods are quite attractive for viscous-inviscid interaction problems. In the present study a three-moment method is employed.

Description of the Flow

The interaction between an incident oblique shock wave and the laminar boundary layer on a flat plate is represented schematically in Figure (1) for the case with injection and Figure (2) for no injection.

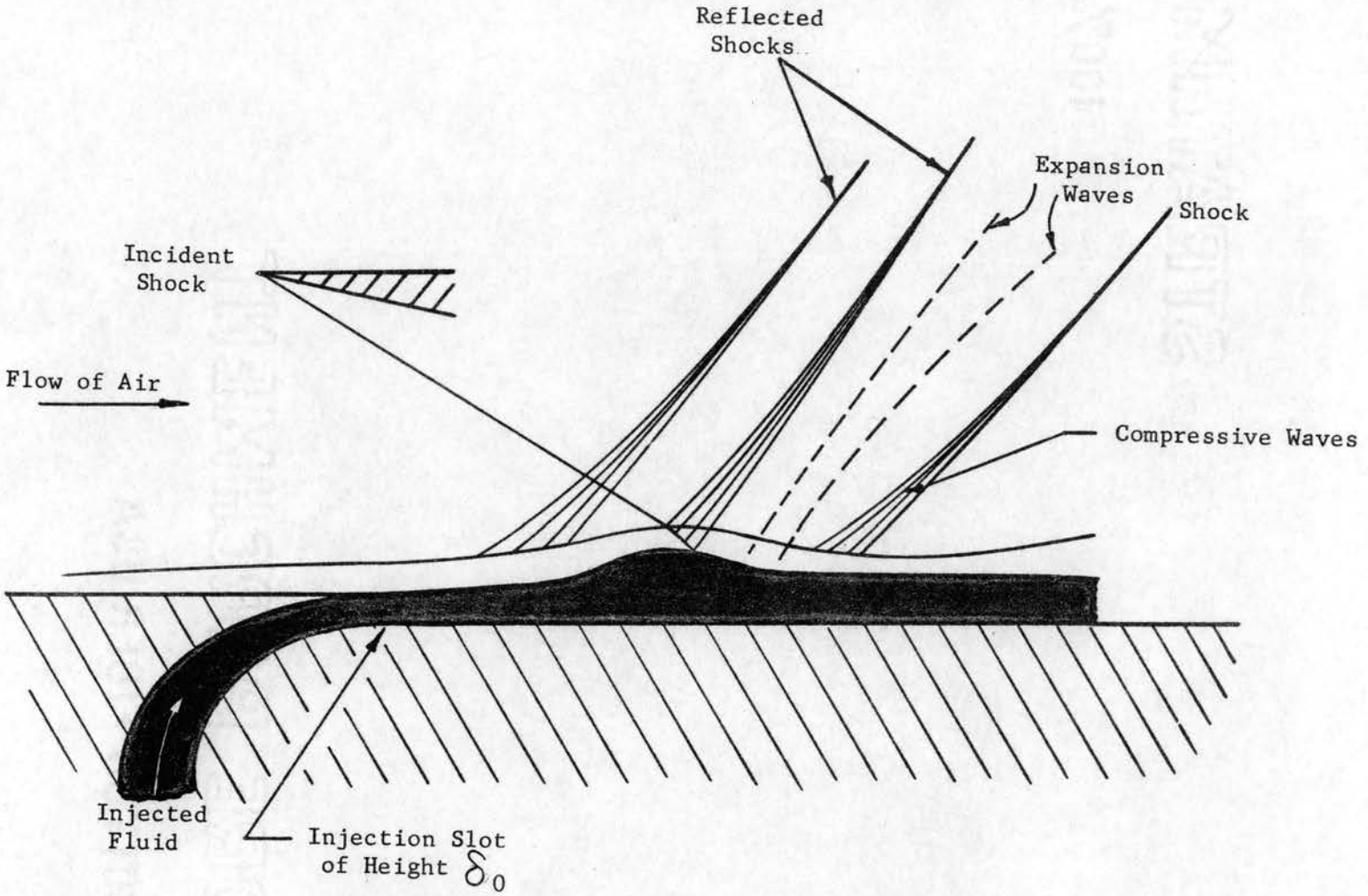

Fig. 1. Scheme for the Shock-Wave-Boundary Layer Interaction with Tangential Injection

Upstream of the shock impingement point, the second fluid is injected tangentially. It is assumed that the thickness of the first layer along the wall is determined by the equilibrium between the two layers. At the interface this equilibrium condition means the continuity of both the velocity and the shear stress. No mixing or mass transfer is assumed between the two layers.

As many authors have shown in the case of no injection, the positive pressure disturbance caused by the shock wave propagates upstream through the subsonic portion of the boundary layer. Unless the shock wave is very weak the laminar boundary layer separates from the surface upstream of shock impingement (7). The subsonic portion of the viscous layer cannot support a sudden pressure rise; therefore, the incident shock is reflected as an expansion fan that just cancels the pressure jump across the shock. Because of this reflection condition the flow at the outer edge of the viscous layer is squeezed against the surface and forced to turn as it flows downstream, and this turning produces a pressure rise and a deceleration of the flow in the viscous layer.

The pressure rise imposed on the boundary layer by the incident shock has an influence on the flow upstream of the shock. The pressure begins to rise above its upstream value, and this causes the boundary layer to thicken, because near the wall there is a region of low speed subsonic flow. The thickening of the boundary layer deflects the external flow outwards from its original direction, so generating a band of compression waves. Clearly the boundary layer thickening must be matched to the associated compression waves, and finding the conditions under which the two processes can be in equilibrium constitutes the principal task of any theory of shock wave boundary layer interaction.

Integral Methods of Solution

Because of the complexity of this problem all the known approaches utilize integral or moment methods that describe the flow in some average sense. Gadd (8) and Curle (9) employed a modified Karman-Pohlhausen method that is actually an extension of Thwaite's technique (13,14).

It is well known that the Karman-Pohlhausen integral method is a rather poor approximation for the analysis of laminar boundary layers in regions of adverse pressure gradient, particularly when separation occurs. The Karman-Pohlhausen method may also be completely inadequate downstream of separation, between the separation and reattachment points. The region where the static pressure is virtually constant (plateau) Figure (3), gives rise to much of the difficulty, since the Karman-Pohlhausen method must produce an attached, Blasius type velocity profile whenever the pressure gradient vanishes. Hence, the Karman-Pohlhausen method must predict reattachment upstream of the plateau, whereas in reality it occurs downstream of the plateau.

Apparently what is needed is an integral method which exhibits velocity profiles containing reverse-flow for vanishingly small adverse pressure gradients analogous to the "lower branch" solutions of the Falkner-Skan equation, which were found by Stewartson. In order to avoid the above mentioned difficulties, Crocco-Lees devised a method that utilizes a shape parameter $\gamma(x)$ that is not explicitly related to the local pressure gradient, or to the momentum thickness $\theta(x)$. Because they employed only the zeroth moment, or momentum integral and no higher moments, a second relation is required in order to determine the behavior of the two independent quantities $\gamma(x)$ and $\theta(x)$. This relation is supplied by specifying the "mixing rate", or rate of mass en-

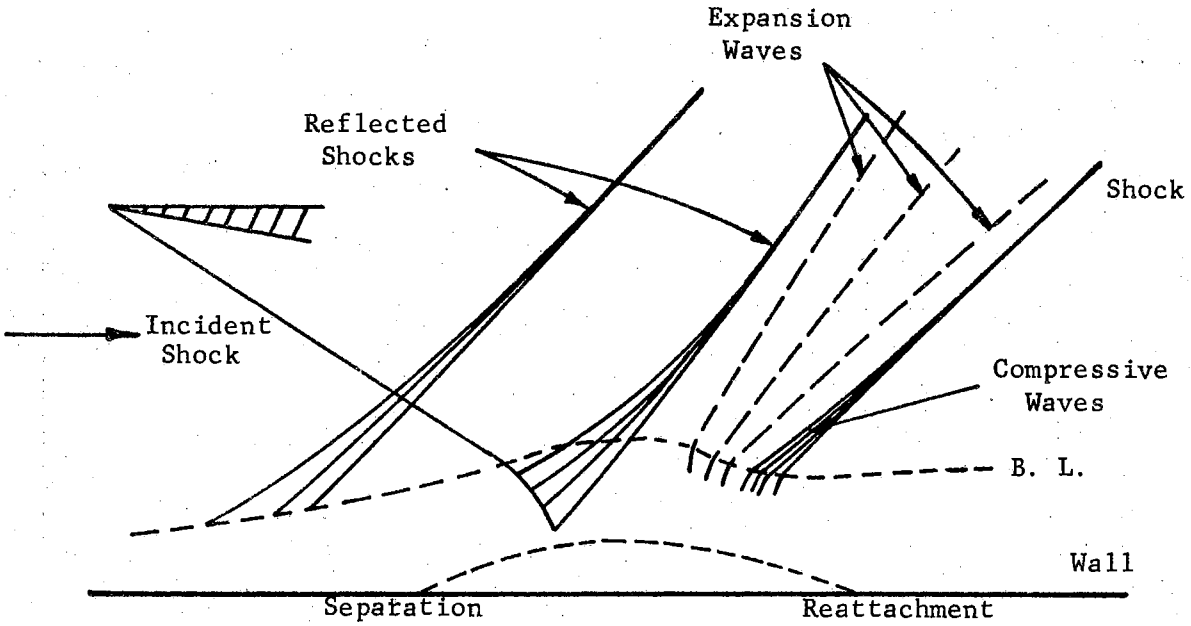

Fig. 2. Reflection of an Oblique Shock from the Boundary Layer on Flat Plate (No Injection)

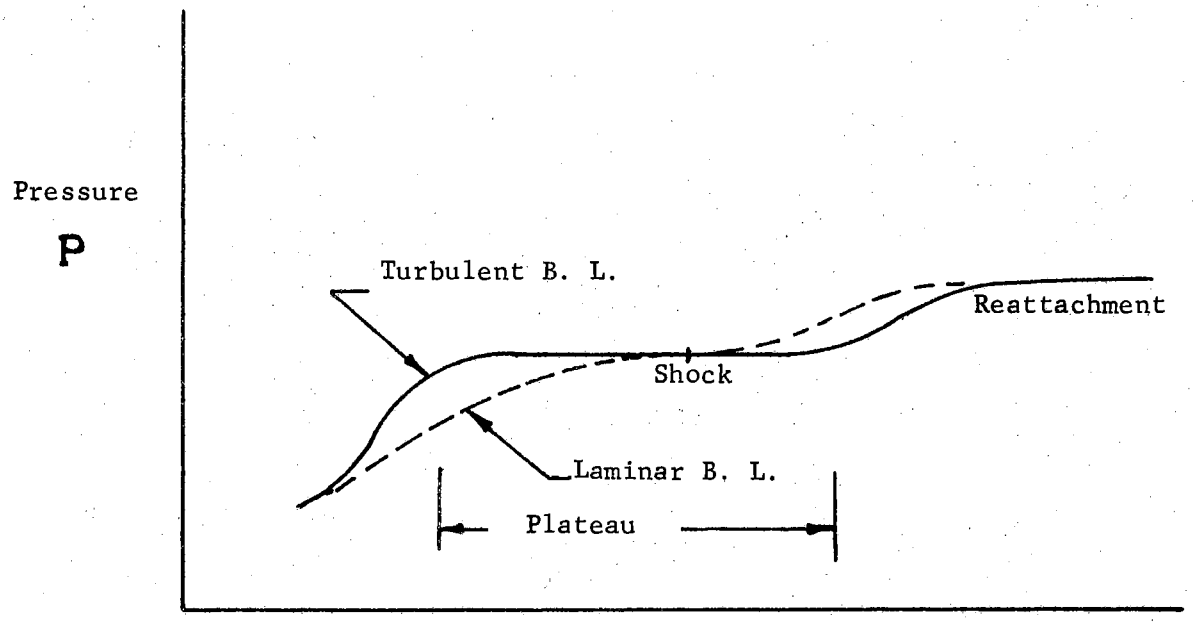

Fig. 3. Typical Surface Pressure Distributions (No Injection)

trainment from the external inviscid flow. For attached viscous layer, this relation offers no difficulty in principle, but the extension to separated and reattached flows is necessarily semi-empirical.

Glick (12) made significant improvements in the Crocco-Lees method, especially in the specification of the mixing rate function. He showed that previous quantitative disagreements between theory and experiment (1) in the region upstream of separation could be attributed to an incorrect mixing rate function $C(\gamma)$ based on the Falkner-Skan similar solutions. These solutions do not properly account for the history of the boundary layer flow, so far as mixing is concerned. When $C(\gamma)$ is based on a suitable average of experimental data and theoretical calculations that include flow history, excellent agreement is obtained between predicted and measured surface pressure distributions upstream of separation. In the region between separation and shock impingement Glick (12) determined the mixing rate function by matching the predicted static pressure distribution with the results of a single experiment. When this mixing rate is applied to another experiment at about the same Mach number, but at a Reynolds number ten times higher, agreement between theory and experiment is quite satisfactory. The "dip" in static pressure between separation and shock impingement and other anomalies found by Bray et al (1) are totally eliminated. However, one has no way of knowing in advance whether Glick's semi-empirical function can be extended to higher Mach numbers or to flows with heat transfer.

In order to avoid the semi-empirical features of the Crocco-Lees method for separated and reattaching flows, at least one additional moment of the momentum equation must be employed. This idea seems to

recur constantly in boundary layer theory; it was proposed by Sutton (15), by Walz (16), and most recently by Tani (17). Tani specifies the velocity profiles in terms of a single independent parameter a(x) proportional to the slope at the surface. By abandoning the condition on $(\partial^2 u/\partial y^2)$ at the plate surface and utilizing the zeroth and first moments of the momentum equation, he obtained two simultaneous, first-order, ordinary non-linear differential equations for a(x) and $\Theta(x)$. Tani's method gives excellent agreement with "exact solution" for prescribed adverse pressure gradients (17). Lees and Reeves (18) have shown that Tani's method is also quite suitable for describing a non-similar "relaxation" of the boundary layer flow, even for uniform static pressure.

When Abbott (11), Holt and Nielsen applied Tani's method to the boundary layer-shock wave interaction problem they found good agreement between theory and experiment for adiabatic flow up to separation. However, except at very low Reynolds numbers, their calculations showed a physically unrealistic static pressure maximum on the plate surface downstream of separation.

In an attempt to remove this anomaly, Abbott (11), Holt and Nielsen abandoned the Tani method downstream of separation, and treated this region by means of a separate analysis.* They integrated the momentum and first moment of momentum equations across the viscous layer between the dividing streamline and the "outer" edge. A quartic velocity profile was employed and the velocity ratio $(u/u_e)_{\psi = 0}$ along the dividing streamline was taken as one independent parameter, often the condi-

* They were interested mainly in "free interaction", in which the flow upstream of the pressure rise is independent of the agency causing separation.

tion of zero mass flux between the surface and the dividing streamline was applied. Unfortunately the no-slip condition at the surface was not satisfied. In the present study, the velocity ratio H(x) along the interface is taken as an independent parameter.

When a one-parameter family of velocity profiles is not sufficiently flexible one could adopt Wieghardt's (19) procedure of retaining the boundary condition on $(\partial^2 u/\partial y^2)$ at the surface, and employing the zeroth and first moments of the momentum equation. Makofski (20) applied this method to the laminar boundary layer-shock wave interaction problem for an insulated flat plate with satisfactory results.

In the present study, there are two layers, thus adding one more unknown to the problem. Therefore, a two-parameter family of velocity profiles is employed in the two layers. Either parameter is not directly proportional to the boundary condition on $(\partial^2 u/\partial y^2)$.

The basic assumptions to be utilized in this approach are:

1. Boundary layer theory is applicable, i.e. the pressure is constant across the layer and none of the other neglected terms become significant.
2. The details at the point of shock impingement are only of local interest.
3. The changes in the external flow caused by the boundary layer growth are isentropic.

The above assumptions are common to all of the analyses discussed. In addition, the following conditions are used.

4. The study will be limited to a compressible laminar boundary layer on an insulated flat plate.
5. The gas is thermally and calorically perfect and its viscosity is proportional to the absolute temperature.

CHAPTER II

SOME REMARKS ON THE PREVIOUS WORK

It seems appropiate here to mention the previous work which has been published in the line of this investigation.

Most of this work was experimental and the main concern was to determine the effect of injecting a liquid on the heat transfer between streaming hot gases and the surface along which the gases flow. No cases involving shock waves or supersonic flows were reported, however, some of the findings were pertinent to this investigation. Although the geometry of most of the reported cases was different from the present case, some of the results were similar. One other difference was that most of these cases involved turbulent flow of gases with a laminar sublayer near the surface. The extent of the theoretical analysis done in these cases, to the author's knowledge, is limited to using Reynolds analogy for joining the laminar sublayer and the turbulent core as done by Sellers (23) and Knuth (24) who extended the analogy to include the effect of the heat and momentum transported in the transverse direction by the diffusing vapor upon the momentum transfer in the turbulent core. Both authors used Von Karman's dimensionless velocity distribution for single phase flow since no information was available for the thickness of the laminar sublayer with mass addition at the wall. Sellers used the Fanning equation for the shear stress, and for the friction coefficient he used the value corresponding to that of single phase in

smooth pipes. Emmons (25) employed a method that did not require the use of the thickness of the laminar sublayer. He also found an expression for the shear stress. Although Emmons' work was conducted with the emphasis on heat transfer, some of his findings were of interest to this work.

Emmons used one injection slot for injecting the film coolant onto the test sections. He reported that for the most part the liquid film was hydrodynamically stable except in certain cases when the flow rate of film coolant becomes excessive, the liquid film becomes unstable and portions of the liquid coolant are torn away by the high velocity gas stream. Consequently, a further increase of the flow rate of the film coolant does not result in a proportional increase in the protected area. Emmons' analysis was applied to a model similar to Figure (4). This type of model was also used by Knuth (24) who reported some results on the attachment of the film coolant to the surface.

Warner and Reese (26) investigated the factors affecting the attachment of a liquid film to a solid surface. They investigated different geometries, as shown in Figure (6). They defined a critical velocity of injection V_i^*, as the mean liquid velocity flowing through the injection slot corresponding to the maximum rate of liquid flow obtained with no visible separation of the liquid film from the surface of the test section. Their results can be summarized as follows:

1. The injection of liquid through slots resulted in the establishment of stable films attached to solid surfaces.
2. The critical velocity of injection V_i^*:
   a. Increased with increases in air velocity.
   b. Decreased with increases in slot width.

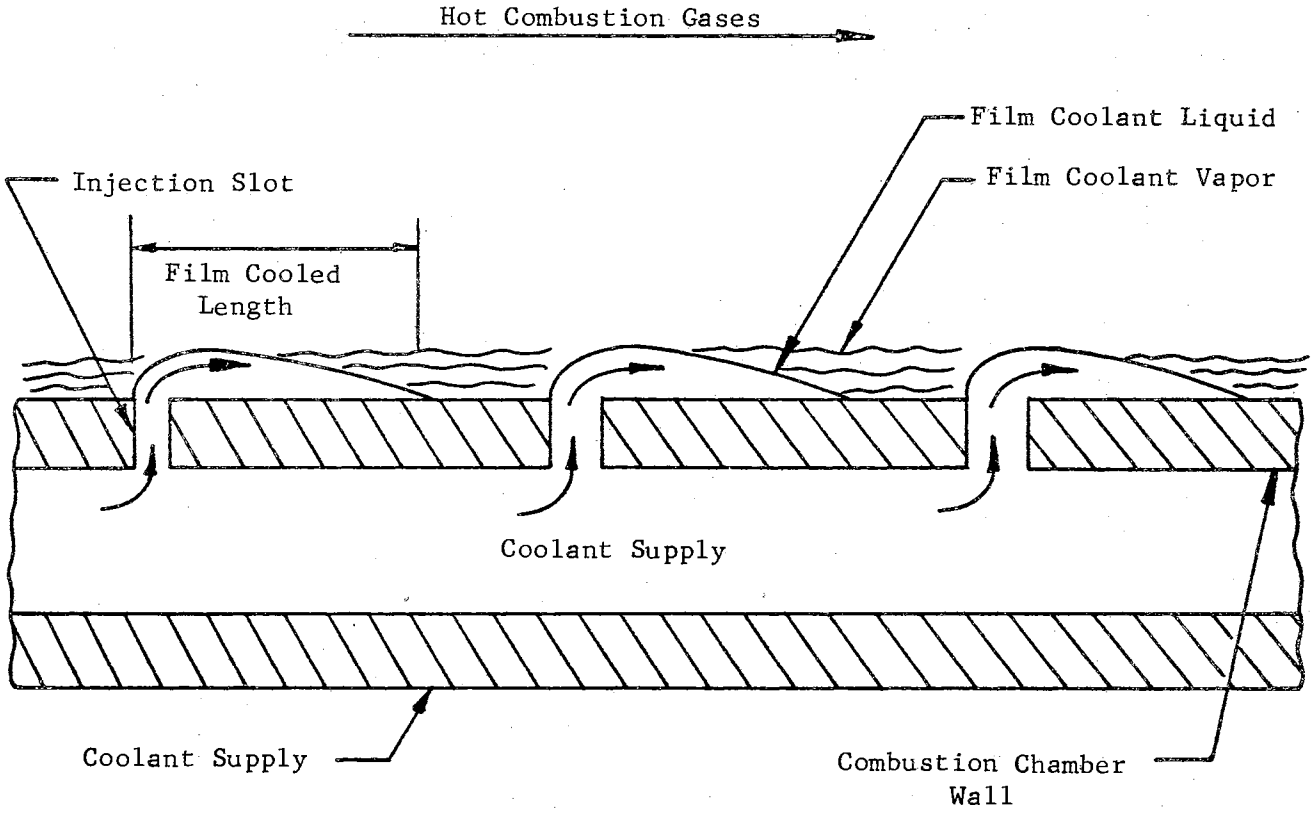

Fig. 4. Model Used by Emmons (25)

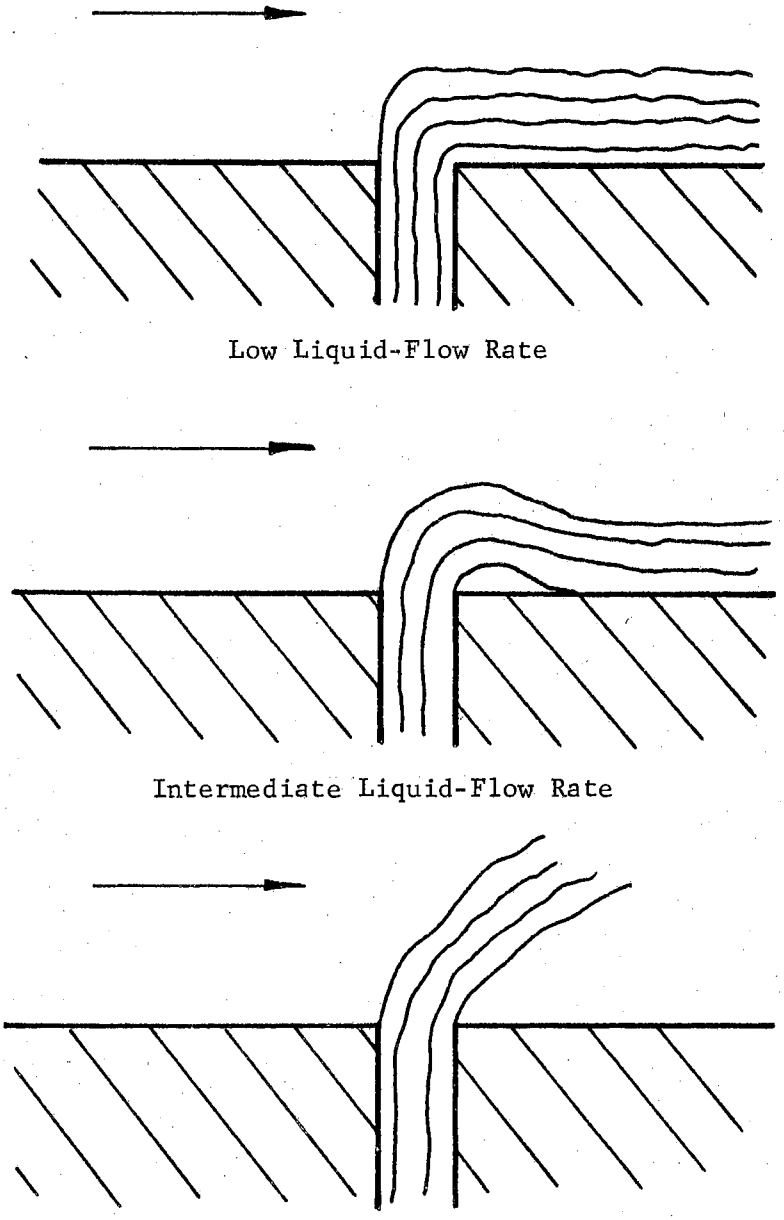

Fig. 5. Liquid-Flow Paths for Different Liquid-Flow Rates at Constant Air Velocity as Reported by Knuth (24)

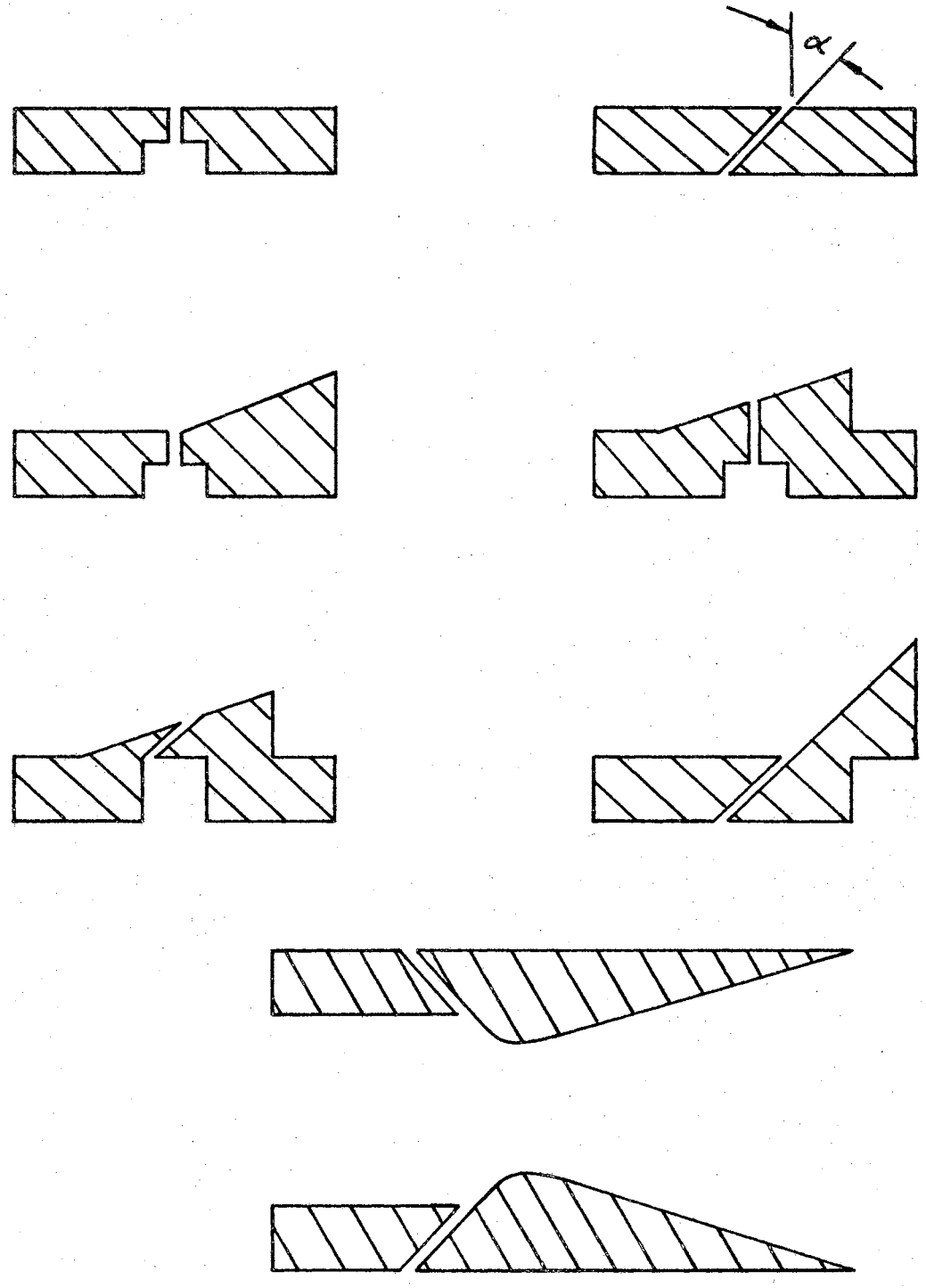

Fig. 6. Slot Configurations Investigated by Warner and Reese (26)

c. Increased with increases in angle of injection α ; separation could not be obtained with angles larger than 75 degrees.

3. The value of V_i^* was independent of liquid surface tension and viscosity, but was a function of liquid density (momentum).

4. The value of V_i^* was a function of air density (momentum).

5. The use of large velocities of injection, below but approaching V_i^*, resulted in the formation of surface disturbances upon the surface, and the entrainment of a considerable portion of the injected liquid by the air stream.

In this investigation the injection slot is tangential to the surface, Figure (1). This allowed the use of high injection velocities without separation at the point of injection.

CHAPTER III

THEORETICAL CONSIDERATIONS

Analysis

The method of analysis used here consists of transforming the compressible laminar boundary layer equations into incompressible form, obtaining integral relations and finally, solving these relations by use of a fourth-degree polynomial representation of the velocity profile in the outside layer and a second-degree polynomial representation of the velocity profile in the inside layer. This method is then applied to the shock wave-boundary layer interaction problem and the method of computation is discussed.

Basic Equations

The partial differential equations describing the steady, two-dimensional, laminar-boundary layer flow of a compressible gas along an adiabatic surface are

$$u \frac{\partial u}{\partial x} + v \frac{\partial u}{\partial y} = \rho_e U_e \frac{dU_e}{dx} + \frac{\partial}{\partial y} \left(\mu \frac{\partial u}{\partial y}\right)$$

$$\frac{\partial}{\partial x} (\rho u) + \frac{\partial}{\partial y} (\rho v) = 0$$

$$\rho / \rho_e = T_e / T \ .$$

These equations may be transformed into incompressible form by the use of the Stewartson (21) transformation as modified by Cohen and Reshotko (22). These relations are

$$x = \int_0^x C \frac{A_e}{A_o} \frac{P_e}{P_o} \, dx$$
$$y = \frac{A_e}{A_o} \int_0^y \frac{\rho}{\rho_o} \, dy \, . \qquad (1)$$

Application of these relations results in the incompressible boundary layer equations (20), where the transformed and physical longitudinal velocities are related by

$$u_i = \frac{A_o}{A_e} u, \quad \frac{u_i}{U_{e_i}} = \frac{u}{U_e} = q$$

so (2)

$$\frac{U_{e_i}}{A_o} = \frac{U_e}{A_e} = M_e \, .$$

Multiplying the momentum equation by u^n, n = 0, 1, 2, and integrating across the two boundary layers from y = 0 to y = δ_2, yields

$$\frac{d}{d_x} U_e^2 \theta + U_e U_{e_x} \delta_* = \nu_1 U_e \left(\frac{\partial q_1}{\partial y} \right)_{wall} \qquad (3) *$$

$$\frac{d}{d_x} U^3_e \, \theta_* = 2 \int_0^{\delta_2} \nu \, U^2_e \, (\frac{\partial q}{\partial y})^2 \, dy \qquad (4)$$

$$\frac{d}{d_x} U^4_e \, \theta_{**} - 3U^3_e U_{e_x} \theta = 6U^3_e \int_0^{\delta_2} \nu \, q \, (\frac{\partial q}{\partial y})^2 \, dy \qquad (5)$$

Equations (3), (4), and (5) are the zeroth, first and second moments of momentum, respectively.

In the above equations δ_* , θ , θ_* , θ_{**} are the incompressible displacement, momentum, energy and a moment of momentum thickness.

---

* The subscript i, meaning incompressible is dropped for convenience.

Velocity Profiles

To solve equations (3) to (5), a fourth degree polynomial is chosen for the velocity profile in the second layer and a second degree polynomial in the first layer, (see Appendix A).

$$q_1 = \frac{u_1}{U_e} = H\eta_1 - F\eta_1 + F\eta_1^2 \tag{6}$$

where $\eta_1 = y/\delta_1$, and

$$q_2 = \frac{u_2}{U_e} = H + (1 - H)(1 - 3.67\eta_2^3 + 2.67\eta_2^4) \tag{7}$$

where $$\eta_2 = \frac{\delta_2 - y}{\delta_2 - \delta_1}$$

The velocity profiles (6) and (7) satisfy the conditions that at,

$$\begin{aligned} &y = 0 \ (\eta_1 = 0) && q_1 = 0 \\ &y = \delta_2 \ (\eta_2 = 0) && q_2 = 1 , \ \frac{\partial q_2}{\partial \eta_2} = \frac{\partial^2 q_2}{\partial \eta_2^2} = 0 \\ &y = \delta_1 \ (\eta_1 = \eta_2 = 1) && q_1 = q_2 = H \end{aligned} \tag{8}$$

It is seen that there are two parameters H(x) and F(x) in the velocity profiles. If the boundary condition at the wall is satisfied for $\partial^2 u/\partial y^2$, one obtains

$$F = \frac{\delta_1^2}{2\nu_1} \frac{dU_e}{dx} ,$$

which is proportional to the pressure gradient and related to the Pohlhausen parameter. This would lead to the complications mentioned earlier. Therefore, this condition will not be satisfied; instead, the continuity

of the shear stress at the interface of the two layers is satisfied. Thus giving

$$F = -H + .332 \left(\frac{\mu_2}{\mu_1}\right) \left(\frac{\delta_1}{\delta_2 - \delta_1}\right) (1 - H)$$

For convenience, write $\delta = \delta_2 - \delta_1$; and $C = .332\ \mu_2/\mu_1$.

Then,

$$F = -H + C\ (\delta_1/\delta)\ (1 - H) \tag{9}$$

The shear stress at the wall is represented as

$$\frac{\tau_0\ \delta_1}{\mu_1\ U_e} = H - F = 2H - C(\delta_1/\delta)\ (1 - H)$$

and the shear stress at the interface is

$$\frac{\tau_{\delta_1}\ \delta_1}{\mu_1\ U_e} = H + F = C\ \frac{\delta_1}{\delta}\ (1 - H) .$$

It is easy to see now that

$$\frac{\tau_{\delta_1}\ \delta_1}{\mu_1\ U_e} > \frac{\tau_0\ \delta_1}{\mu_1\ U_e}$$

when H(x) is negative. Also $\frac{\tau_0 \delta_1}{\mu_1 U_e}$ goes to zero only if H(x) becomes negative. Therefore, the crucial parameter is $\frac{\tau_0 \delta_1}{\mu_1 U_e}$ and investigating its behavior will determine whether separation takes place or not.

By studying the velocity profiles given by equations (6) and (7) it is seen that they both combine to give different shapes depending on the choice of the values of H, C and δ_1/δ . This could be seen in Figures (26,27 and 28). The previous researchers who investigated the same problem but with no injection, employed velocity profiles that involved polynomials of degrees up to the eleventh. This was done in order to give the profile the ability to accomodate geometrical qualities, such as points of inflexion which would permit reverse flows. The present profiles do not need to be represented by such high degree polynomials. This is because there are two of them and they are connected by a point at the interface, whose position relative to a fixed point, can be controlled to some extent by varying the velocity of injection H(0), the relative thicknesses δ_1/δ or μ_2/μ_1 .

When these profiles are used in equations (3) (4) and (5) one obtains the following equations

$$\frac{d}{d_x}\Theta + (2\Theta + \Delta_*)\,VR = \frac{1}{\Delta_1 \, R\delta_0}(H - F) \qquad (10)$$

$$\frac{d}{d_x}\Theta_* + 3\Theta_*\,VR = \frac{2}{\Delta_1 \, R\delta_0}(H^2 + .33F^2) + \frac{2.8}{R\delta_0}(1 - 2H + H^2) \qquad (11)$$

$$\frac{d}{d_x}\Theta_{**} + (4\Theta_{**} - 3\Theta)\,VR = \frac{1}{\Delta_1 \, R\delta_0}(3.0H^3 + .96HF^2 + .96H^2F)$$

$$+ \frac{1}{R\delta_0}(7.2 - 13.2H + 4.8H^2 + 1.2H^3) \qquad (12)$$

where

$$VR = \frac{U_{ex}}{U_e}\,,\ \Theta = \theta/\delta_0\,,\ \Delta_1 = \delta_1/\delta_0\,,\ \Delta = \delta/\delta_0\,,$$

$$\Delta_* = \delta_* / \delta_0 , \quad \Theta_* = \theta_* / \delta_0 , \quad \Theta_{**} = \theta_{**} / \delta_0 , \quad {}^R\delta_0 = \frac{U_\infty \delta_0}{\nu_1} \cdot \delta_0$$

And δ_0 is the height of the injection slot. Also H, Δ_*, Θ_* and Θ_{**} are functions of H, Δ_1, and Δ. (For the complete relations, see Appendix A.)

The Attached Boundary Layer

Upstream of the region of interaction where the pressure is constant (VR = 0), equations (10) to (12) can be solved for $H(x), \Delta_1(x)$ and $\Delta(x)$. However, in the interaction region, the surface pressure is not specified a priori. Therefore, a fourth relation is needed that couples the growth of the boundary layer with the changes in the external stream. With the assumption that changes in the external stream are isentropic, the boundary layer growth may be related to the external velocity by

$$\frac{d^2 \delta_*}{dx^2} = - \frac{\sqrt{M_0^2 - 1}}{U_e} \frac{dU_e}{dx} . \qquad (13)$$

This relation is obtained by observing that the angle of deflection, α, of the external stream from the free-stream direction parallel to the wall is related to the pressure upstream of the shock by (3)

$$\alpha = \sqrt{M_0^2 - 1} \; (P - P_\infty) / \gamma M_e^2 P_\infty .$$

Where there are sharp longitudinal pressure gradients α is, in fact, somewhat indefinite, since the divergence of the stream lines in the external flow is of the same order as that within the boundary layer. With a flat wall

$$\alpha = \left[d \delta_* (x) / dx \right] - \left[d \delta_* (x - \Delta x) / dx \right] .$$

Hence, upstream of the shock

$$\frac{d}{dx}\left[\delta_*(x) - \delta_*(x - \Delta x)\right] = \frac{\sqrt{M_0^2 - 1}}{\gamma M_0^2 P_\infty}(P - P_\infty) \qquad (14)$$

and since

$$U_e \frac{dU_e}{dx} = -\frac{1}{\rho_e}\frac{d}{dx}(P - \underset{\sim}{P}),$$

equation (13) follows by differentiating equation (14).

For use in equations (10) and (12), equation (13) must be transformed into the incompressible plane using Stewartson transformation, equation (1). The result of this transformation (see Appendix A) is

$$\frac{d\Delta_*}{dx} + \frac{0.2M_e^2}{(1 + 0.2M_e^2)}\frac{d\tilde{\ }}{dx} + \left[\left\{\frac{0.24M_e^4}{(1 + 0.2M_e^2)^2} + \frac{0.8M_e^2}{(1 + 0.2M_e^2)}\right\}\tilde{\ } + \frac{1.6M_e^2}{(1 + 0.2M_e^2)}\Delta_* + (\Delta x/\delta_0)\sqrt{M_e^2 - 1}\right] VR = G_0 . \qquad (15)$$

By expanding equations (10), (11), (12) and (15), (see Appendix A) one obtains

$$S_1\frac{d\Delta_1}{dx} + S_2\frac{d\Delta}{dx} + S_3\frac{dH}{dx} + S_4 VR = S_5 \qquad (17)$$

$$P_1\frac{d\Delta_1}{dx} + P_2\frac{d\Delta}{dx} + P_3\frac{dH}{dx} + P_4 VR = P_5 \qquad (18)$$

$$H_1\frac{d\Delta_1}{dx} + H_2\frac{d\Delta}{dx} + H_9\frac{dH}{dx} + H_{10}VR = H_{11} \qquad (19)$$

$$D_1\frac{d\Delta_1}{dx} + D_2\frac{d\Delta}{dx} + D_3\frac{dH}{dx} + D_4 VR = D_7 \qquad (20)$$

Equations (17), (18), (19) and (20) are first order, non-linear ordinary differential equations. They are to be solved for $\frac{d\Delta_1}{dx}$, $\frac{d\Delta}{dx}$, $\frac{dH}{dx}$, and VR. This is done by considering the differential equations as algebraic equations in the above unknowns.

With a set of initial conditions on Δ_1, Δ, H and VR (Appendix A), one obtains

$$\Delta_1 (x + \Delta x) = \Delta_1 (x) + \Delta x \left. \frac{d\Delta_1}{dx} \right)_x \tag{21}$$

$$\Delta (x + \Delta x) = \Delta(x) + \Delta x \left. \frac{d\Delta_1}{dx} \right)_x \tag{22}$$

$$H (x + \Delta x) = H (x) + \Delta x \left. \frac{dH}{dx} \right)_x \tag{23}$$

$$P/P_\infty = 1 + \gamma M_e^2 \int_0^x VR(x)dx \tag{24}$$

CHAPTER IV

RESULTS AND DISCUSSION

The experimental work which has been mentioned earlier has guided the author to use the input data which closely resembled actual cases whenever this was possible.

In order to report the results it is necessary to specify the parameters which are varied in the input data and the parameters whose behavior is to be studied.

The input data or the initial conditions consist of the following parameters:

1. The upstream Mach numbers M_0 = 2 to 5.
2. The shock strength PR, which is defined as the pressure rise across the shock over the upstream pressure, PR = P_s/P_∞.
3. The injection velocity ratio H(0) = 0.05 to 0.50.
4. The height of the injection slot δ_0 = 0.001 to 0.005.
5. The position of injection relative to the leading edge x_0. This is specified by the choice of $\Delta(0)$, the thickness of the gas layer at the point of injection. This is because the boundary layer growth upstream of that point is a function of the distance from the leading edge according to the theory of flow over flat surfaces. $\Delta(0)$ = 0.6 to 5.0.
6. The physical properties of the injected fluid as indicated by the reduced Reynolds number, R_{δ_0} = 2 to 5.

7. The ratio of the viscosity of the injected fluid to that of the flowing gas (air), as indicated by $C = 0.332\mu_2/\mu_1 = 0.0332$ to 0.332.

The effect of the position of the shock impingement point relative to the point of injection is taken into account by using the dimensionless distance x/L. In this case L is the distance from the shock impingement point to the injection slot for $M_0 = 2.0$.

The main concern of this investigation is to determine whether or not separation occurs. Therefore, the most important parameter to discuss is the shear stress parameter $\frac{\tau_0 \delta_1}{\mu_1 U_e}$.

Although this investigation is not concerned with the surface pressure, it was important to check whether or not the surface pressure rises up to the value at the shock impingement point.

It was noticed that the shear stress parameter is sensitive to the variation of the injection velocity ratio H(0). It was also noticed that for the high values of H(0), the interface velocity ratio, H(x), did not become negative. Because the shear stress assumed negative values when H(x) became negative, the behavior of H(x) was of significant interest.

The last parameter to discuss will be the boundary layer thicknesses. In the case of no injection the gas layer deflects upward, thus generating compression waves; but when the layer of the injected fluid grows beneath the gas layer, the latter is pushed upward and its curvature is changed, thus changing the pattern of the compression waves. This is not as sharp and localized as in the case of no injection.

Variation of the Shear Stress

Effect of the initial interface velocity ratio:

As mentioned before, the most influential factor on the behavior of the shear stress is the injection velocity ratio H(0). The behavior shown in Figures (7,8 and 9) is obviously due to the fact that the higher the injection velocity, the higher the momentum associated with the moving fluid particles in the boundary layers which enables the latter to withstand higher adverse pressure gradients. For the low range of H(0), it is seen that the shear stress increases at first and then drops sharply and separation takes place. This early increase is due to the fact that momentum is added to the layers by the injected fluid while the pressure gradient there is nearly zero. For H(0) = 0.50 the shear stress decreases steadily along the surface but does not go to zero even past the shock impingement point. Therefore, the phenomenon of separation was eliminated completely for the high values of H(0) and delayed for the low range of H(0). The conditions leading to this result do not specify whether the injected fluid was a gas or a liquid; therefore, either could be the case; however, the validity of some of the assumptions made earlier would be questionable. For instance, the Prandtl number of the injected fluid might not be unity for some liquids. Also the viscosity-temperature relationship which may hold for gases, does not hold for liquids. It should not be overlooked that these assumptions were made only to facilitate the mathematical analysis, and it is felt that they would not change the trend of the results.

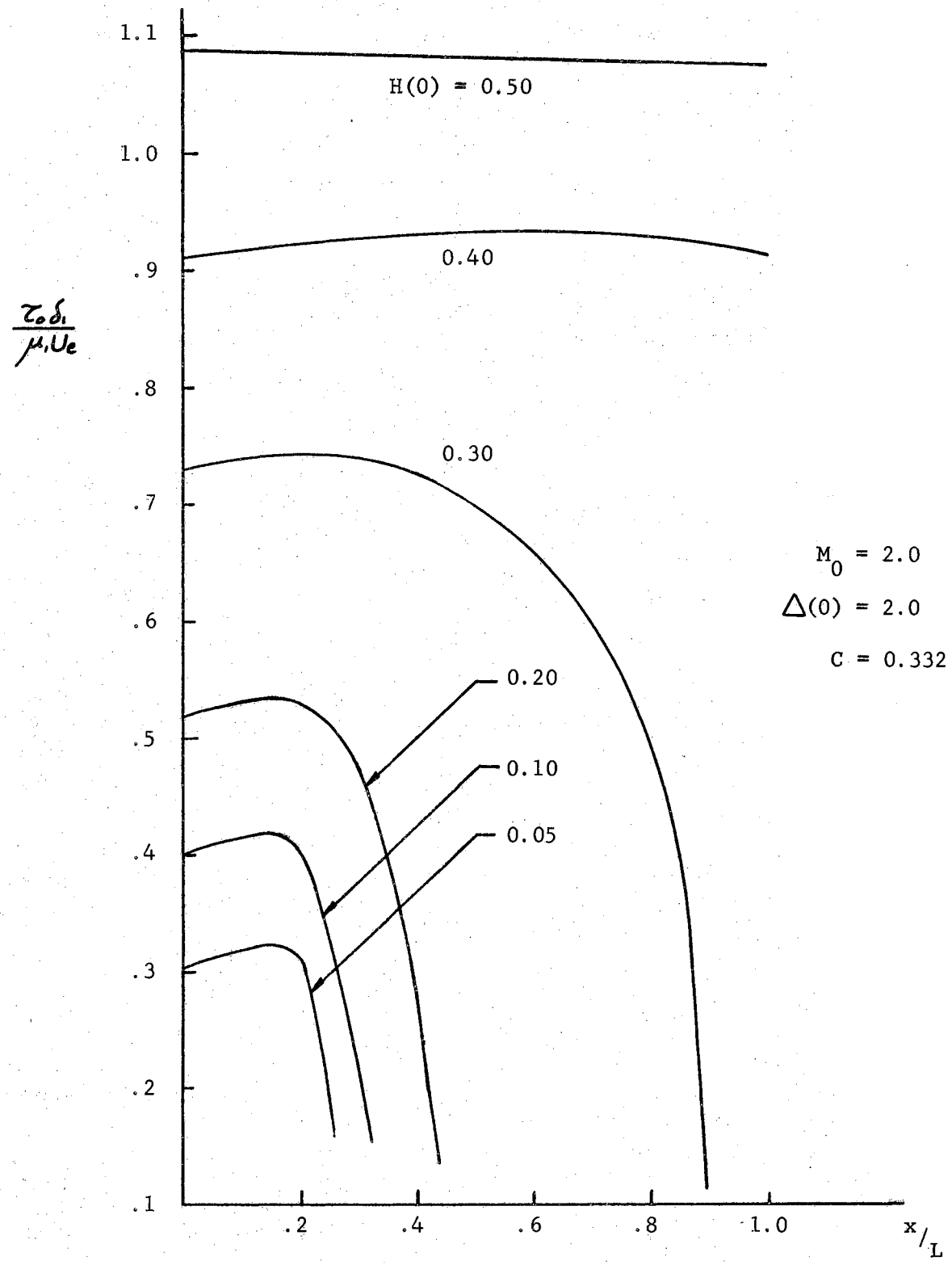

Fig. 7. Effect of Initial Injection Velocity Ratio H(0) on Shear Stress

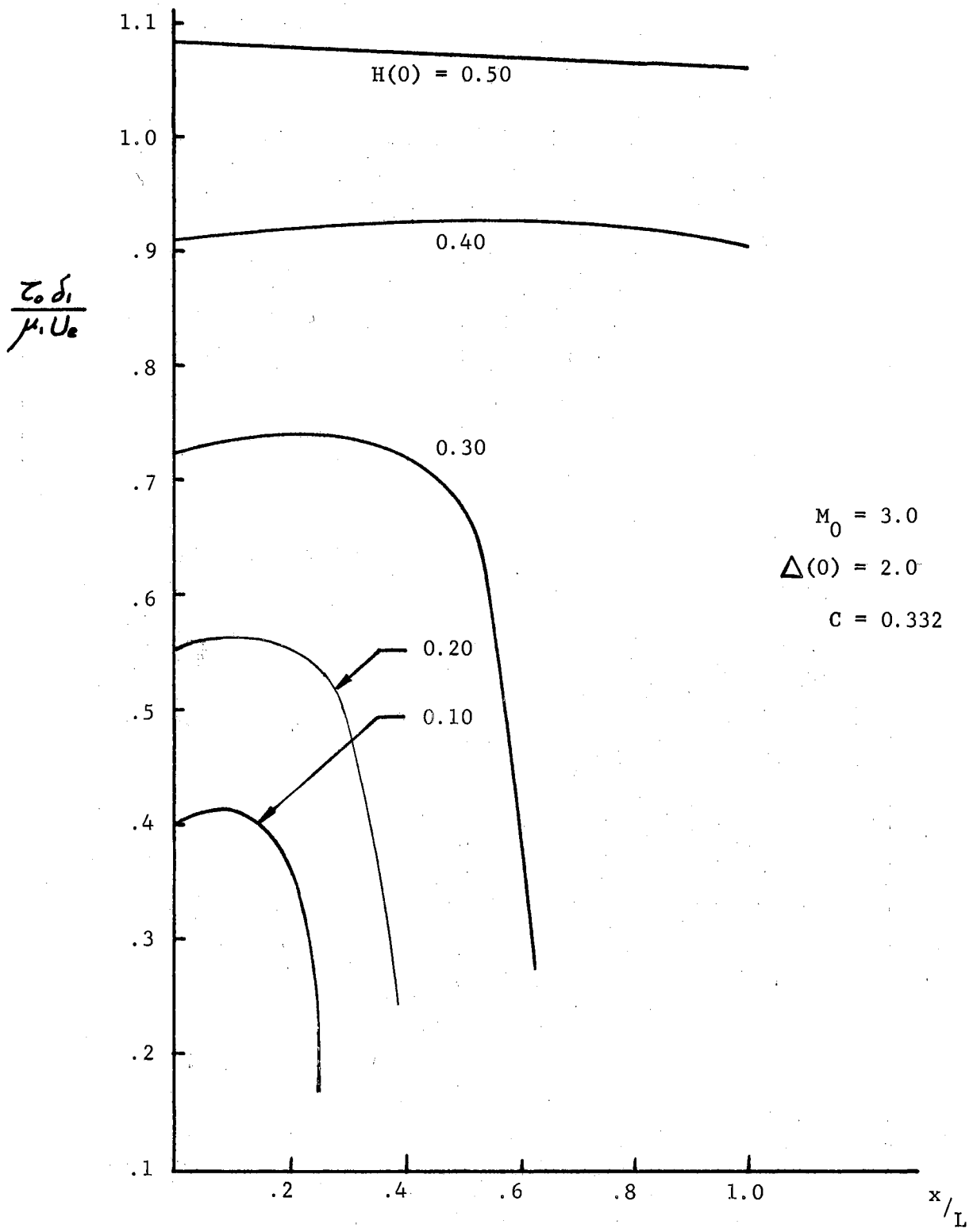

Fig. 8. Effect of H(0) on the Shear Stress

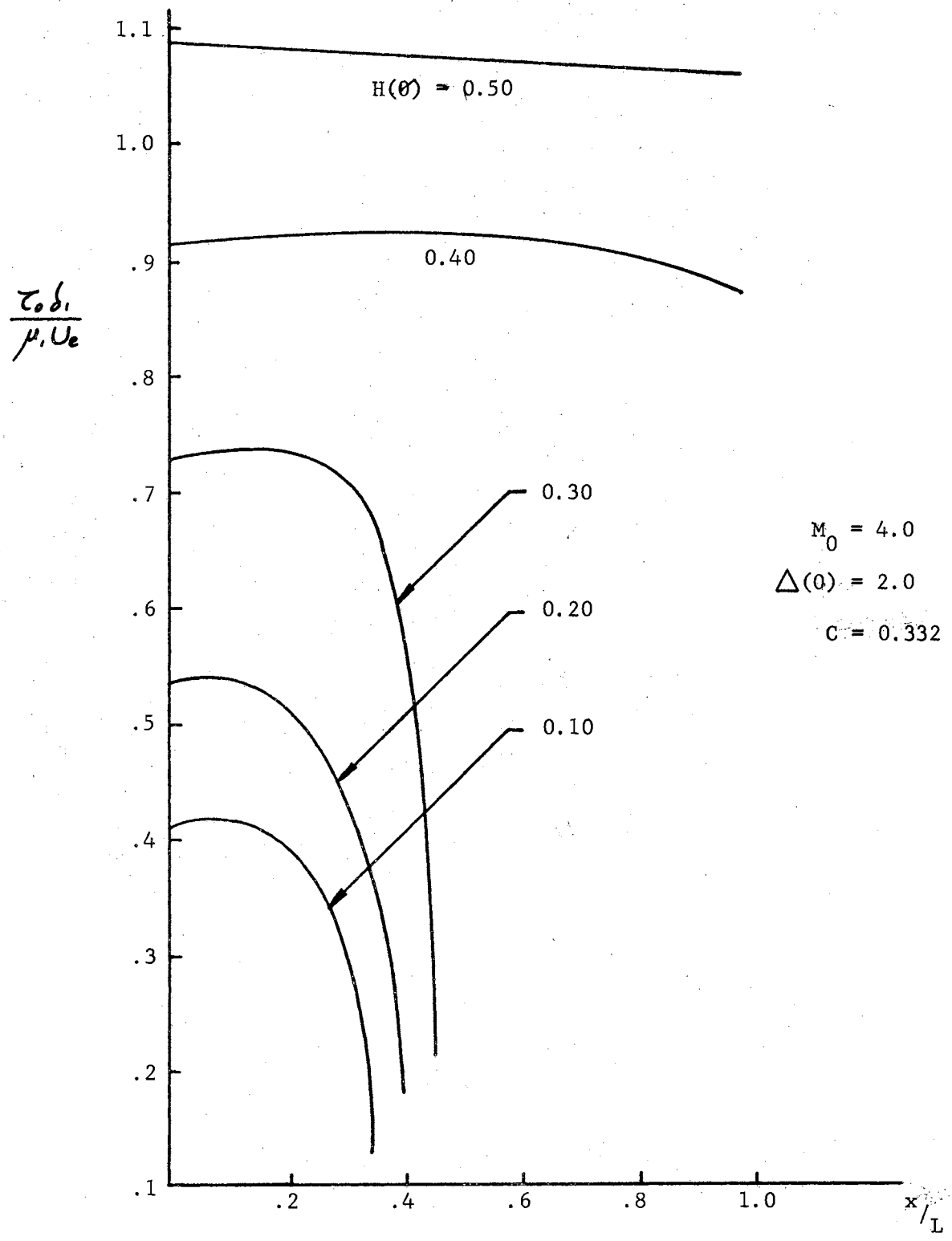

Fig. 9. Effect of H(0) on the Shear Stress

Effect of the upstream Mach Number:

The effect of the upstream Mach number, M_0, on the shear stress is small, only speeding separation at the lower range of H(0) for the higher range of Mach numbers.

Effect of the initial Boundary Layer thickness ratio:

The effect of the initial boundary layer thickness ratio, $\Delta(0)$, on the shear stress is shown in Figure (10). It is observed that $\Delta(0)$ has a slight effect, and in general the higher the value of $\Delta(0)$, the higher the value of the shear stress.

Effect of the slot height:

Figure (12) shows the effect of using different heights for the injection slot. The smaller sizes correspond to the slot heights which were used by the previous investigations (23,24). The shear stress decreases with increasing slot height. This is logical since H(x) does not vary much with δ_0; thus, the shear stress is inversely proportional to δ_0.

Effect of the fluid viscosity ratio:

The effect of varying the fluid viscosity as indicated by C is shown in Figure (13). Since the case of $\Delta(0) = 1.0$ leads to separation even for $H(0) = 0.50$, the effect of C on the shear stress was investigated for this particular case. As shown, it is seen that increasing the viscosity of the injected fluid or decreasing C does delay separation even for the case where the boundary layer could not withstand any adverse pressure gradient at all.

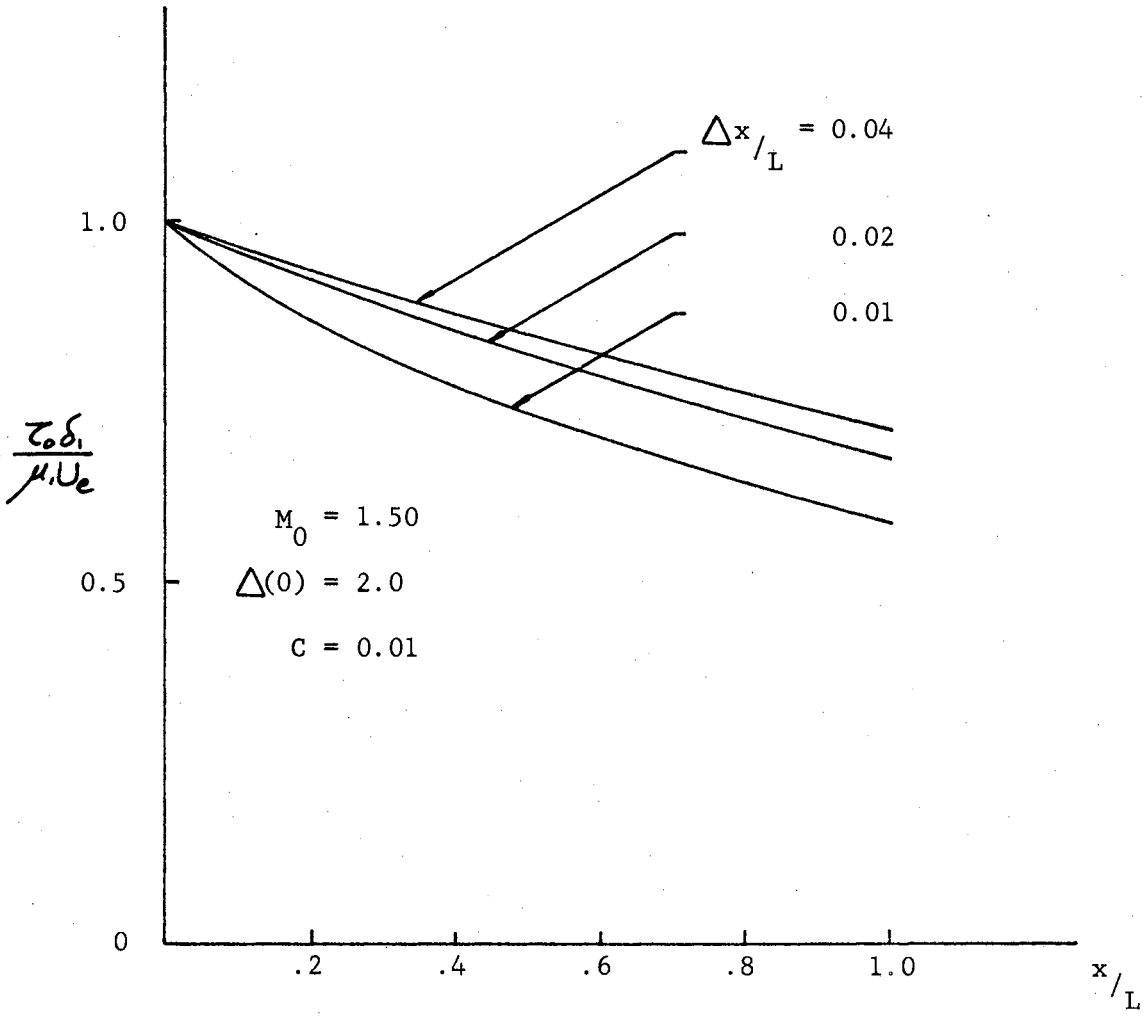

Fig. 11. Effect of $\Delta x/L$ on the results of the Numerical Integration

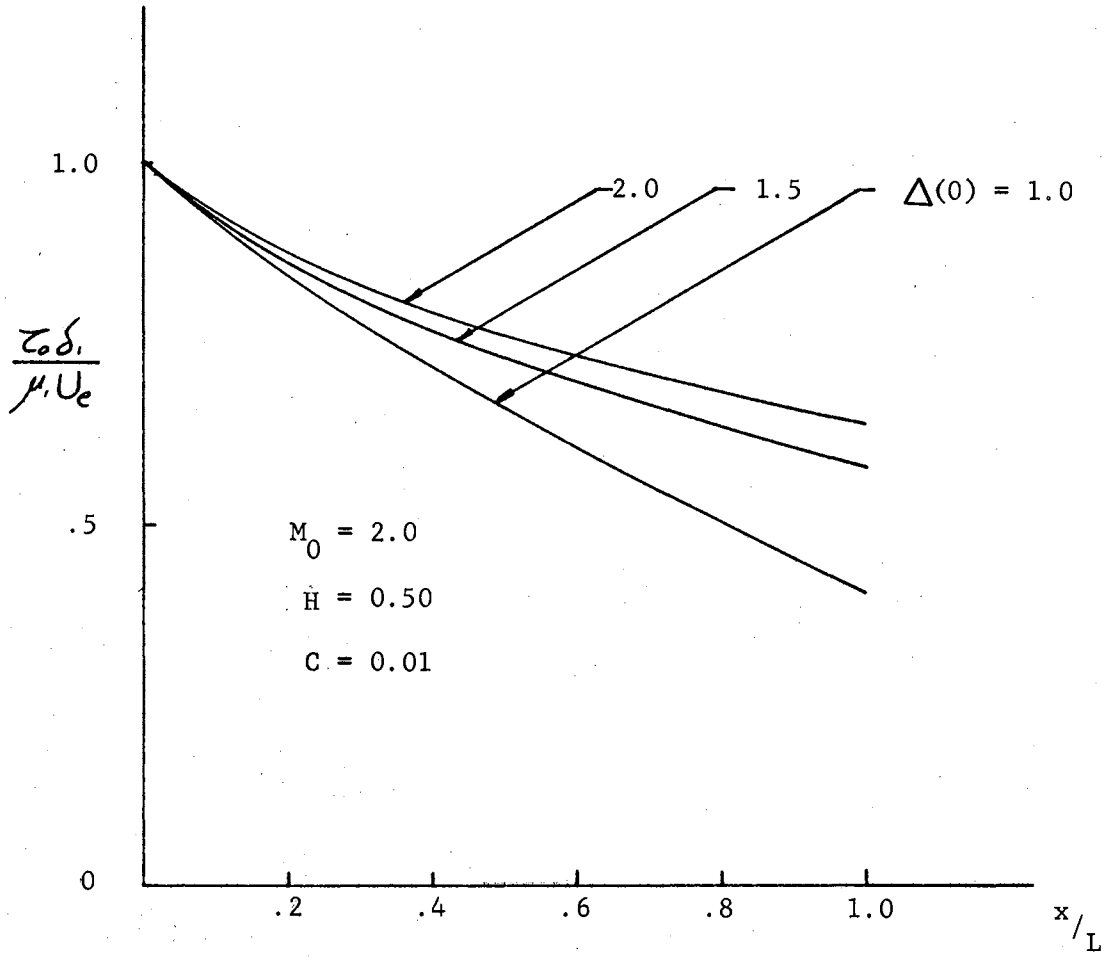

Fig. 10. Effect of $\Delta(0)$ on the Shear Stress

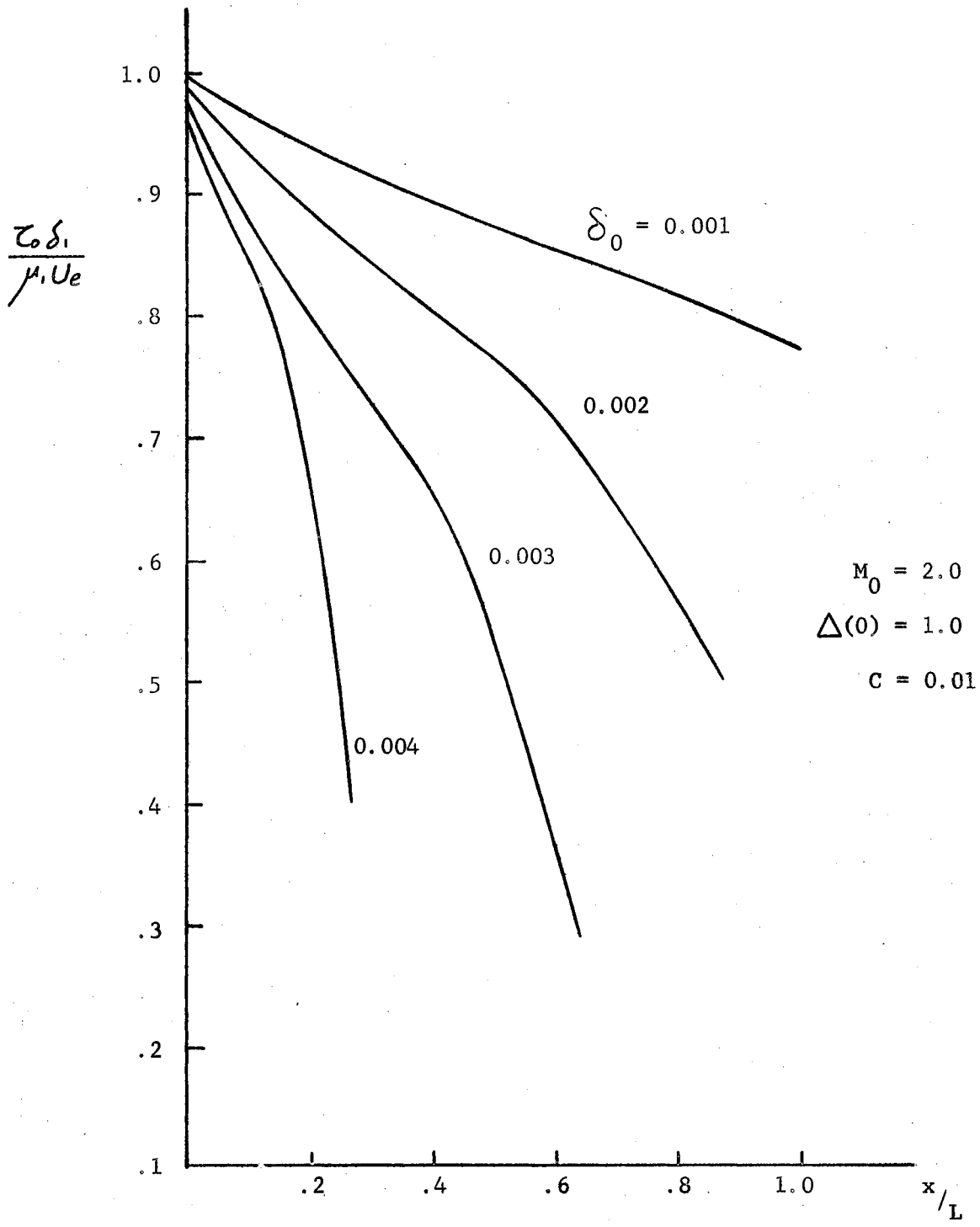

Fig. 12. Effect of the Size of δ_0 on the shear stress

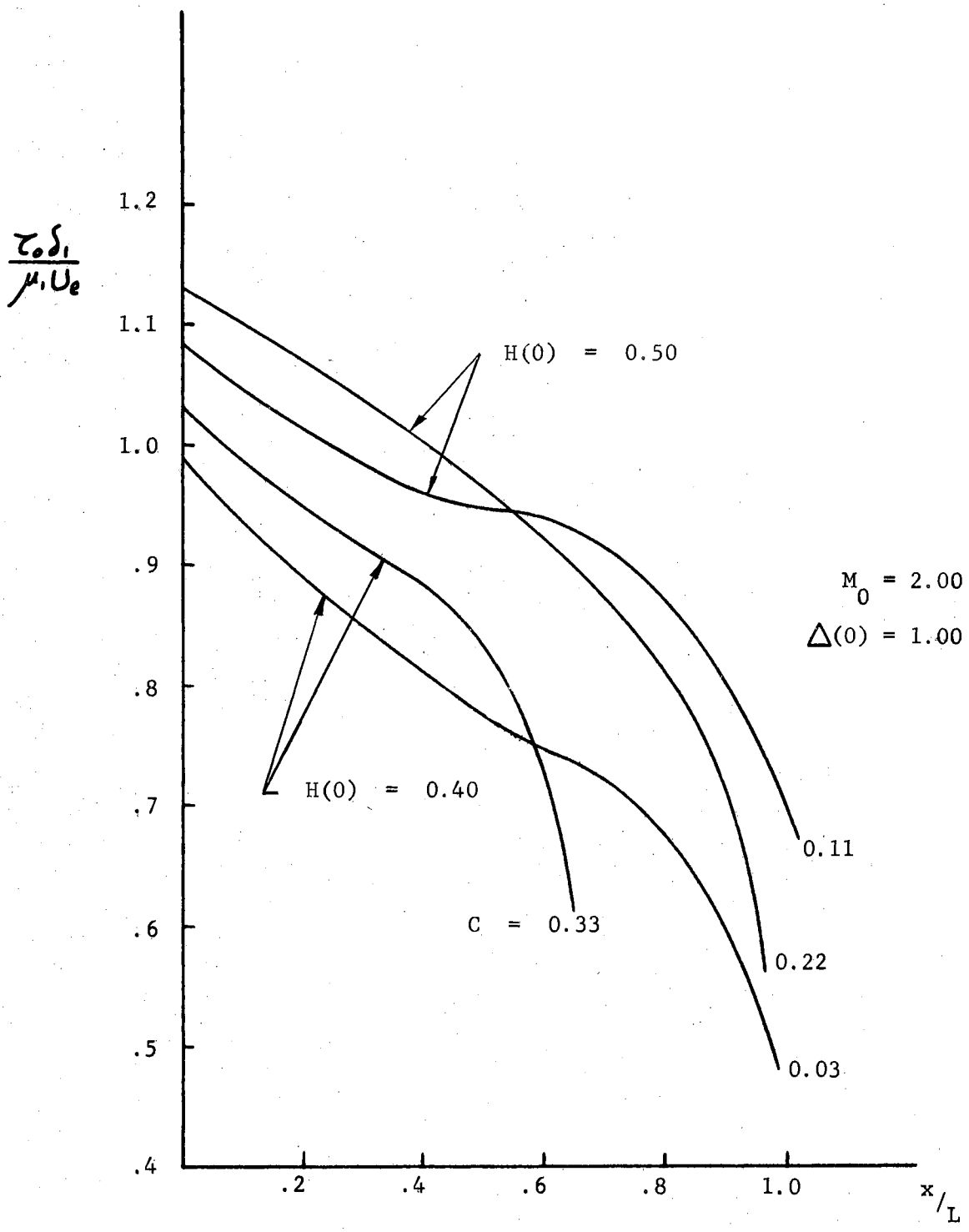

Fig. 13. Effect of C on the Shear Stress

Effect of the reduced Reynolds number:

This effect is shown in Figure (14). For the case of $H(0) > 0.3$ the effect of $R\delta_0$ on the shear stress is small. However, for $H(0) = 0.3$, $R\delta_0 \leqslant 2.0$, it was noticed that separation took place. When $R\delta_0$ was increased separation was delayed.

Variation of the Interface Velocity Ratio

Effect of $R\delta_0$ and $\Delta(0)$:

It was mentioned earlier that the interface velocity has a marked effect on the shear stress; therefore, we expect that $R\delta_0$ would have the same effect on $H(x)$ as it did on the shear stress. Indeed this was the case, as shown in Figure (15). Increasing $R\delta_0$ extends the ranges of $H(x)$ above the zero level, thus delaying separation.

The effect of $\Delta(0)$ on $H(x)$ is seen to be similar to that of $R\delta_0$ as shown in Figure (16).

Variation of the Surface Pressure

The surface pressure, Figures (17,18,19 and 20), is seen to be gradually increasing up to the values specified by the shock strength PR. At the high values of PR, which correspond to the higher Mach numbers, the surface pressure is seen to attain its peak value just before the shock impingement point and stays approximately constant past that point. This region may correspond to the plateau pressure region in separated flows without injection, but the extent is not as large. As mentioned earlier, the rise in the surface pressure along the surface is sharper for high Mach numbers than for low Mach numbers. It was also mentioned before that the growth of the fluid layer beneath

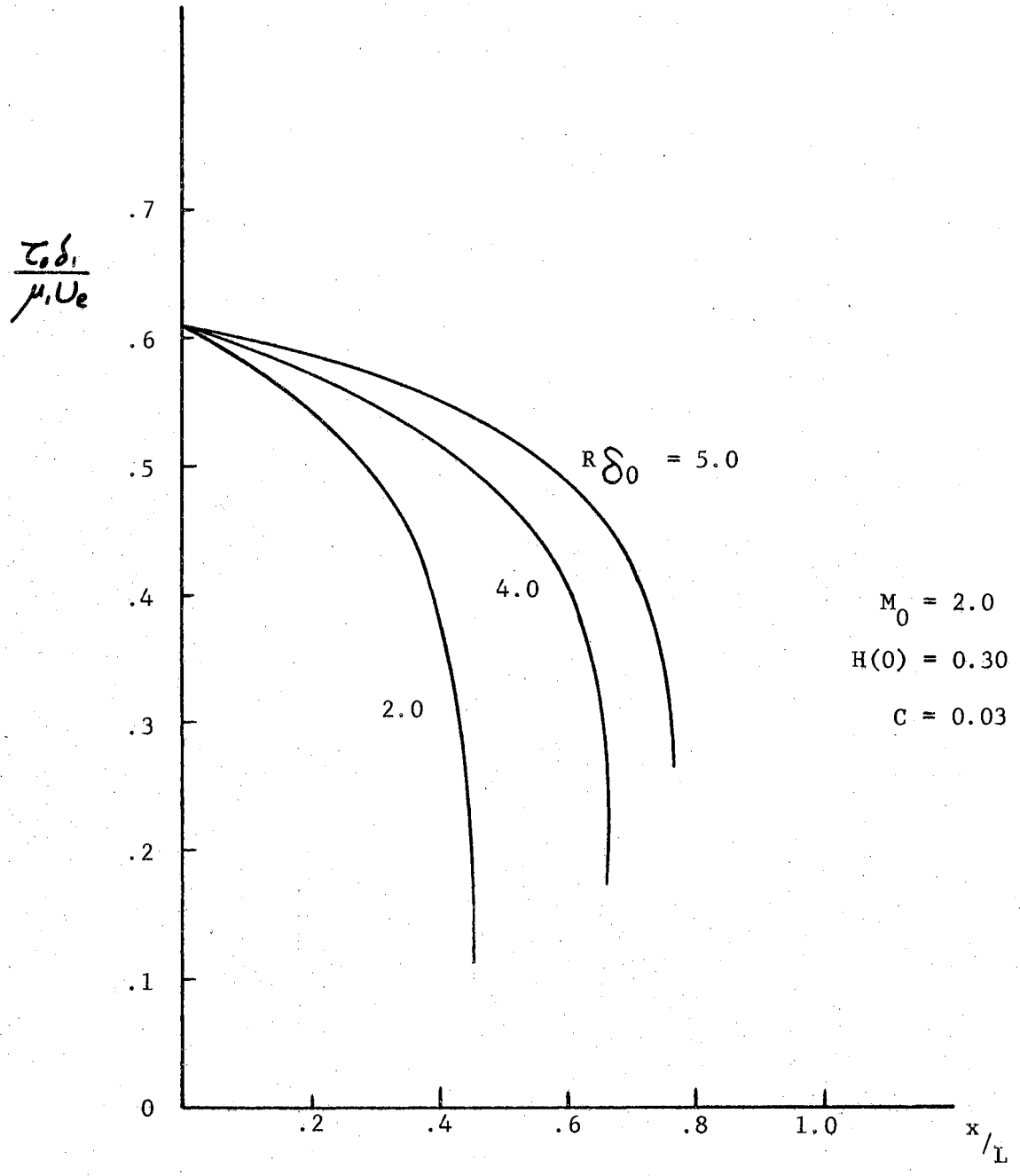

Fig. 14. Effect of $R\delta_0$ on the Shear Stress

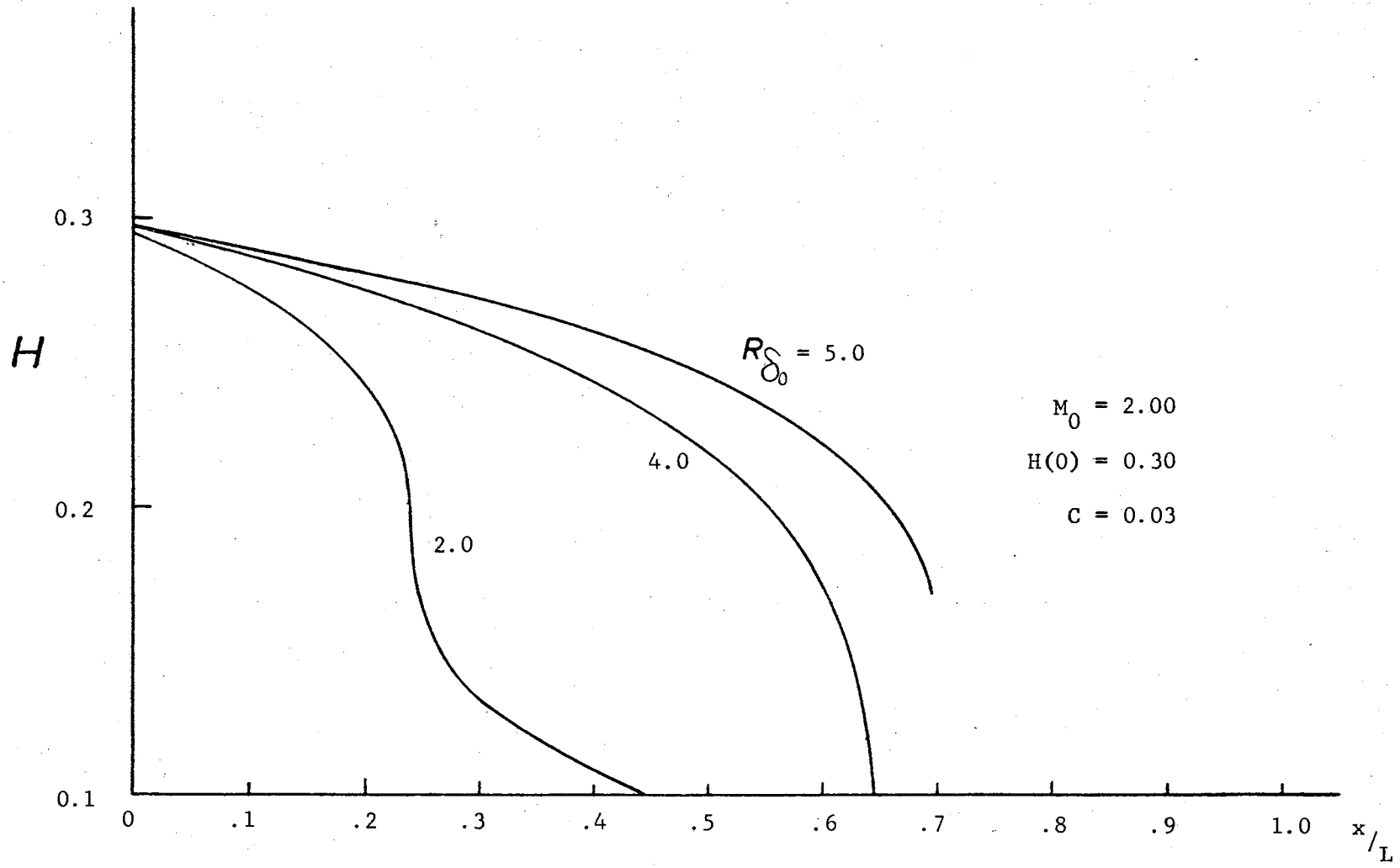

Fig. 15. Effect of R_{δ_0} on the Interface Velocity Ratio

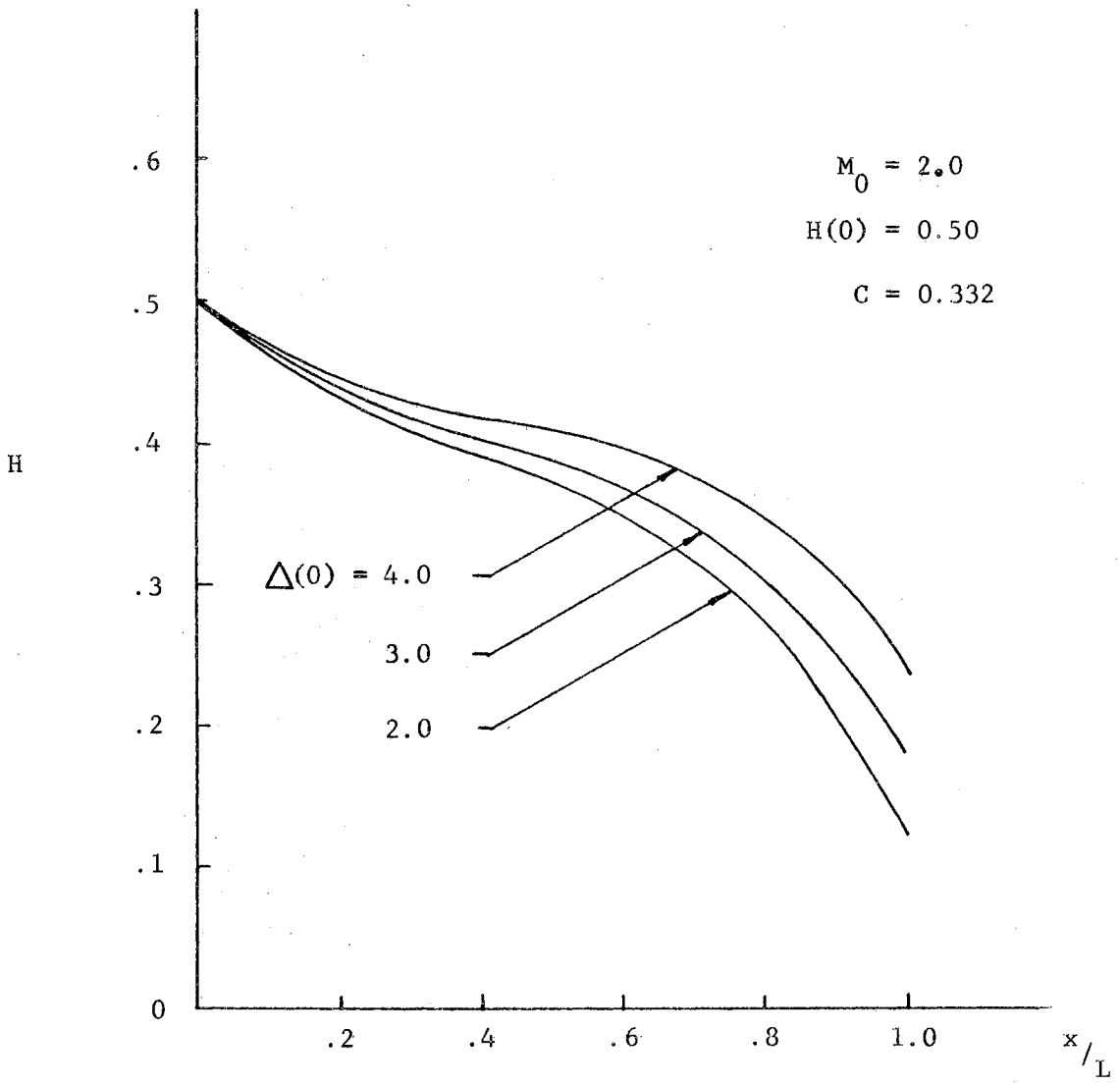

Fig. 16. Effect of $\Delta(0)$ on H(x)

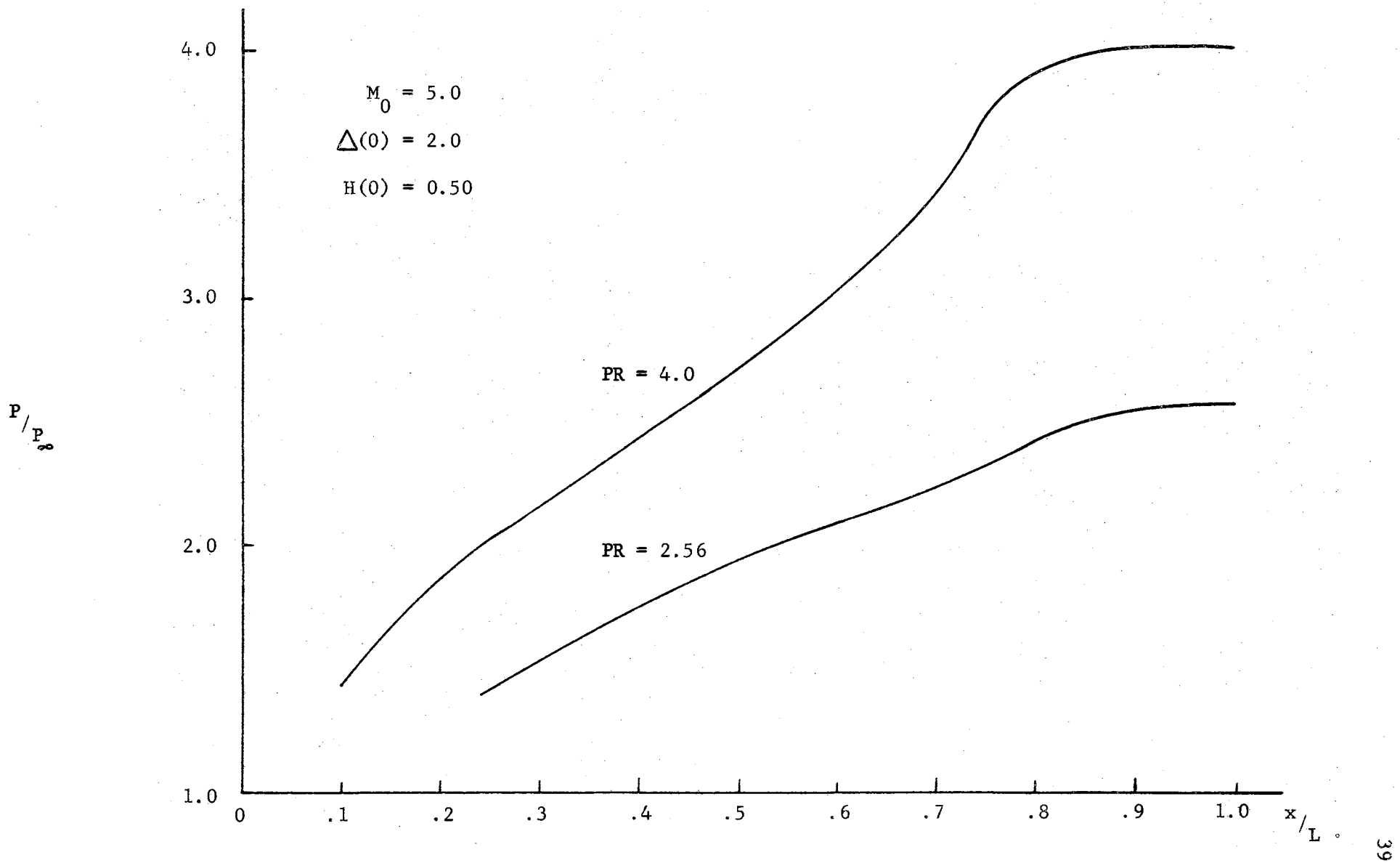

Fig. 17. Variation of Surface Pressure with Shock Strength

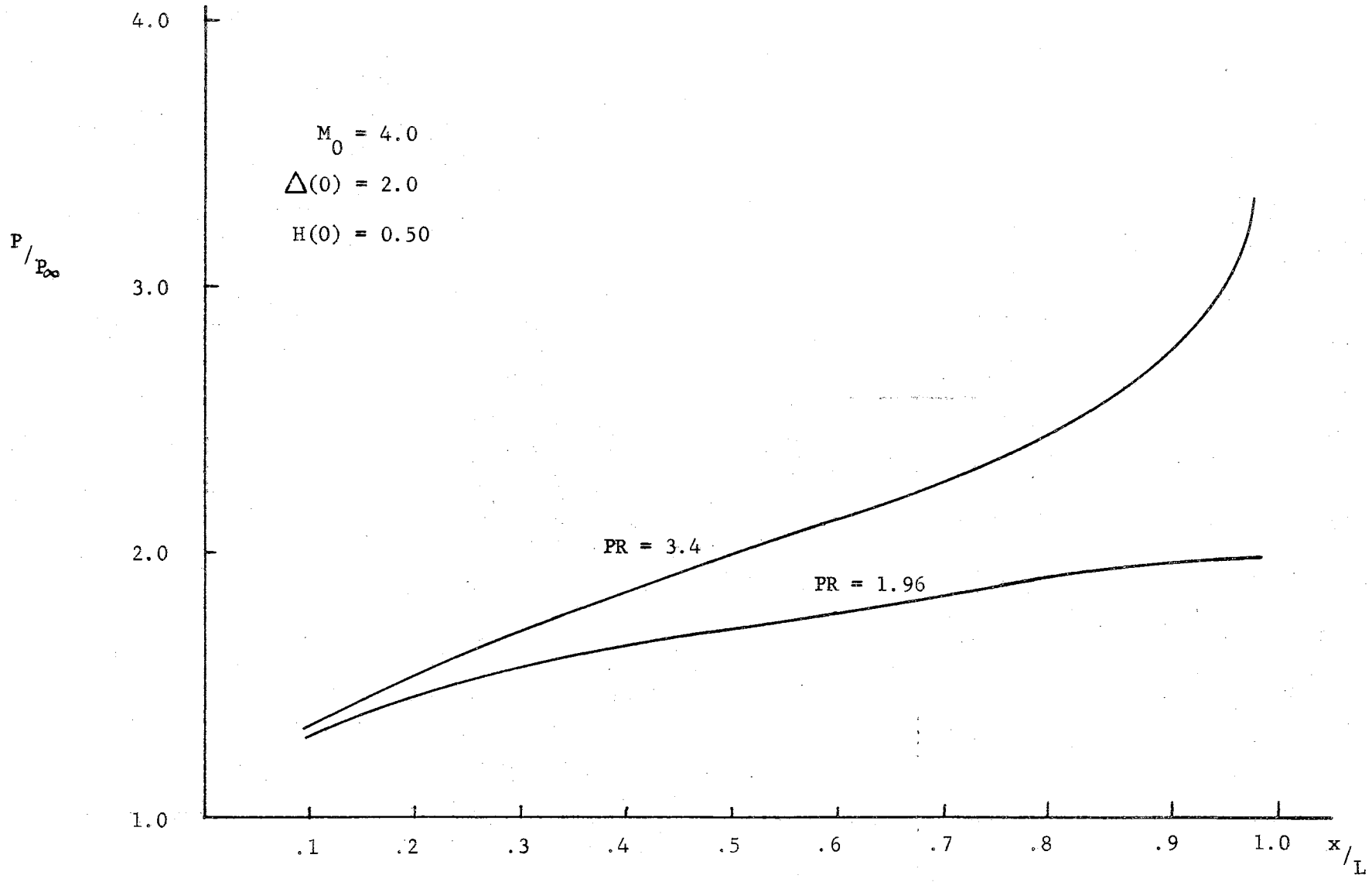

Fig. 18. Variation of Surface Pressure with Shock Strength

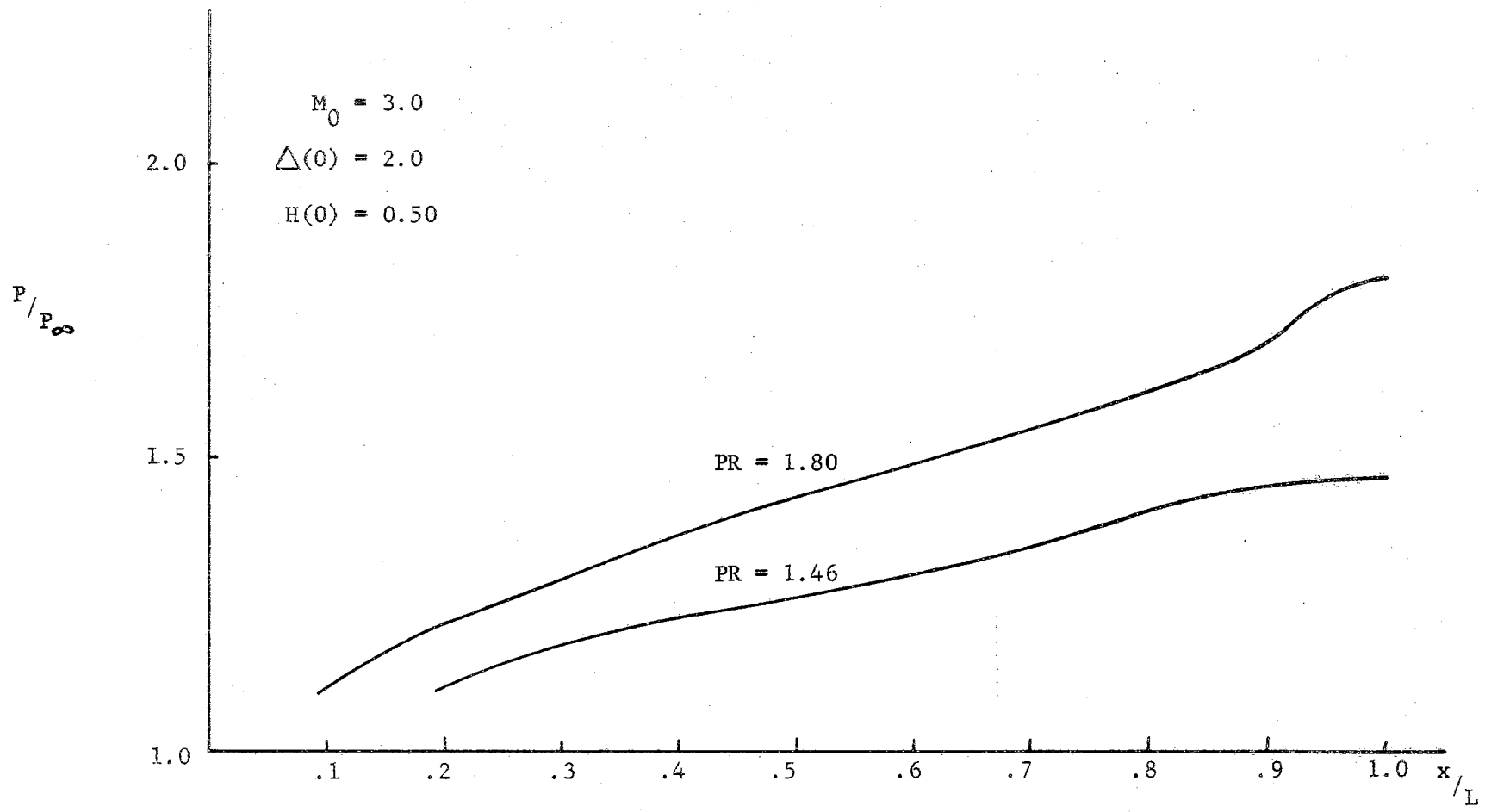

Fig. 19. Variation of Surface Pressure with Shock Strength

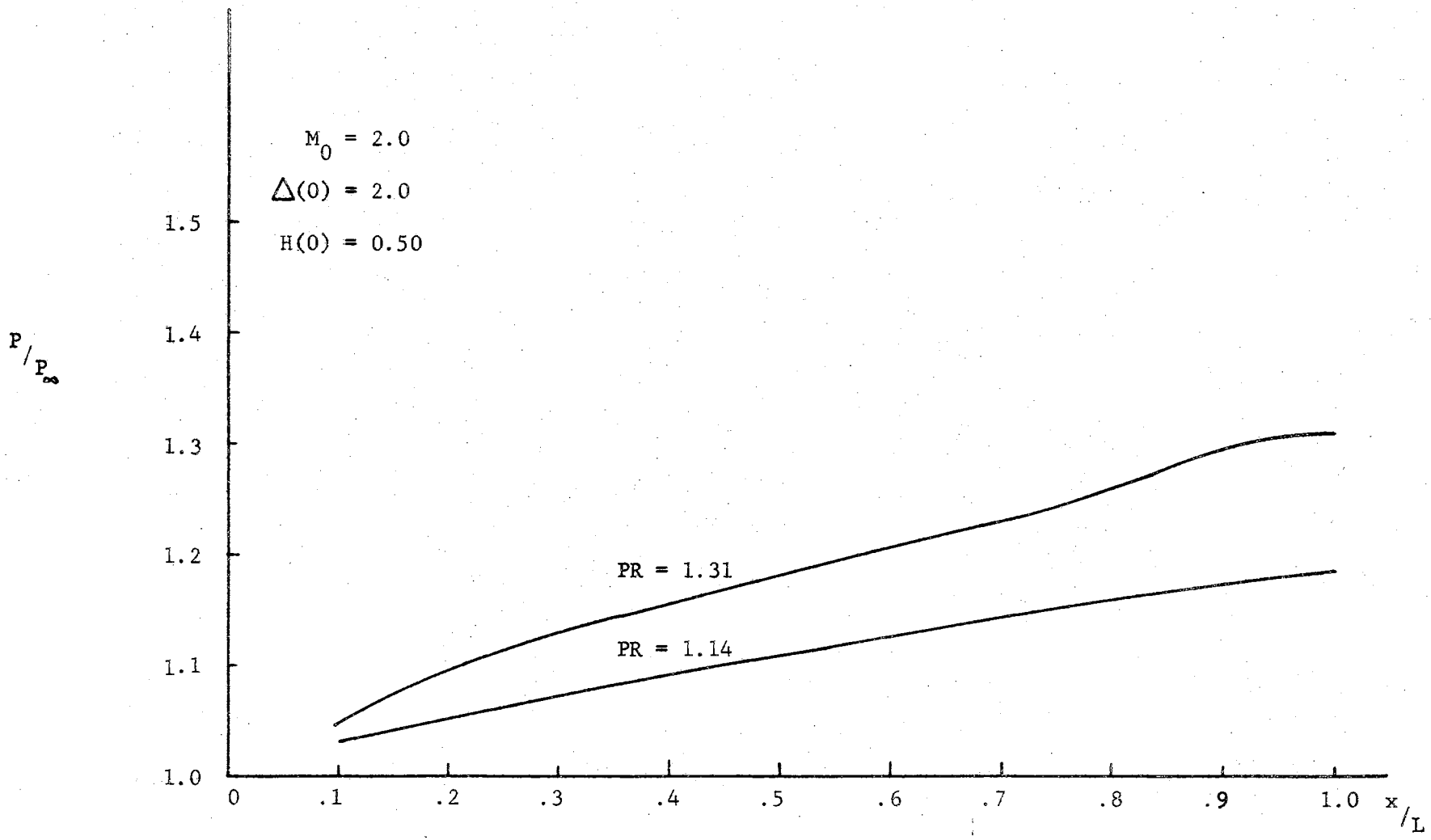

Fig. 20. Variation of Surface Pressure with Shock Strength

the gas layer pushes the latter upwards. This changes the pattern of the compressive waves which originate at the boundary layer edge and maintain the equilibrium between the viscous and the inviscid layers. This in turn changes the rate of increase of the surface pressure. The fluid layer grows thicker and faster than the gas layer since it consists mainly of a subsonic flow region. This growth of $\Delta_1(x)$, and the effect of $R\delta_0$ on it, is shown in Figure (21) for a case where separation did not occur. As expected, the high $R\delta_0$ corresponded to the thinner $\Delta_1(x)$.

Figure (22) shows a typical variation of $\Delta_1(x)$ and $\Delta(x)$ for a case where the boundary layer separates. The variation of Δ_1 for $x/_L$ 1.0 is physically unrealistic. From continuity considerations, the fluid in the first layer cannot disappear and thus Δ_1 cannot go to zero. Therefore, the solution should not be considered as representing a real case for $x/_L > 1.0$.

Figure (23) shows a critical case where separation takes place because the injected fluid velocity was not high enough to eliminate separation. This particular case was also investigated for higher $R\delta_0$, Figure (24), and as mentioned before, the result was to delay separation and cause the boundary layer thicknesses to grow smoothly.

Figure (25) shows a typical case for high Mach numbers and high shock strength. The boundary layer thicknesses grow sharply near the shock impingement point. The boundary layer did not separate due to the high velocity of flow.

Velocity Profiles

Figures (26,27 and 28) show the different velocity profiles which are obtained for different values of H, C and δ_1/δ. It is seen that

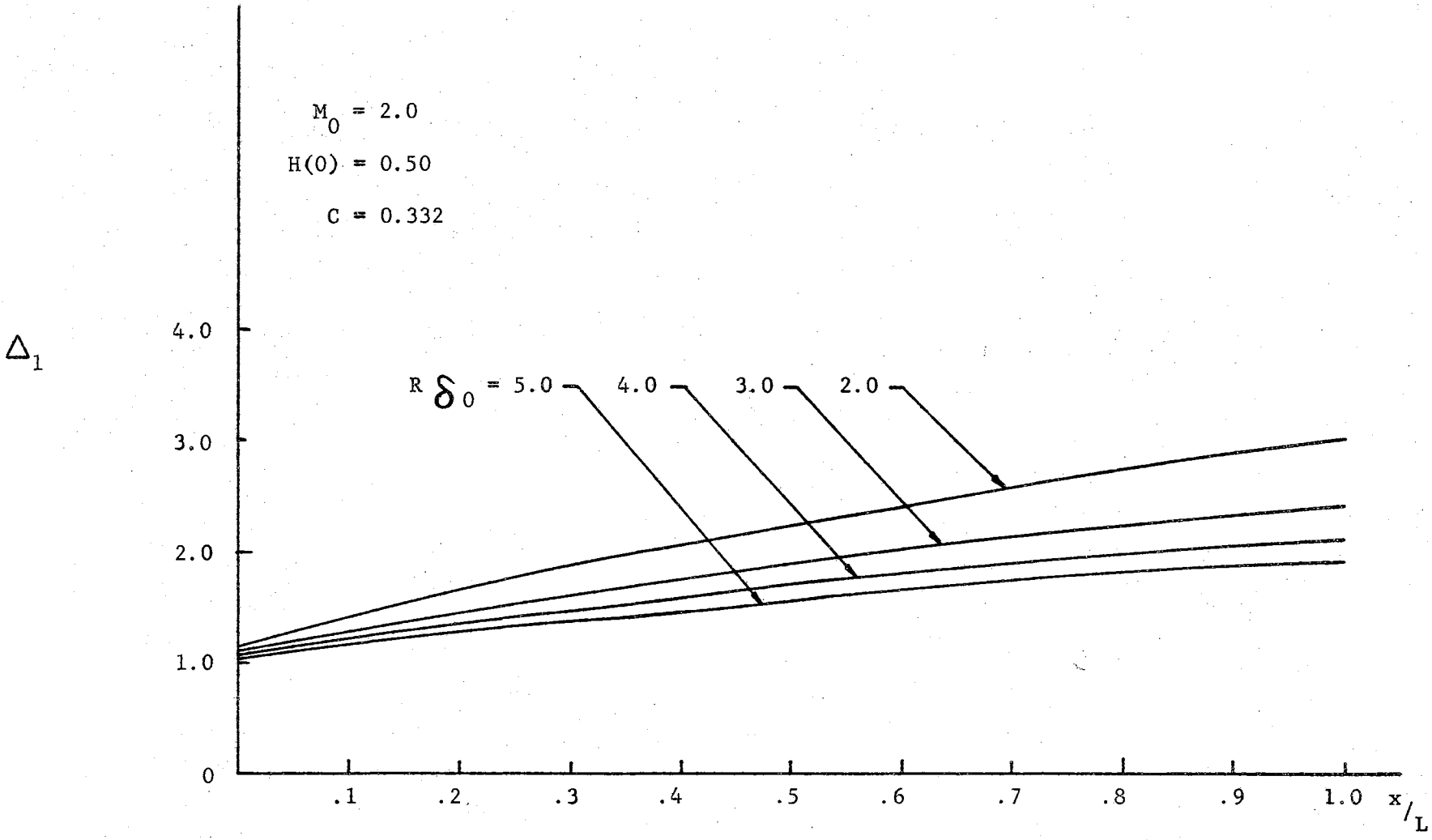

Fig. 21. Effect of R δ_0 on the Growth of Δ_1

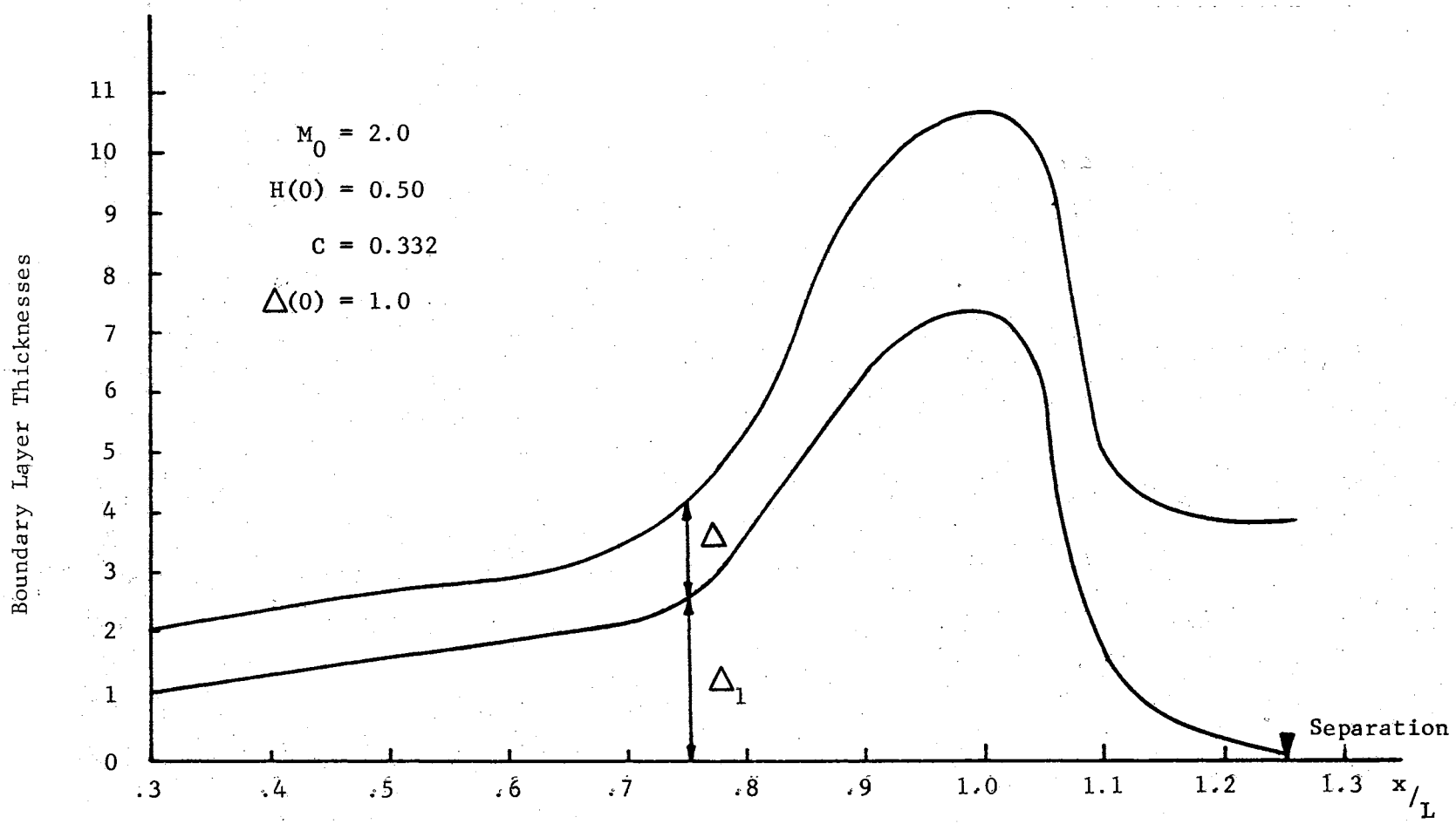

Fig. 22. Typical Variation of Δ and Δ_1 for a Separated B. L.

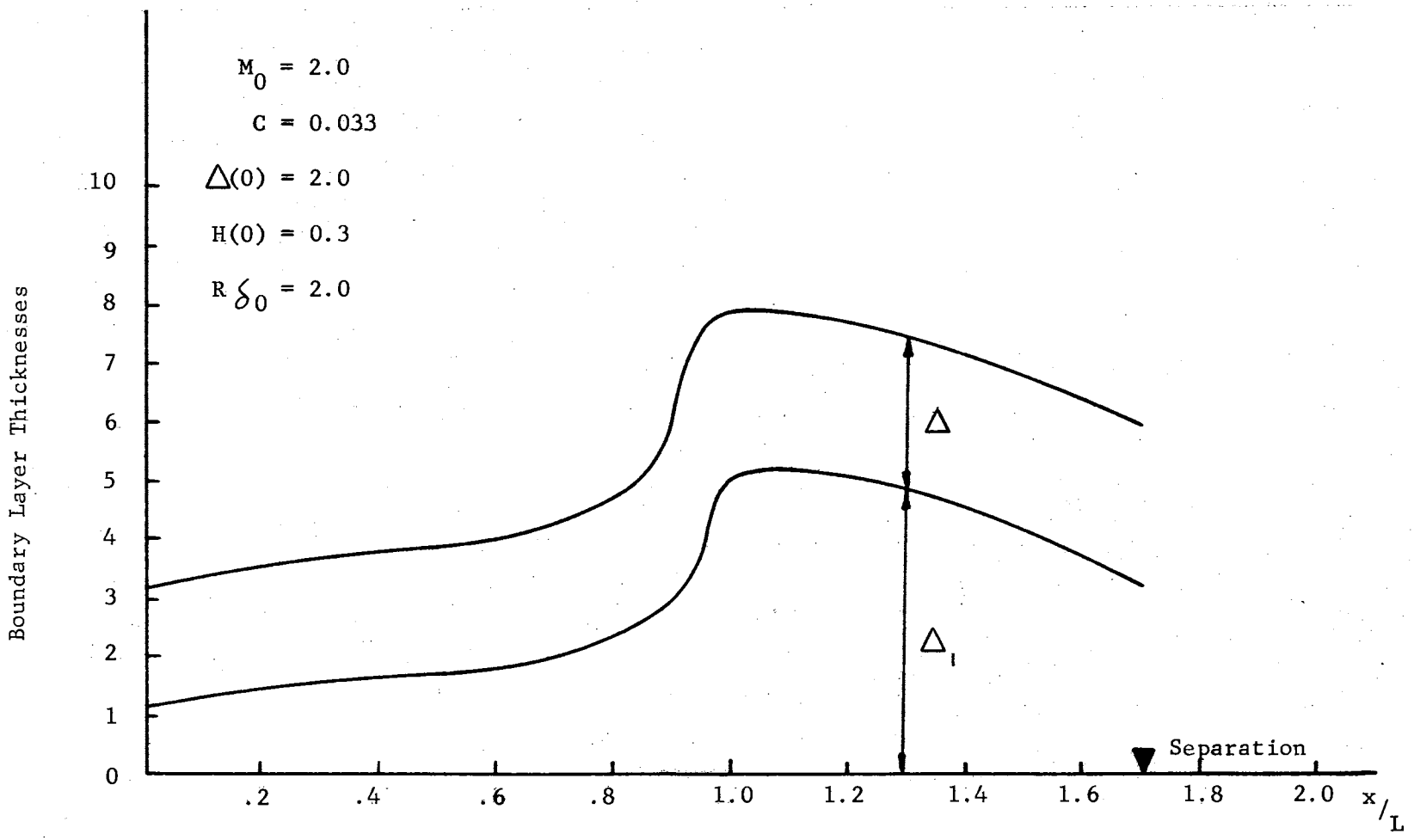

Fig. 23. Separated B. L. for Small H(0)

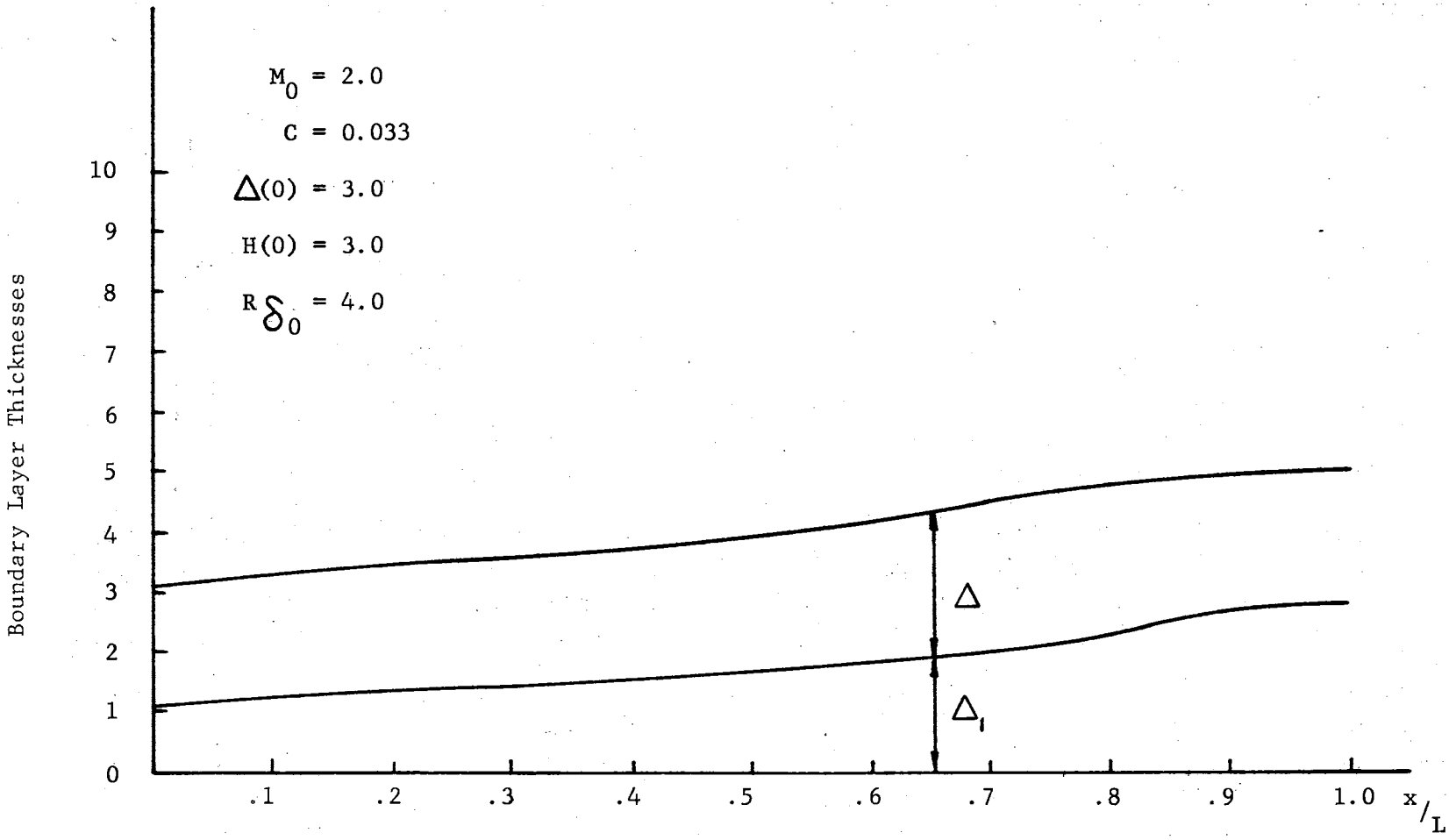

Fig. 24. Effect of $R\delta_0$ in Delay in Separation

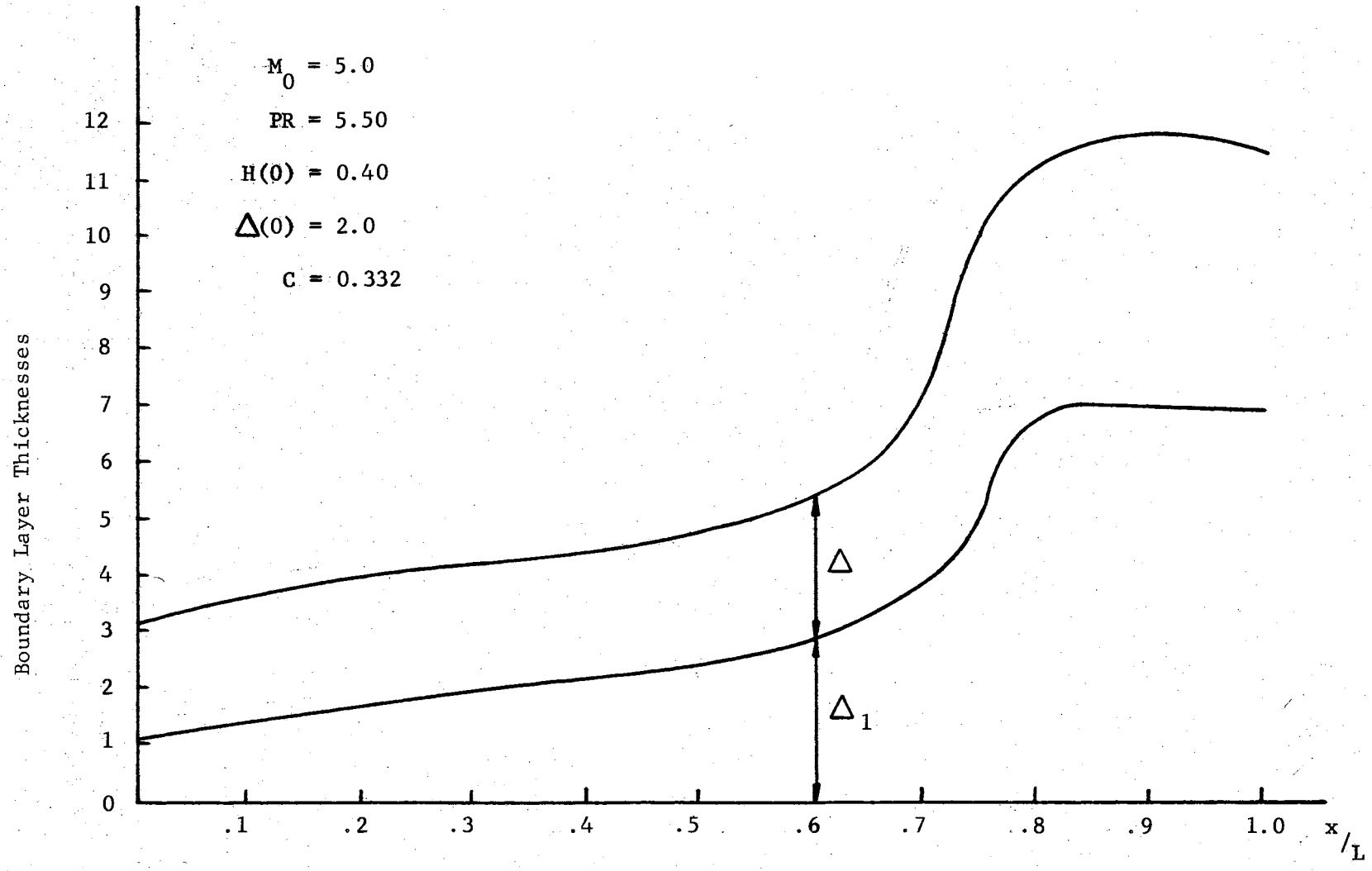

Fig. 25. Typical Variation of Δ and Δ_1 for a Non-Separated B. L. at High M_0

the profiles allow for various geometrical properties to occur such as negative velocity gradients at the wall and inflexion points. The effect of H(x) is the most influential on the velocity profile and the velocity gradient at the wall which is proportional to the shear stress. The effect of C is seen to be small, Figure (28). For the same values of C and H(x), it is seen that the effect of δ_1/δ is also pronounced, Figure (27). The velocity gradient at the wall is changed by stretching or shrinking the thickness δ_1 .

Numerical Technique

Figure (11) shows the effect of using different increments, $\Delta x/_L$; in the step-by-step numerical integration. Most of the results were obtained using $\Delta x/_L = 0.02$. When $\Delta x/_L = 0.04$ and 0.01 the results varied between $\pm$ 5 percent. However, the trend did not change.

When $\Delta x/_L = 0.05$ and C = 0.332 the behavior of the shear stress was unrealistic. While the boundary layer thickness increased and the surface pressure did not change very much; the shear stress dropped and then increased sharply at $x/_L = 0.5$. This behavior was due to the lack of convergence and this anomaly was eliminated by using smaller increments of $\Delta x/_L$.

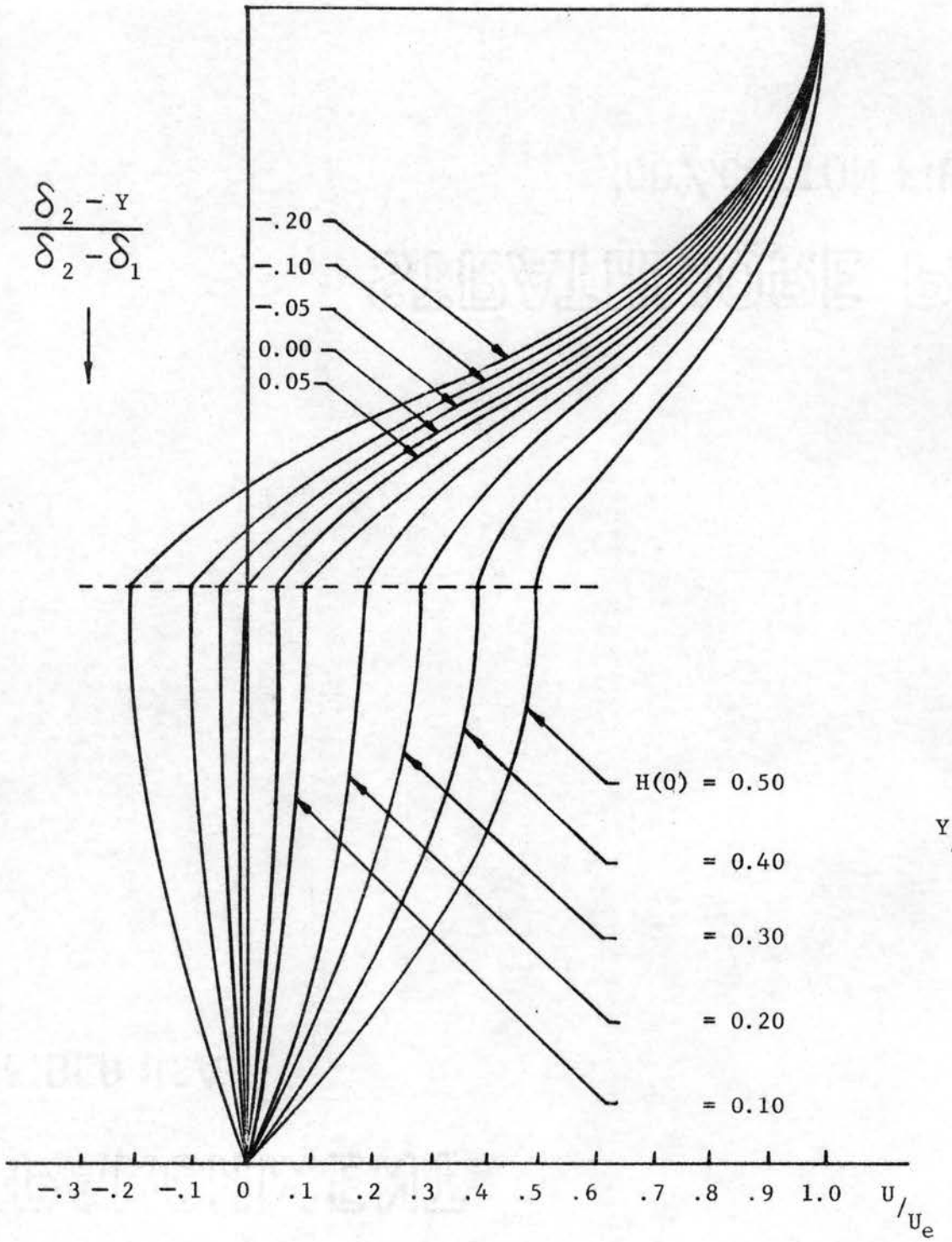

Fig. 26. Effect of H(x) on the Velocity Profiles

$C = 0.01$, $\delta_1/\delta = 1.0$

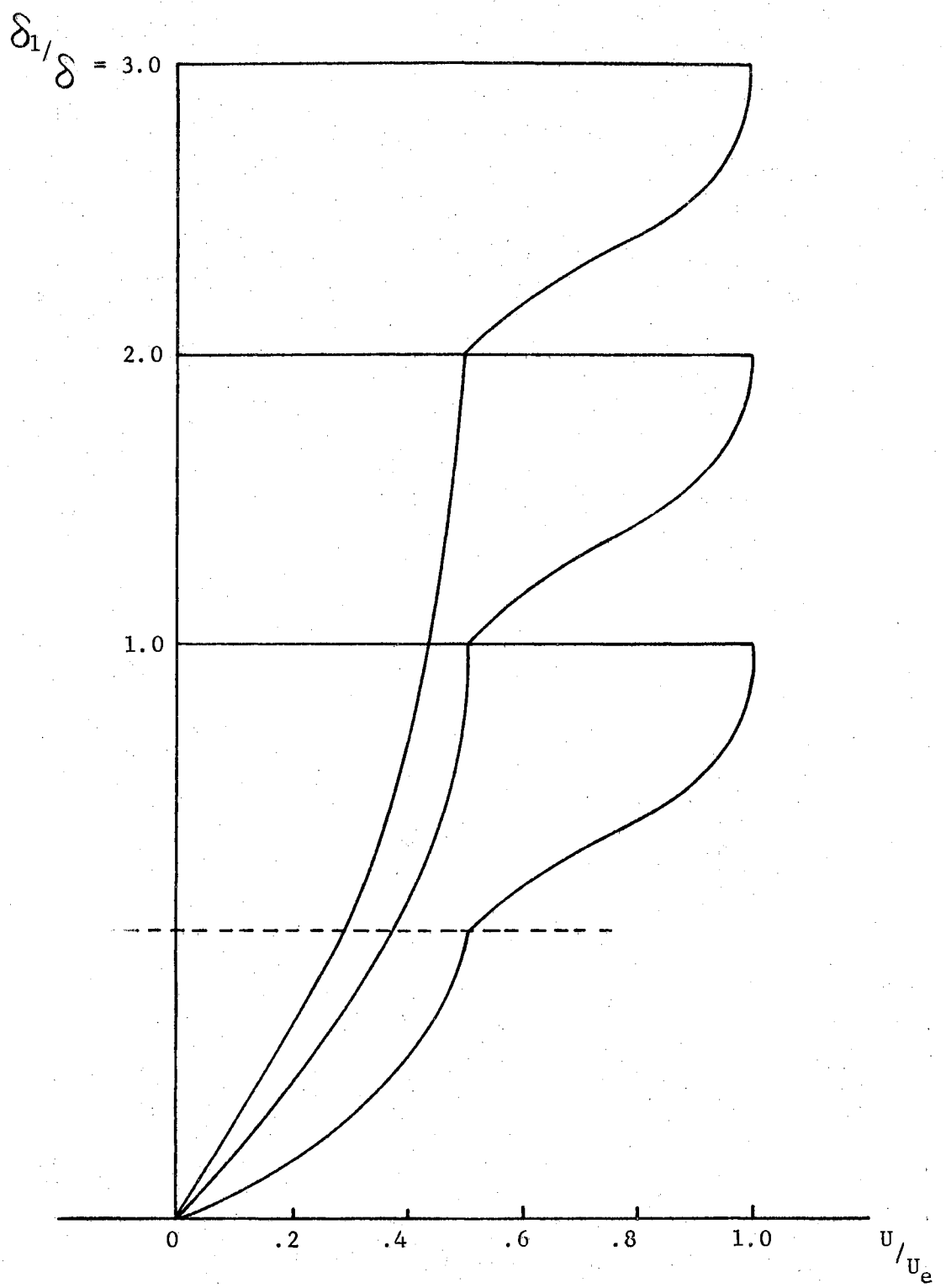

Fig. 27. Velocity Profiles at Locations Indicated by δ_1/δ

H = 0.5 , C = 0.01

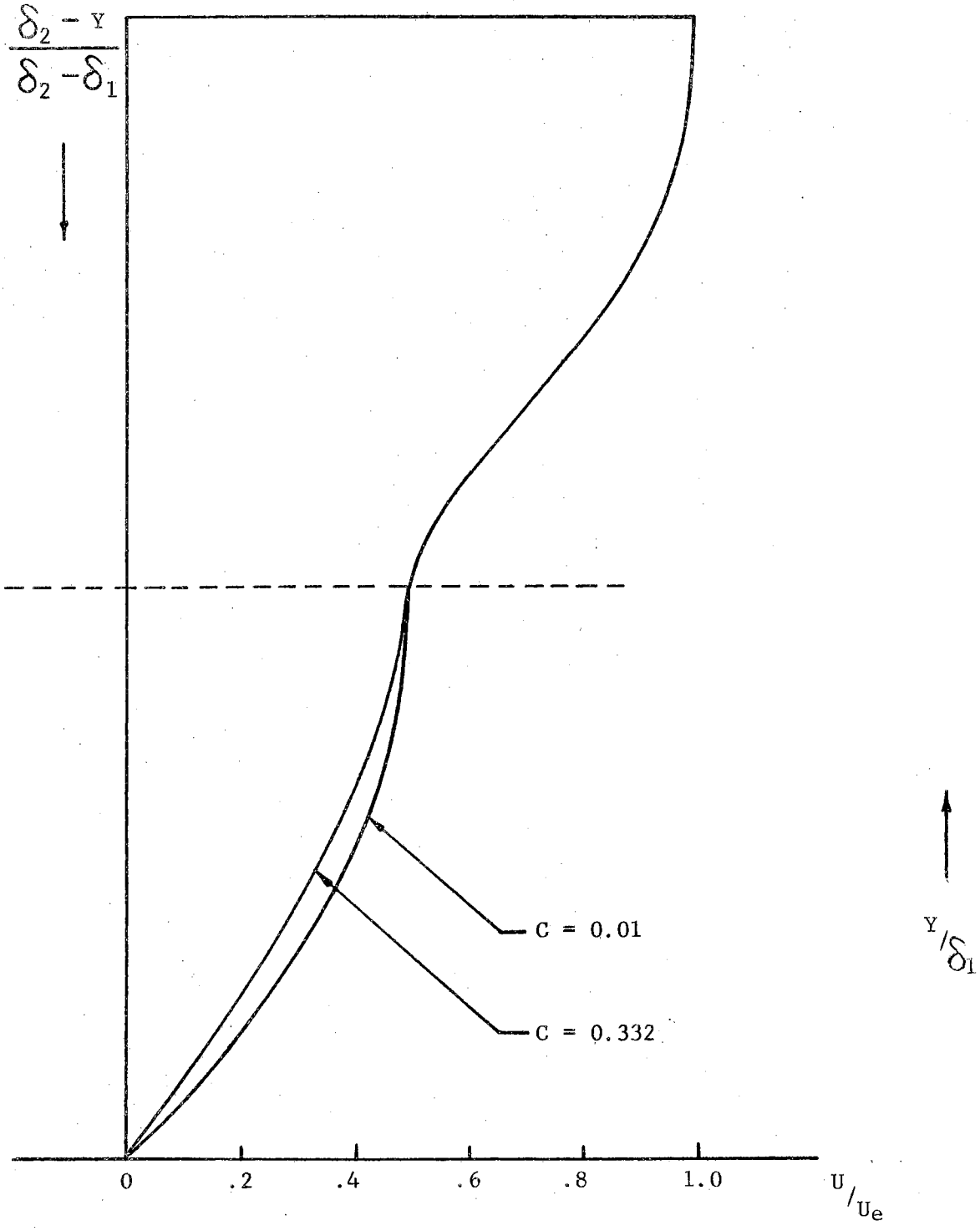

Fig. 28. Effect of C on the Velocity Profile

$H = 0.5$, $\delta_1/\delta = 1.0$

CHAPTER V

CONCLUSIONS

The current theoretical investigation has shown that separation of laminar boundary layers caused by the interaction of the boundary layer and an incident oblique shock wave can be delayed, and in some cases eliminated. The method utilizes a tangential injection of a second fluid through a slot contained within the boundary layer.

One of the assumptions utilized in the analysis ignores the evaporation of the injected fluid when it is in the form of a liquid. However, this should not minimize the importance of the findings. The injected fluids are usually liquid; however, gases could be used instead. In the latter case one has to pause and question the assumption of no mixing between the fluids in the two layers. This overall criticism may limit the applicability of this method to liquid injection where evaporation effects are not great.

In addition, the method and results are of academic value. The solution should be considered as the first attempt towards solving the complete problem of shock wave-boundary layer interaction with heat transfer and possibly chemical reaction. More complicated geometries can also be considered.

It was mentioned earlier that in "free interaction" problems the solution for the case of no injection is the same whether the shock strikes the boundary layer or emanates from within the flow geometry.

In the present study, the case of a shock wave forming from within the flow geometry (a forward facing step) does not have the same solution as in the case of an incident oblique shock on the boundary layer. This is because the injected fluid would accumulate and cause trouble at the corner of the step. Unless some means is introduced to suck away this accumulated fluid, the boundary layer will separate when the accumulated fluid pushes up the gas layer and mixes with the flowing gas.

SELECTED BIBLIOGRAPHY

1. Lees, L. and Reeves, B. L., "Supersonic Separated and Reattaching Laminar Flows," GALCIT 574, Part I, 1963.

2. Bray, K. N., Gadd, G. E. and Woodger, M., "Some Calculations by the Crocco-Lees and Other Methods of Interactions Between Shock Waves and Laminar Boundary Layers, Including Effects of Heat Transfer and Suction," Aeronautical Research Council, Report 21, 834, FM 2937, 1960.

3. Crocco, L. and Lees, L., "A Mixing Theory for the Interaction Between Dissipative Flows and Nearly Isentropic Streams," Journal of the Aerospace Sciences, Vol. 19, No. 10, 1952, pp. 649-676.

4. Ackeret, J., Feldmann, F. and Rott, N., "Investigations of Compression Shocks and Boundary Layers in Gases Moving at High Speed," Translated as NACA TM 1113, 1947.

5. Liepmann, H. W., "The Interaction Between Boundary Layer and Shock Waves in Transonic Flow," Journal of the Aerospace Sciences, Vol. 13, No. 12, 1946, pp. 623-637.

6. Oswatitsch, K. and Wieghardt, K., "Theoretical Analysis of Stationary Potential Flows and Boundary Layers at High Speeds," Translated as NACA TN No. 1189, 1948.

7. Lees, L., "Interaction Between the Laminar Boundary Layer over a Plate Surface and an Incident Oblique Shock Wave," Princeton University, Aeronautical Engineering Laboratory, Report No. 143, 1949.

8. Gadd, G. E., "Boundary Layer Separation in the Presence of Heat Transfer," AGARD Report No. 280, 1960.

9. Curle, N., "The Effects of Heat Transfer on Laminar-Boundary-Layer Separation in Supersonic Flow," The Aeronautical Quarterly, Vol. XII, 1961, pp. 309-336.

10. Honda, M., "A Theoretical Investigation of the Interaction Between Shock Waves and Boundary Layers," Journal of the Aerospace Sciences, Vol. 25, No. 11, 1958, pp. 667-678.

11. Abbot, D. E., Holt, M. and Nielsen, J. N., "Investigation of Hypersonic Flow Separation and Its Effects on Aerodynamic Control Characteristics," Vidya Report No. 81, 1962.

See also, "Studies of Separated Laminar Boundary Layers at Hypersonic Speed with Some Low Reynolds Number Data," Paper No. 63-172, presented at the AIAA Summer Meeting, Los Angeles, California, 1963.

12. Glick, H. S., "Modified Crocco-Lees Mixing Theory for Supersonic Separated and Reattaching Flows," GALCIT, Hypersonic Research Project, Memorandum No. 53, 1960. See also, Journal of the Aerospace Sciences, Vol. 29, No. 10, 1962, pp. 1238-1244.

13. Thwaites, B., "Approximate Calculation of the Laminar Boundary Layer," The Aeronautical Quarterly, Vol. 1, 1949, pp. 245-280.

14. Rott, N. and Crabtree, L. F., "Simplified Laminar Boundary Layer Calculations for Bodies of Revolution and for Yawed Wings," Journal of the Aeronautical Sciences, Vol. 19, No. 8, 1952, pp. 553-565.

15. Sutton, W. G., "An Approximate Solution of the Boundary Layer Equations for a Flat Plate," Philosophical Magazine, Vol. 23, 1937, pp. 1146-1152.

16. Walz, A., "Anwendung des Energiesatzes von Wieghardt anf Einparametrige Geschwindig Keitsprofile in Laminaren Grenzschichten," Ingenieur-Archiv, Vol. 16, 1948, pp. 243-248.

17. Tani, L., "On the Approximate Solution of the Laminar Boundary Layer Equations," Journal of the Aerospace Sciences, Vol. 21, No. 7, 1954, pp. 487-504.

18. Lees, L. and Reeves, B. L., "Some Remarks on Integral Moment Methods for Laminar Boundary Layers with Application to Separation and Reattachment," GALCIT, Separated Flows Research Project, Report No. 1, AFOSR Report No. 1920, 1961.

19. Wieghardt, K., "Uber Einen Energiesatz zur Berechnung Laminarer Grenzschichten," Ingenieur-Archiv, Vol. 16, Nos. 3 and 4, 1948, pp. 231-242.

20. Makofski, R., "A Two-Parameter Method for Shock Wave-Laminar Boundary Layer Interaction and Flow Separation," Proceedings of the 1963 Heat Transfer and Fluid Mechanics Institute, 1963, pp. 112-127.

21. Stewartson, K., "Correlated Incompressible and Compressible Boundary Layers," Proceedings of the Royal Society of London (A), Vol. 200, No. 10, No. 1060, 1949, pp. 84-100.

22. Cohen, C. B. and Reshotko, E., "Similar Solutions for the Compressible Laminar Boundary Layer with Heat Transfer and Pressure Gradient," NACA Report 1293, 1956.

23. Sellers, J. P., Jr., "Experimental and Theoretical Study of the Application of Film-Cooling to a Cylinderical Rocket Thrust Chamber," Ph. D. Thesis - Purdue University, 1958.

24. Knuth, E. L. "A Study of the Mechanics of Liquid Films as Applied to Film Cooling," JPL-CIT, Progress Report No. 1-79, 1951

25. Emmons, D. L., "Effects of Selected Gas Stream Parameters and Coolant Physical Properties on Film Cooling of Rocket Motors," JPL, Purdue University, Report No. TM-62-5, 1962.

26. Warner, C. F. and Reese, B. A., "Investigation of the Factors Affecting the Attachment of a Liquid Film to a Solid Surface," JPL, Purdue University, 1957.

ADDITIONAL REFERENCES*

27. Prandtl, L., "Zur Berechnung der Grenzschichten," Zeit. Angew., Math. U. Mech., Vol. 18, No. 1, 1936, pp. 77-82.

28. Lees, L., "On the Boundary Layer Equations in Hypersonic Flow and Their Approximate Solutions," Journal of the Aeronautical Sciences, Vol. 20, No. 2, 1953, pp. 143-145.

29. Hayes, W. D. and Probstein, R. F., Hypersonic Flow Theory, especially Chapter IX, Academic Press, New York, 1959.

30. Chapman, D. R., Kuehn, D. M. and Larson, H. K., "Investigation of Separated Flows in Supersonic and Subsonic Streams with Emphasis on the Effect of Transition," NACA Report 1356, 1958.

31. Curle, N., "The Effects of Heat Transfer on Laminar-Boundary-Layer Separation in Supersonic Flow," The Aeronautical Quarterly, Vol. XII, 1961, pp. 309-336.

32. Hakkinen, R. J., Greber, I., Trilling, L. and Abarbanel, S. S., "The Interaction of an Oblique Shock Wave with a Laminar Boundary Layer," NASA, Memorandum 2-18-59 W, 1959.

33. Oswatitsch, K., "Die Ablösungs Bedingung von Grengschichten," Symposium on Boundary Layer Research, Freiburg/Br., 1957, H. Gortler, Ed., Springer-Verlag, 1958, pp. 357-367.

34. Crocco, L., "Considerations on the Shock-Boundary Layer Interaction," Proceedings of Conference on High-Speed Aeronautics, Polytechnique Institute of Brooklyn, 1955, pp. 75-112.

35. Crocco, L. and Probstein, R. F., "The Peak Pressure Rise Across an Oblique Shock Emerging from a Tubrulent Boundary Layer Over a Plane Surface," Princeton University, Aeronautical Engineering Department, Report No. 254, 1954.

---

* Those references which helped in understanding the problem, but were not referred to directly in the text.

36. Rott, N. and Crabtree, L. F., "Simplified Laminar Boundary Layer Calculations for Bodies of Revolution and for Yawed Wings," Journal of the Aeronautical Sciences, Vol. 19, No. 8, 1952, pp. 553-565.

37. Martellucci, A. and Libby, P. A., "Heat Transfer Due to the Interaction Between a Swept Planar Shock Wave and a Laminar Boundary Layer," Proceedings of the USAF ASD Symposium on Aeroclasticity, Dayton, Ohio, 1960. See also, Technical Report ASD-TR-61-727, Vol. II, 1962.

38. Wieghardt, K., "Uber Einen Engergiesatz zur Berechnung Laminarer Grenzschichten," Ingenieur-Archiv, Vol. 16, Nos. 3 and 4, 1948, pp. 231-242.

39. Chapman, D. R., "Laminar Mixing of a Compressible Fluid," NACA Report 958, 1959.

40. Savage, S. B., "The Effect of Heat Transfer on Separation of Laminar Compressible Boundary Layers," GALCIT, Separated Flows Research Project, Report No. 2, 1962.

41. Sterrett, J. R. and Emery, J. C., "Extension of Boundary-Layer Separation Criteria to a Mach Number of 6.5 by Utilizing Flat Plates with Forward-Facing Steps," NASA TN D-618, 1960.

42. Lankford, J. L., "The Effect of Heat Transfer on the Separation of Laminar Flow over Axisymmetric Compression Surfaces," NAVWEPS Report No. 7402, 1961.

43. Gadd, G. E., Holder, D. W. and Regan, J. D., "An Experimental Investigation of the Interaction Between Shock Waves and Boundary Layers," Proceedings of Royal Society of London (A), Vol. 226, No. 1165, 1954, pp. 227-253.

44. Fage, A. and Sargent, R. F., "Shock-Wave and Boundary-Layer Phenomena near a Flat Surface," Proceedings of Royal Society of London (A), Vol. 190, No. 1020, 1947, pp. 1-20.

APPENDIX A

VELOCITY PROFILES AND INITIAL CONDITIONS

Velocity Profiles

The velocity profiles assumed are of the form

$$q_1 = A_0 + A_1\eta_1 + A_2\eta_1^2 \qquad \text{(A-1)}$$

$$q_2 = B_0 + B_1\eta_2 + B_2\eta_2^2 + B_3\eta_2^3 + B_4\eta_2^4 \qquad \text{(A-2)}$$

where,

$$\eta_1 = y/\delta_1 \quad ; \quad \eta_2 = (\delta_2 - y) / (\delta_2 - \delta_1) = (\delta_2 - y)/\delta$$

Boundary Conditions

$$\eta_1 = 0 \ (y = 0) \quad ; \quad q_1 = 0 \qquad \text{(i)}$$

$$\eta_1 = \eta_2 = 1 (y = \delta_1) \quad ; \quad q_1 = q_2 = H(x) \qquad \text{(ii,iii)}$$

$$\frac{\mu_1}{\delta_1}\frac{\partial q_1}{\partial \eta_1} = -\frac{\mu_2}{\delta}\frac{\partial q_2}{\partial \eta_2} \qquad \text{(iv)}$$

$$\eta_2 = 0 \ (y = \delta_2) \quad ; \quad q_2 = 1.0 \qquad \text{(v)}$$

$$\frac{\partial q_2}{\partial \eta_2} = \frac{\partial^2 q_2}{\partial \eta_2^2} = 0 \qquad \text{(vi,vii)}$$

These are seven conditions. The eighth condition is specified by noticing that the flow field in the gas layer is to be continuous as the gas flows over the flat plate and past the injection slot. This will be explained after determining some of the eight unknowns.

From B. C. (i,vi and vii), one obtains

$$A_0 = B_1 = B_2 = 0$$

and from B. C. (ii)

$$A_1 + A_2 = H \tag{A-3}$$

It is possible now to rewrite q_2, without any loss of generality and in accordance with B. C. (iii), in the form

$$q_2 = H + (1 - H)\,(B_0^{\,1} + B_3^{\,1}\,\eta_2^{\,3} + B_4^{\,1}\,\eta_2^{\,4}), \tag{A-4}$$

so that upstream of the injection point, when $H(x) = 0$, the velocity profile in the gas layer becomes

$$q_2 = B_0^{\,1} + B_3^{\,1}\,\eta_2^{\,3} + B_4^{\,1}\,\eta_2^{\,4}\ . \tag{A-5}$$

From B. C. (V), one obtains

$$B_0^{\,1} = 1.0\ .$$

Now, we can specify the eighth boundary condition by utilizing the result obtained by Blasius for the flow over flat plates. Namely,

$$\frac{\tau_0 \delta}{\mu_2 U_e} = -\frac{\partial q_2}{\partial \eta_2} = 0.332 \tag{viii}$$

or,

$$3B_3^{\,1} + 4B_4^{\,1} = -\ 0.332\ . \tag{A-6}$$

Also from B. C. (iii)

$$1 + B_3^{\,1} + B_4^{\,1} = 0\ . \tag{A-7}$$

From (A-6) and (A-7), one obtains

$$B_3^1 = -3.67$$

$$B_4^1 = 2.67 \quad .$$

Therefore,

$$q_2 = H + (1 - H)(1 - 3.67\,\eta_2^3 + 2.67\,\eta_2^4) \quad . \qquad \text{(A-8)}$$

From B. C. (iv)

$$\frac{\mu_1}{\delta_1}(A_1 + 2A_2) = 0.332\,\frac{\mu_2}{\delta}(1 - H)$$

or,

$$A_1 + 2A_2 = 0.332\,\frac{\mu_2}{\mu_1}\,\frac{\delta_1}{\delta}(1 - H) \quad . \qquad \text{(A-9)}$$

From (A-3) and (A-9) it follows that

$$A_2 = -H + 0.332\,\frac{\mu_2}{\mu_1}\,\frac{\delta_1}{\delta}(1 - H) \quad . \qquad \text{(A-10)}$$

Later on the R. H. S. of (A-10) will be denoted by F. Therefore, one writes

$$A_1 = H - F \quad \text{and} \quad q_1 = H\eta_1 - F\eta_1 + F\eta_1^2 \quad . \qquad \text{(A-11)}$$

From (A-8) and (A-11) it is possible now to write δ_*, θ, θ_* and θ_{**} noting that for any function f(y),

$$\int_0^{\delta_2} f(y)dy = \delta_1 \int_0^1 f(\eta_1)d\eta_1 + \delta \int_0^1 f(\eta_2)d\eta_2 \quad .$$

The results are as follows:

$$\Delta_* = \delta_*/\delta_0 = \frac{1}{\delta_0}\int_0^{\delta_2} (1-q)\,dy$$

$$= \Delta_1(1 - .5H + .167F) + \Delta(.38 - .38H)$$

$$\Theta = \theta/\delta_0 = \frac{1}{\delta_0}\int_0^{\delta_2} q(1-q)\,dy$$

$$= \Delta_1(.5H - .167F + .167HF - .033F^2 - .33H^2)$$

$$+ \Delta(.16H - .27H^2 + .11)$$

$$\Theta_* = \theta_*/\delta_0 = \frac{1}{\delta_0}\int_0^{\delta_2} q(1-q^2)\,dy$$

$$= \Delta_1(.5H - .167F - .85HF^2 - .55H^2F - .25H^3$$

$$+ .825F^3) + \Delta(0.05 + .89H - 1.17H^2 - 0.23H^3$$

$$\Theta_{**} = \frac{\theta_{**}}{\delta_0} = \frac{1}{\delta_0}\int_0^{\delta_2} q(1-q^3)\,dy$$

$$= \Delta_1(.5H - .17F + .34HF^3 + .13H^3F - .2H^4)$$

$$+ \Delta(.88 - 2.94H + 6.0H^2 - 5.56H^3 - 3.34H^4)$$

Differentiating the above relations w.r.t.x., and substituting into equations (10,11 and 12) then grouping similar terms, one obtains equations (17,18 and 19), where

$$S_1 = A_2 + \Delta_{20}\, T_1$$

$$S_1 = B_2 + \Delta_{20}\, T_2$$

$$S_3 = C_2 + \Delta_{20}\, T_3$$

$$S_4 = 2\tilde{\Theta} + \Delta_*$$

$$S_5 = (H - F) \,/\, (\Delta_1\, R\delta_0)$$

$$P_1 = A_3 + D_{30}\, T_1$$

$$P_2 = B_3 + D_{30}\, T_2$$

$$P_3 = C_3 + D_{30}\, T_3$$

$$P_4 = 3\,\textcircled{\sim}_{*}$$

$$P_5 = (2H^2 + 0.67F^2)/(\Delta_1 R\delta_0) + (2.8 - 5.6H + 2.8H^2)\,(\Delta R\delta_0)$$

$$H_1 = A_4 + D_{40}\, T_1$$

$$H_2 = B_4 + D_{40}\, T_2$$

$$H_9 = C_4 + D_{40}\, T_3$$

$$H_{10} = (4\,\textcircled{\sim}_{**} - 3\,\textcircled{\sim})$$

$$H_{11} = (3H^3 + .96HF^2 + .96H^2F) \,/\, (\Delta_1 R\delta_0) + (5.6 - 7.8H - .6H^2 - 3H^3) \,/\, (\Delta R\delta_0)$$

and

$$T_1 = C\,(1 - H) \,/\, \Delta$$

$$T_2 = -\,C\,(1 - H)\,\Delta_1 \,/\, \Delta^2$$

$$T_3 = -\,1 - C\,\Delta_1 \,/\, \Delta$$

$$C = 0.332\,\mu_2 \,/\, \mu_1$$

$$\Delta_{10} = \Delta_1\,(0.167)$$

$$\Delta_{20} = \Delta_1\,(-.167 + .167H - .067F)$$

$$\Delta_{30} = \Delta_1\,(-.167 + 1.7HF - .55H^2 + 2.48F^2)$$

$$\Delta_{40} = \Delta_1\,(-.167 + HF^2 + .13H^3)$$

$$A_2 = .5H - .167F + .167HF - .033F^2 - .33H^2$$

$$B_2 = .16H - .27H^2 + .11$$

$$C_2 = \Delta_1 (-.167 + .167H - .067F) + (.16 - .54H)$$

$$A_3 = .5H - .167F - .85HF^2 - .55H^2F - .25H^3 + .825F^3$$

$$B_3 = 0.05 + 0.89H - 1.17H^2 - 0.23H^3$$

$$C_3 = \Delta_1 (.5 - .85F^2 - 1.1HF - .75H^2) + \Delta (.87 - 2.34H - .69H^2)$$

$$A_4 = .5H - .167F + .34HF^3 + .13H^3F - .2H^4$$

$$B_4 = .88 - 2.94H + 6.0H^2 - 5.56H^3 - 3.34H^4$$

$$C_4 = \Delta_1 (.5 + .34F^3 + .39H^2F - .8H^3) + \Delta (-2.94 + 12H - 16.68H^2 - 13.36H^3)$$

$$R_{\delta_0} = \left(\frac{U_\infty \delta_0}{\nu_1}\right) \delta_0$$

Initial Conditions

The initial conditions at x/L = 0 are necessary to start the step-by-step integration of the differential equations. Some of them are chosen arbitrarily and some are determined from the flow conditions upstream of the region of interactions. The first group includes $\Delta(0)$ and H(0). The latter consists of

$$\frac{d\Delta_1}{dx}(0) = 0$$

since injection is tangential,

$$\frac{d\Delta}{dx}(0) = \frac{12.5}{R\delta_0 \Delta(0)}$$

since for $x/L < 0$, $\Delta = \frac{5\sqrt{x}}{\sqrt{R\delta_0}}$, (according to the theory of flow over a flat plate) and

$$VR(0) = 0$$

since $\frac{dp}{dx} = 0$ upstream of interaction.

This leaves out $\frac{dH}{dx}(0)$. Since the equations are valid at $x/L = 0$, $\frac{dH}{dx}(0)$ is determined from any differential equation by substituting the above mentioned conditions. This gives

$$\frac{dH}{dx}(0) = \frac{S_2(0)}{S_3(0)} - \frac{S_2(0)}{S_3(0)} \frac{d\Delta(0)}{dx}$$

A Note on the Choice of Parameters

It may seem to the reader that the problem is as easy as it may look. The fact that the problem is presented in the form of differential equations and initial conditions together with the two velocity profiles, tends to eliminate any imagination of the difficulty encountered in solving the problem. The reader should not be misled by that. Perhaps the most difficult part was the choice of the parameters and the independent variable. Many trials were completed, without success, before the present results were arrived at. Another difficulty encountered in the process of the step-by-step integration was that the wrong choice of parameter led the solution to blow up which appeared as error message in the computer work.

APPENDIX B

TRANSFORMATION OF THE ISENTROPIC EXPANSION RELATION

Application of the Stewartson transformation, Equation (1), to the definitions for δ_{*_c} and θ_c will result in (21)

$$\theta_c = \theta \frac{\rho_0 A_0}{\rho_e A_e} \tag{B-1}$$

$$\delta_{*_c}/\theta_c = \delta_*/\theta + \frac{\gamma - 1}{2} M_e^2 (\delta_*/\theta + 1) \tag{B-2}$$

The coupling equation (13) is transformed to

$$\frac{d}{dx}\left[\left(\frac{A_e P_e}{A_0 P_0}\right)\frac{d}{dx}\left(\frac{\rho_0 A_0}{\rho_e A_e}\right)\left\{\delta_* + \frac{\gamma - 1}{2} M_e^2 (\delta_* + \theta)\right\}\right] + \left(\frac{M_e^2 - 1}{M_e}\right)\frac{dM_e}{dx} = 0 . \tag{B-3}$$

Equation (B-3) is second-order and in order to unify the order of the equations to be solved, it is necessary to reduce the order from second to first. This is accomplished by utilizing a finite difference rule which is an approximation of Taylor's expansion.

$$\left.\frac{df}{dx}\right)_x = \left.\frac{\partial f}{\partial x}\right)_{x-\Delta x} + \Delta x \left.\frac{\partial^2 f}{\partial x^2}\right)_{x-\Delta x} \tag{B-4}$$

Applying Equation (B-4) to (B-3), one obtains

$$\left[\left(\frac{A_e P_e}{A_0 P_0}\right)\frac{d}{dx}\left(\frac{\rho_0 A_0}{\rho_e P_0}\right)\left\{\delta_* + \frac{\gamma - 1}{2} M_e^2 (\delta_* + \theta)\right\}\right]_{x-\Delta x} + \frac{(M_e^2 - 1)^{\frac{1}{2}}}{M_e}\frac{dM_e}{dx}\Delta x = \left[\left(\frac{A_e P_e}{A_0 P_0}\right)\frac{d}{dx}\left(\frac{\rho_0 A_0}{\rho_e A_e}\right)\left\{\delta_* + \frac{\gamma - 1}{2} M_e^2 (\delta_* + \theta)\right\}\right]_x . \tag{B-5}$$

For isentropic flow relations, for $\gamma = 1.4$

$$\frac{A_e P_e}{A_0 P_0} = (1 + 0.2M_e^2)^{-4}$$

$$\frac{\rho_0 A_0}{\rho_e A_e} = (1 + 0.2M_e^2)^3$$

Therefore, Equation (B-5) becomes

$$\frac{d\Delta_*}{dx} + \frac{0.2M_e^2}{(1 + 0.2M_e^2)} \frac{d\omega}{dx} + \left[\frac{1.6M_e^2}{(1 + .2M_e^2)} \Delta_* + \left\{ \frac{0.24M_e^4}{(1 + .2M_e^2)^2} + \frac{0.8M_e^2}{(1 + .2M_e^2)} \right\} \omega + \sqrt{M_e^2 - 1} \quad (\Delta x / \delta_0) \right] VR = G_0 \tag{B-6}$$

where

$$G_0 = \frac{d\Delta_*}{dx} + \frac{0.2M_e^2}{(1 + .2M_e^2)} \frac{d\omega}{dx} + \left[\frac{1.6M_e^2}{(1 + .2M_e^2)} \Delta_* + \left\{ \frac{.24M_e^4}{(1 + .2M_e^2)} + \frac{.8M_e^2}{(1 + .2M_e^2)} \right\} \omega \right] VR$$

at the position $(x - \Delta x)$.

Using the results of Appendix A, one can write Equation (B-6) in the form of Equation (20) where

$$D_1 = A_1 + D_{10} T_1 + \left(\frac{.2M_e^2}{1 + .2M_e^2} \right) S_1$$

$$D_2 = B_1 + D_{10}\, T_2 + \left(\frac{.2M_e^{\,2}}{1 + .2M_e^{\,2}}\right) S_2$$

$$D_3 = C_1 + D_{10}\, T_3 + \left(\frac{.2M_e^{\,2}}{1 + .2M_e^{\,2}}\right) S_3$$

$$D_4 = \left[\frac{1.6M_e^{\,2}}{(1 + .2M_e^{\,2})}\, \Delta_* + \left\{\frac{.24M_e^{\,4}}{(1 + .2M_e^{\,2})^2} + \frac{.8M_e^{\,2}}{(1 + .2M_e^{\,2})}\right\}\right.$$

$$\left. + (M_e^{\,2} - 1)^{\frac{1}{2}} \left(\frac{\Delta x}{\delta_0}\right)\right]$$

$$D_7 = G_0$$

$$A_1 = 1 - .5H + .167F$$

$$B_1 = .38 - .38H$$

$$C_1 = -.5\,\Delta_1 - .38\,\Delta$$

APPENDIX C

1410 IBM COMPUTER PROGRAM

```
C       SHOCK WAVE BOUNDARY LAYER INTERACTION WITH TANGENTIAL INJECTION
C       THE REGION OF INTERACTION
100     FORMAT(5F5.2,F6.2,3F5.2,F6.2,F7.4)
200     FORMAT(1X,5F5.2,F6.2,3F5.2,F6.2,F7.4)
300     FORMAT(F5.2,5F15.6)
1       READ(1,100)X0,H0,DEL10,DEL0,DEL1D0,Z,R,DX,XM,C,DELTA
        WRITE(3,200)X0,H0,DEL10,DEL0,DEL1D0,Z,R,DX,XM,C,DELTA
        X=X0
        H=H0
        G=0.
        VR1=0.
        DEL1=DEL10
        DEL=DEL0
        DEL1D=DEL1D0
        DELD=DEL0
        FZ=1.+0.2*Z
        Z1=SQRT(Z)
        F=-H-C*DEL1*(1.-H)/DEL
        T2=C*(1.-H)*DEL1/(DEL*DEL)
        T3=(C*DEL1/DEL)-1.
        B1=0.216-0.216*H
        B2=0.22*H-0.13*H*H-0.09
        C1=-0.5*DEL1-0.216*DEL
        C2=DEL1*(0.5+0.167*F-0.67*H)+DEL*(0.22-0.26*H)
        D10=0.167*DEL1
        D20=DEL1*(-0.167+0.167*H-0.067*F)
        S2=B2+D20*T2
        S3=C2+D20*T3
        S5=(H-F)/(DEL1*R)
        D2=B1+D10*T2+S2*(0.2*Z/FZ)
        D3=C1+D10*T3+S3*(0.2*Z/FZ)
        HD=(S5-S2*DELD)/S3
        FUN=D2*DELD+D3*HD
        PM=(Z-2.)/(2.8*Z)
5       F=-H-C*DEL1*(1.-H)/DEL
        X1=X-X0
        T1=-C*(1.-H)/DEL
        T2=C*(1.-H)*DEL1/(DEL*DEL)
        T3=(C*DEL1/DEL)-1.
        A1=1.-0.5*H+0.167*F
        B1=0.216-0.216*H
        C1=-0.5*DEL1-0.216*DEL
        D10=0.167*DEL1
        A2=0.5*H-0.167*F+0.167*H*F-0.033*F*F-0.33*H*H
        B2=0.22*H-0.13*H*H-0.09
        C2=DEL1*(0.5+0.167*F-0.67*H)+DEL*(0.22-0.26*H)
        D20=DEL1*(-0.167+0.167*H-0.067*F)
        A3=0.5*H-0.167*F-0.85*H*F*F-0.55*H*H*F-0.25*H*H*H+0.825*F*F*F
```

```
 B3=-5.06-8.87*H-7.2*H*H+6.3*H*H*H
 C3=DEL1*(0.5-0.85*F*F-1.1*H*F-0.75*H*H)
1+DEL*(-8.87-14.24*H+18.93*H*H)
 D30=-0.167-1.7*H*F-0.55*H*H+2.48*F*F
 A4=0.5*H-0.167*F+0.34*H*F*F*F+0.13*H*H*H*F-0.2*H*H*H*H
 B4=68.42+276.42*H-416.2*H*H-278.*H*H*H-69.9*H*H*H*H
 C4=DEL1*(0.5+0.34*F*F*F+0.39*H*H*F-0.8*H*H*H)
1+DEL*(-0.167+H*F*F+0.13*H*H*H)
 D40=DEL1*(-0.167+H*F*F+0.13*H*H*H)
 S1=A2+D20*T1
 S2=B2+D20*T2
 S3=C2+D20*T3
 THD=DEL1*(1.-0.5*H+0.167*F)+DEL*(0.216-0.216*H)
 THM=DEL1*(0.5*H-0.167*F+0.167*H*F-0.033*F*F-0.33*H*H)
1+DEL*(0.22*H-0.13*H*H-0.09)
 THE=DEL1*(0.5*H-0.167*F-0.85*H*F*F-0.55*F*H*H-0.25*H*H*H+0.825
1*F*F*F)+DEL*(-5.06-8.87*H-7.12*H*H+6.31*H*H*H)
 THEE=DEL1*(0.5*H-0.17*F+0.34*H*F*F*F+0.13*F*H*H*H-0.2*H*H*H*H)
1+DEL*(68.42+276.42*H-416.21*H*H-278.1*H*H*H-69.9*H*H*H*H)
 S4=2.*THM+THD
 S5=(H-F)/(DEL1*R)
 P1=A3+D30*T1
 P2=B3+D30*T2
 P3=C3+D30*T3
 P4=3.*THE
 P5=(2.*H*H+0.67*F*F)/(DEL1*R)+(2.8-5.6*H+2.8*H*H)/(DEL*R)
 H1=A4+D40*T1
 H2=B4+D40*T2
 H9=C4+D40*T3
 H10=4.*THEE-3.*THM
 H11=(3.*H*H*H+0.96*H*F*F+0.96*H*H*F)/(DEL1*R)
1+(7.2-13.2*H+4.8*H*H+1.2*H*H*H)/(DEL*R)
 D1=A1+D10*T1+S1*(0.2*Z/FZ)
 D2=B1+D10*T2+S2*(0.2*Z/FZ)
 D3=C1+D10*T3+S3*(0.2*Z/FZ)
 D4=(0.4*Z*(THM+THD)+Z1*(DX/DELTA))/FZ
 D7=FUN
 DET=S1*P2*H9*D4+S1*P3*H10*D2+S1*P4*H2*D3-S1*D2*H9*P4
1-S1*D3*H10*P2-S1*P3*D4*H2-S2*P1*H9*D4-S2*P3*H10*D1
2-S2*P4*H1*D3+S2*D1*H9*P4+S2*D3*H10*P1+S2*D4*P3*H1
3+S3*P1*H2*D4+S3*P2*H10*D1+S3*P4*H1*D2-S3*D1*H2*P4
4-S3*D2*H10*P1-S3*D4*P2*H1-S4*P1*H2*D3-D1*S4*P2*H9
5-S4*P3*H1*D2+S4*D1*H2*P3+S4*D2*H9*P1+S4*D3*H1*P2
 DET100 =S5*P2*H9*D4+S5*P3*H10*D2+S5*P4*H2*D3-S5*D2*H9*P4
1-S5*D3*H10*P2-S5*D4*H2*P3-S2*P5*H9*D4-S2*P3*H10*D7
2-S2*P4*H11*D3+S2*D7*H9*P4 +S2*D3*H10*P5+S2*D4*H11*P3
3+S3*P5*H2*D4+S3*P2*H10*D7+S3*P4*H11*D2-S3*D7*H2*P4
4-S3*D2*H10*P5-S3*D4*H11*P2-S4*P5*H2*D3-S4*P2*H9*D7
5-S4*P3*H11*D2+S4*D7*H2*P3+S4*D2*H9*P5+S4*D3*H11*P2
```

```
 DETDEL=S1*P5*H9*D4+S1*P3*H10*D7+S1*P4*H11*D3-S1*D7*H9*P4
1-S1*D3*H10*P5-S1*D4*H11*P3-S5*P1*H9*D4-S5*P3*H10*D1
2-S5*P4*H1*D3+S5*D1*H9*P4+S4*D3*H10*P1+S5*D4*H1*P3
3+S3*P1*H11*D4+S3*P5*H10*D1+S3*P4*H1*D7-S3*D1*H11*P4
4-S3*D7*H10*P1-S3*D4*H1*P5-S4*P1*H11*D3-S4*P5*H9*D1
5-S4*P3*H1*D7+S4*D1*H11*P3+S4*D7*H9*P1+S4*D3*H1*P5
 DETA=S1*P2*H11*D4+S1*P5*H10*D2+S1*P4*H2*D7-S1*D2*H11*P4
1-S1*D7*H10*P2-S1*D4*H2*P5-S2*P1*H11*D4-S2*P5*H10*D1
2-S2*P4*H1*D7+S2*D1*H11*P4+S2*H10*D7*P1+S2*D4*H1*P5
3+S5*P1*H2*D4+S5*P2*H10*D1+S5*P4*H1*D2-S5*D1*H2*P4
4-S5*D2*H10*P1-S5*D4*H1*P2-S4*P1*H2*D7-S4*P2*H11*D1
5-S4*P5*H1*D2+S4*D1*H2*P5+S4*D2*H11*P1+S4*D7*H1*P2
 DETB=S1*P2*H9*D7+S1*P3*H11*D2+S1*P5*H2*D3-S1*D2*H9*P5
1-S1*P2*D3*H11-S1*D7*H2*P3-S2*D7*H2*P3-S2*P3*H11*D1
2-S2*P5*H1*D2+S2*D1*H9*P5+S2*D2*H11*P1+S2*D7*H1*P3
3+S3*P1*H2*D7+S3*P2*H11*D1+S3*P5*H1*D2-S3*D1*H2*P5
4-S3*DI*H11*P1-S3*D7*H1*P2-S5*P1*H2*D3-S5*P2*H9*D1
5-S5*P3*H1*D2+S5*D1*H2*P3+S5*D2*H9*P1+S5*D3*H1*P2
 DEL1D=DET100/DET
 DELD=DETDEL/DET
 HD=DETA/DET
 VR=DETB/DET
 DEL1=DEL1+DX*DEL1D
 DEL=DEL+DX*DELD
 H=H+DX*HD
 FUN=D1*DEL1D+D2*DELD+D3*HD+D4*VR
 VR1=DETB/DET+VR1
 PR=1.-1.4*Z*DX*VR1
 B=H-F
 WRITE(3,300)X,DEL1,DEL,H,PR,B
 X=X+DX
 IF(X.LE.XM)GO TO 5
 GO TO 1
  END
```

APPENDIX D

TABLES OF RESULTS

TABLE I

EFFECT OF THE MACH NUMBER

$H(0) = 0.50$, $R\delta_0 = 2.0$, $C = 0.332$, $\delta_0 = 0.001$, $\Delta(0) = 2.0$

$M_0 = 2.0$, $PR = 1.20$

x/L	Δ_1	Δ	H	P/P_∞	$\frac{\tau_0 \delta_1}{\mu_1 U_e}$
0.0	1.1695	2.0415	.4904	1.0207	1.0904
.1	1.4549	2.1120	.4747	1.0543	1.0883
.2	1.6962	2.1699	.4618	1.0801	1.0868
.3	1.9080	2.2188	.4510	1.1007	1.0861
.4	2.0994	2.2620	.4415	1.1178	1.0858
.5	2.2768	2.3024	.4327	1.1329	1.0858
.6	2.4448	2.3421	.4244	1.1469	1.0854
.7	2.6069	2.3827	.4163	1.1602	1.0346
.8	2.7650	2.4251	.4082	1.1733	1.0832
.9	2.9210	2.4702	.4002	1.1862	1.0801
1.0	3.0758	2.5186	.3922	1.1992	1.0788

TABLE II

EFFECT OF THE MACH NUMBER

$H(0) = 0.50$, $R\delta_0 = 2.0$, $C = 0.332$, $\delta_0 = 0.001$, $\Delta(0) = 2.0$

$M_0 = 3.0$, $PR = 1.50$

x/L	Δ_1	Δ	H	P/P_∞	$\frac{\tau_0 \delta_1}{\mu_1 U_e}$
0.0	1.1709	2.0430	.4902	1.0487	1.0902
.1	1.4588	2.1162	.4740	1.1276	1.0873
.2	1.7024	2.1765	.4608	1.1887	1.0852
.3	1.9168	2.2277	.4497	1.2376	1.0841
.4	2.1110	2.2732	.4398	1.2788	1.0834
.5	2.2915	2.3160	.4308	1.3154	1.0829
.6	2.4631	2.3582	.4221	1.3495	1.0820
.7	2.6292	2.4015	.41372	1.3823	1.0808
.8	2.7919	2.4469	.4053	1.4144	1.0790
.9	2.9530	2.4951	.3969	1.4464	1.07665
1.0	3.1137	2.5470	.3887	1.4786	1.07365

TABLE III

EFFECT OF THE MACH NUMBER

$H(0) = 0.50$, $R_{\delta_0} = 2.0$, $C = 0.332$, $\delta_0 = 0.00.$, $\Delta(0) = 2.0$

$M_0 = 4.0$, PR = 2.00

x/L	Δ_1	Δ	H	P/P	$\frac{\tau_0 \delta_1}{\mu_1 U_e}$
0.0	1.1763	2.0490	.48915	1.0997	1.0891
.1	1.4736	2.1324	.4713	1.2607	1.0835
.2	1.7255	2.2012	.4570	1.3855	1.0795
.3	1.9475	2.2598	.4450	1.4859	1.0769
.4	2.1491	2.3122	.4344	1.5711	1.0750
.5	2.3378	2.3622	.4246	1.6479	1.0732
.6	2.5189	2.4124	.4152	1.7206	1.0712
.7	2.6960	2.4645	.4059	1.7915	1.0687
.8	2.8717	2.5199	.3967	1.8620	1.0656
.9	3.0482	2.5799	.3873	1.9332	1.0617
1.0	3.2275	2.6457	.3778	2.0059	1.0571

TABLE IV

EFFECT OF THE MACH NUMBER

$H(0) = 0.50$, $R_{\delta_0} = 2.0$, $C = 0.332$, $\delta_0 = 0.001$, $\Delta(0) = 2.0$

$M_0 = 5.0$, PR = 3.00

x/L	Δ_1	Δ	H	P/P_∞	$\frac{\zeta_0 \delta_1}{\mu_1 U_e}$
0.0	1.1836	2.0571	.4877	1.1832	1.0877
.1	1.4940	2.1545	.4677	1.4788	1.0783
.2	1.7577	2.2351	.4518	1.7074	1.0718
.3	1.9905	2.3039	.4386	1.8919	1.0672
.4	2.2032	2.3663	.4270	2.0506	1.0636
.5	2.4046	2.4270	.4162	2.1966	1.0602
.6	2.6013	2.4896	.4056	2.3381	1.0565
.7	2.7977	2.5566	.3950	2.4796	1.0520
.8	2.9970	2.6301	.3842	2.6241	1.0467
.9	3.2057	2.7131	.3730	2.7750	1.0402
1.0	3.4277	2.8098	.3611	2.9369	1.0323

TABLE V

EFFECT OF THE MACH NUMBER

$H(0) = 0.50$, $R\delta_0 = 2.0$, $C = 0.332$, $\delta_0 = 0.00$ $\Delta(0) = 2.0$

$M_0 = 4.0$, $PR = 2.23$

x/L	Δ_1	Δ	H	P/P_∞	$\frac{\tau_0 \delta_1}{\mu_1 U_e}$
0.0	1.1613	2.0388	.3921	1.0759	.9121
.1	1.4365	2.1043	.3786	1.1980	.9186
.2	1.6763	2.1613	.3666	1.2990	.9226
.3	1.8987	2.2164	.3551	1.3913	.9250
.4	2.1143	2.2736	.3435	1.4808	.9256
.5	2.3301	2.3355	.3315	1.5709	.9247
.6	2.5532	2.4052	.3187	1.6647	.9219
.7	2.7939	2.4882	.3045	1.7666	.9170
.8	3.0743	2.5965	.2875	1.8866	.9086
.9	3.4807	2.7783	.2626	2.0630	.8913
1.0	3.8640	2.9529	.2388	2.2297	.8733

TABLE VI

EFFECT OF THE MACH NUMBER

$H(0) = 0.50$, $R\delta_0 = 2.0$, $C = 0.332$, $\delta_0 = 0.001$, $\Delta(0) = 2.0$

$M_0 = 5.0$, $PR = 5.50$

x/L	Δ_1	Δ	H	P/P_∞	$\frac{\tau_0 \delta_1}{\mu_1 U_e}$
0.0	1.1689	2.0456	.3910	1.1413	.9110
.1	1.4577	2.1228	.3758	1.3692	.9150
.2	1.7117	2.1912	.3622	1.5605	.9169
.3	1.9517	2.2590	.3490	1.7394	.9170
.4	2.1909	2.3319	.3354	1.9180	.9152
.5	2.4408	2.4147	.3208	2.1055	.9112
.6	2.7195	2.5169	.3041	2.3158	.9043
.7	3.0796	2.6662	.2820	2.5899	.8914
.8	7.0542	4.7612	.0354	5.6764	.6536
.9	4.0195	4.7176	.0357	5.6421	.6441
1.0	6.9157	4.6596	.0346	5.4734	.6448

TABLE VII

EFFECT OF THE MACH NUMBER

$H(0) = 0.40$, $R\delta_0 = 2.0$, $C = 0.332$, $\quad_0 = 0.001$, $\Delta(0) = 2.0$

$M_0 = 2.0$, $PR = 1.20$

x/L	Δ_1	Δ	H	P/P_∞	$\frac{\tau_0 \delta_1}{\mu_1 U_e}$
0.0	1.1545	2.0327	.3931	1.0155	.9131
.1	1.4169	2.0869	.3813	1.0401	.9219
.2	1.6432	2.1331	.3709	1.0599	.9282
.3	1.8501	2.1766	.3609	1.0776	.9326
.4	2.0468	2.2208	.3511	1.0945	.9355
.5	2.2388	2.2675	.3410	1.1111	.9369
.6	2.4302	2.3183	.3305	1.1278	.9369
.7	2.6253	2.3751	.3195	1.1450	.9354
.8	2.8293	2.4410	.3076	1.1633	.9323
.9	3.0513	2.5211	.2944	1.1835	.9269
1.0	3.3104	2.6276	.2786	1.2075	.9179

TABLE VIII

EFFECT OF THE MACH NUMBER

$H(0) = 0.40$, $R\delta_0 = 2.0$, $C = 0.332$, $\delta_0 = 0.001$, $\Delta(0) = 2.0$

$M_0 = 3.0$, $PR = 1.50$

x/L	Δ_1	Δ	H	P/P_∞	$\frac{\tau_0 \delta_1}{\mu_1 U_e}$
0.0	1.1559	2.0340	.3929	1.0367	.9129
.1	1.4213	2.0908	.3807	1.0955	.9212
.2	1.6512	2.1398	.3698	1.1435	.9269
.3	1.8624	2.1864	.3595	1.1867	.93078
.4	1.9639	2.2099	.3543	1.2075	.9330
.5	2.2618	2.2842	.3386	1.2688	.9338
.6	2.4605	2.3390	.3275	1.3100	.9332
.7	2.6649	2.4008	.3158	1.3529	.9310
.8	2.8824	2.4733	.3030	1.3989	.9269
.9	3.1260	2.5643	.2884	1.4512	.9202
1.0	3.4322	2.6950	.2696	1.5179	.9083

TABLE IX

EFFECT OF THE SHOCK STRENGTH

$H(0) = 0.50$, $M_0 = 2.0$, $R\delta_0 = 2.0$, $C = 0.033$, $PR = 1.20$

x/L	Δ_1	Δ	H	P/P_∞	$\frac{\tau_0 \delta_1}{\mu_1 U_e}$
0.0	1.1589	2.0348	.4934	1.0189	1.0034
.1	1.4279	2.0936	.4826	1.0502	.9832
.2	1.6567	2.1413	.4737	1.0754	.9670
.3	1.8592	2.1806	.4663	1.0962	.9535
.4	2.0427	2.2134	.4599	1.1139	.9421
.5	2.2122	2.2413	.4542	1.1295	.9319
.6	2.3716	2.2657	.4489	1.1437	.9227
.7	2.5238	2.2874	.4439	1.1569	.9141
.8	2.6708	2.3071	.4390	1.1696	.9057
.9	2.8144	2.3253	.4343	1.1820	.8976
1.0	2.9559	.23442	.4295	1.1942	.8896

TABLE X

EFFECT OF THE SHOCK STRENGTH

$H(0) = 0.50$, $M_0 = 2.0$, $R\delta_0 = 2.0$, $C = 0.033$, $PR = 1.33$

x/L	Δ_1	Δ	H	P/P_∞	$\frac{\tau_0 \delta_1}{\mu_1 U_e}$
0.0	1.1589	2.0348	.4934	1.0189	1.0034
.1	1.6567	2.1413	.4737	1.0754	.9670
.2	2.0427	2.2134	.4599	1.1139	.9421
.3	2.3716	2.2657	.4489	1.1437	.9227
.4	2.6708	2.3071	.4390	1.1696	.9057
.5	2.9559	2.3442	.4295	1.1942	.8896
.6	3.2367	2.3719	.4201	1.2185	.8735
.7	3.5204	2.3966	.4104	1.2433	.8571
.8	3.8145	2.4153	.4002	1.2692	.8402
.9	4.1292	2.4265	.3894	1.2970	.8223
1.0	4.4812	2.4268	.3774	1.3281	.8029

TABLE XI

EFFECT OF THE SHOCK STRENGTH

$H(0) = 0.50$, $M_0 = 3.0$, $R\delta_0 = 2.0$, $C = 0.033$, $PR = 1.46$

x/L	Δ_1	Δ	H	P/P_∞	$\frac{\tau_0 \delta_1}{\mu_1 U_e}$
0.0	1.1603	2.0362	.4932	1.0445	1.0032
.1	1.4316	2.0974	.4820	1.1181	.9822
.2	1.6627	2.1473	.4728	1.1773	.9653
.3	1.8675	2.1887	.4651	1.2265	.9513
.4	2.0535	2.2235	.4584	1.2686	.9393
.5	2.2259	2.2536	.4524	1.3060	.9287
.6	2.3885	2.2801	.4469	1.3401	.9190
.7	2.5441	2.3041	.4416	1.3722	.9098
.8	2.6950	2.3216	.4365	1.4031	.90.0
.9	2.8429	2.3467	.4315	1.4334	.8923
1.0	2.9992	2.3659	.4265	1.4632	.8837

TABLE XII

EFFECT OF THE SHOCK STRENGTH

$H(0) = 0.50$, $M_0 = 3.0$, $R\delta_0 = 2.0$, $C = 0.033$, $PR = 1.80$

x/L	Δ_1	Δ	H	P/P_∞	$\frac{\tau_0 \delta_1}{\mu_1 U_e}$
0.0	1.1603	2.0362	.4932	1.0445	1.0032
.1	1.6627	2.1473	.4728	1.1773	.9653
.2	2.0535	2.2235	.4584	1.2686	.9393
.3	2.3885	2.2801	.4469	1.3401	.9190
.4	2.6950	2.3261	.4365	1.4031	.9010
.5	2.9992	2.3659	.4265	1.4632	.8837
.6	3.2811	2.4008	.4164	1.5231	.8666
.7	3.5890	2.4307	.4061	1.5844	.8490
.8	3.8922	2.4549	.3953	1.6490	.8308
.9	4.2346	2.4714	.3835	1.7195	.8113
1.0	4.6326	2.4763	.3701	1.8011	.7897

TABLE XIII

EFFECT OF THE SHOCK STRENGTH

$H(0) = 0.50$, $M_0 = 4.0$, $R\delta_0 = 2.0$, $C = 0.033$, $PR = 2.0$

x/L	Δ_1	Δ	H	P/P_∞	$\frac{\tau_0 \delta_1}{\mu_1 U_e}$
0.0	1.1654	2.0416	.4922	1.0911	1.0022
.1	1.4459	2.1120	.4795	1.2417	.9781
.2	1.6856	2.1696	.4692	1.3629	.9588
.3	1.8986	2.2175	.4606	1.4638	.9429
.4	2.0928	2.2581	.4531	1.5508	.9293
.5	2.2737	2.2935	.4464	1.6280	.9172
.6	2.4457	2.3251	.4401	1.7008	.9061
.7	2.6122	2.3541	.4340	1.7697	.8955
.8	2.7757	2.3813	.4281	1.8370	.8851
.9	2.9383	2.4069	.4222	1.9039	.8749
1.0	3.1018	2.4313	.4163	1.9712	.8646

TABLE XIV

EFFECT OF THE SHOCK STRENGTH

$H(0) = 0.50$, $M_0 = 4.0$, $R\delta_0 = 2.0$, $C = 0.033$, $PR = 3.3$

x/L	Δ_1	Δ	H	P/P_∞	$\frac{\tau_0 \delta_1}{\mu_1 U_e}$
0.0	1.1654	2.0416	.4922	1.0911	1.0022
.1	1.6856	2.1696	.4692	1.3629	.9588
.2	2.0928	2.2581	.4531	1.5508	.9293
.3	2.4457	2.3251	.4401	1.7008	.9061
.4	2.7757	2.3813	.4281	1.8370	.8851
.5	3.1018	2.4313	.4163	1.9712	.8646
.6	3.4389	2.4763	.4041	2.1099	.8436
.7	3.8044	2.5155	.3910	2.2600	.8213
.8	4.2318	2.5461	.37606	2.4344	.7963
.9	4.8282	2.5584	.3562	2.6739	.7646
1.0	6.4678	2.4685	.3069	3.3131	.6865

TABLE XV

EFFECT OF THE SHOCK STRENGTH

$H(0) = 0.50$, $M_0 = 5.0$, $R\delta_0 = 2.0$, $C = 0.033$, $PR = 2.87$

x/L	Δ_1	Δ	H	P/P_∞	$\frac{\tau_0 \delta_1}{\mu_1 U_e}$
0.0	1.1725	2.0489	.4910	1.1679	1.0010
.1	1.4659	2.1320	.4762	1.4449	.9725
.2	1.7179	2.2003	.4644	1.6681	.9501
.3	1.9429	2.2572	.4545	1.8546	.9316
.4	2.1495	2.3058	.4459	2.0167	.9158
.5	2.3441	2.3487	.4381	2.1642	.9016
.6	2.5322	2.3879	.4306	2.3039	.8883
.7	2.7182	2.4247	.4234	2.4410	.8754
.8	2.9060	2.4600	.4161	2.5789	.8626
.9	3.0993	2.4943	.4086	2.7206	.8495
1.0	3.3025	2.5276	.4008	2.8693	.8359

TABLE XVI

EFFECT OF THE SHOCK STRENGTH

$H(0) = 0.50$, $M_0 = 5.0$, $R\delta_0 = 2.0$, $C = 0.033$, $PR = 4.0$

x/L	Δ_1	Δ	H	P/P_∞	$\frac{\tau_0 \delta_1}{\mu_1 U_e}$
0.0	1.1725	2.0489	.4910	1.1679	1.0010
.1	1.5960	2.1678	.4700	1.5620	.9607
.2	1.9429	2.2572	.4545	1.8546	.9316
.3	2.2479	2.3278	.4419	2.0918	.9085
.4	2.5322	2.3879	.4306	2.3909	.8883
.5	2.8117	2.4425	.4197	2.5097	.8690
.6	3.0993	2.4943	.4086	2.7206	.8495
.7	3.4095	2.5440	.39674	2.9474	.8288
.8	3.7674	2.5918	.3833	3.2074	.8059
.9	4.2468	2.6370	.3659	3.5510	.7774
1.0			SEPARATION		

TABLE XVII

EFFECT OF THE REYNOLDS NUMBER

$H(0) = 0.50$, $M_0 = 2.0$, $C = 0.332$, $\delta_0 = 0.001$, $\Delta(0) = 2.0$

$R\delta_0 = 2.0$

x/L	Δ_1	Δ	H	P/P_∞	$\frac{\tau_0 \delta_1}{\mu_1 U_e}$
0.0	1.1126	2.0273	.4937	1.0136	1.0937
.1	1.3106	2.0745	.4083	1.0364	1.0924
.2	1.4830	2.1140	.4740	1.0546	1.0917
.3	1.6374	2.1479	.4662	1.0696	1.0916
.4	1.7785	2.1781	.4593	1.0824	1.0919
.5	1.9098	2.2060	.4530	1.0937	1.0923
.6	2.0338	2.2327	.4470	1.1040	1.0926
.7	2.1523	2.2591	.4413	1.1136	1.0928
.8	2.2666	2.2857	.4357	1.1229	1.0927
.9	2.3777	2.3129	.4303	1.1319	1.0924
1.0	2.4863	2.3410	.4249	1.1408	1.0918

TABLE XVIII

EFFECT OF THE REYNOLDS NUMBER

$H(0) = 0.50$, $M_0 = 2.0$, $C = 0.332$, $\delta_0 = 0.001$, $\Delta(0) = 2.0$

$R\delta_0 = 3.0$

x/L	Δ_1	Δ	H	P/P_∞	$\frac{\tau_0 \delta_1}{\mu_1 U_e}$
0.0	1.1126	2.0273	.4937	1.0136	1.0937
.1	1.3106	2.0745	.4830	1.0364	1.0924
.2	1.4830	2.1140	.4740	1.0546	1.0917
.3	1.6374	2.1479	.4662	1.0696	1.0916
.4	1.7785	2.1781	.4593	1.0824	1.0919
.5	1.9098	2.2060	.4530	1.0937	1.0923
.6	2.0338	2.2327	.4470	1.1040	1.0926
.7	2.1523	2.2591	.4413	1.1136	1.0928
.8	2.2666	2.2857	.4357	1.1229	1.0927
.9	2.3777	2.3129	.4303	1.1319	1.0924
1.0	2.4863	2.3410	.4249	1.1408	1.0918

TABLE XIX

EFFECT OF THE REYNOLDS NUMBER

$H(0) = 0.50$, $M_0 = 2.0$, $C = 0.332$, $\delta_0 = 0.001$, $\Delta(0) = 2.0$

$R\delta_0 = 4.0$

x/L	Δ_1	Δ	H	P/P_∞	$\frac{\tau_0 \delta_1}{\mu_1 U_e}$
0.0	1.0842	2.0202	.4953	1.0100	1.0953
.1	1.2358	2.0555	.4872	1.0272	1.0944
.2	1.3706	2.0855	.4803	1.0412	1.0941
.3	1.4931	2.1116	.4743	1.0531	1.0943
.4	1.6061	2.1350	.4688	1.0633	1.0947
.5	1.7119	2.1566	.4638	1.0724	1.0952
.6	1.8120	2.1773	.4591	1.0807	1.0957
.7	1.9077	2.1974	.4545	1.0885	1.0962
.8	1.9999	2.2174	.4502	1.0960	1.0965
.9	2.0893	2.2375	.4459	1.1032	1.0966
1.0	2.1762	2.2579	.4417	1.1101	1.0966

TABLE XX

EFFECT OF THE REYNOLDS NUMBER

$H(0) = 0.50$, $M_0 = 2.0$, $C = 0.332$, $\delta_0 = 0.001$, $\Delta(0) = 2.0$

$R\delta_0 = 5.0$

x/L	Δ_1	Δ	H	P/P_∞	$\frac{\tau_0 \delta_1}{\mu_1 U_e}$
0.0	1.0671	2.0159	.4963	1.0079	1.0963
.1	1.1899	2.0440	.4898	1.0216	1.0957
.2	1.3008	2.0681	.4842	1.0330	1.0956
.3	1.4026	2.0894	.4792	1.0427	1.0958
.4	1.4972	2.1085	.4747	1.0513	1.0963
.5	1.5863	2.1263	.4706	1.0589	1.0984
.6	1.6710	2.1433	.4666	1.0660	1.0974
.7	1.7521	2.1597	.4628	1.0726	1.0979
.8	1.8302	2.1760	.4592	1.0789	1.0984
.9	1.9059	2.1922	.4556	1.0849	1.0987
1.0	1.9794	2.2087	.4521	1.0908	1.0989

TABLE XXI

EFFECT OF THE REYNOLDS NUMBER

$H(0) = 0.4$, $M_0 = 2.0$, $C = 0.332$, $\delta_0 = 0.001$, $\Delta(0) = 2.0$

$R\delta_0 = 3.0$

x/L	Δ_1	Δ	H	P/P_∞	$\frac{\tau_0 \delta_1}{\mu_1 U_e}$
0.0	1.1024	2.0212	.3955	1.0101	.9155
.1	1.2835	2.0573	.3876	1.0268	.9217
.2	1.4442	2.0885	.38055	1.0409	.9268
.3	1.5922	2.1177	.3738	1.0535	.9310
.4	1.7320	2.1463	.3673	1.0653	.9342
.5	1.8664	2.1754	.3607	1.0768	.9367
.6	1.9972	2.2054	.3542	1.0879	.9384
.7	2.1256	2.2366	.3475	1.0990	.9394
.8	2.2529	2.2697	.3407	1.1100	.9398
.9	2.3801	2.3051	.3338	1.1211	.9396
1.0	2.5083	2.3434	.3267	1.1324	.9387

TABLE XXII

EFFECT OF THE REYNOLDS NUMBER

$H(0) = 0.4$, $M_0 = 2.0$, $C = 0.332$, $\delta_0 = 0.001$, $\Delta(0) = 2.0$

$R\delta_0 = 4.0$

x/L	Δ_1	Δ	H	P/P_∞	$\frac{\tau_0 \delta_1}{\mu_1 U_e}$
0.0	1.0763	2.0155	.3966	1.0074	.9166
.1	1.2146	2.0423	.3908	1.0200	.9215
.2	1.3398	2.0659	.3854	1.0309	.9258
.3	1.4562	2.0880	.38036	1.0408	.9294
.4	1.5665	2.1096	.3754	1.0501	.9325
.5	1.6723	2.1311	.3704	1.0590	.9350
.6	1.7748	2.1530	.3656	1.0677	.9370
.7	1.8747	2.1752	.3607	1.0677	.9370
.8	1.9726	2.1982	.3557	1.0846	.9398
.9	2.0691	2.2220	.3508	1.0928	.9406
1.0	2.1648	2.2469	.3458	1.1011	.9411

TABLE XXIII

EFFECT OF THE REYNOLDS NUMBER

$H(0) = 0.4$, $M_0 = 2.0$, $C = 0.332$, $\delta_0 = 0.001$, $\Delta(0) = 2.0$

$R\delta_0 = 5.0$

x/L	Δ_1	Δ	H	P/P_∞	$\frac{\tau_0 \delta_1}{\mu_1 U_e}$
0.0	1.0607	2.0120	.3974	1.0058	.9174
.1	1.1725	2.0333	.3927	1.0159	.9214
.2	1.2751	2.0522	.3884	1.0247	.9251
.3	1.3714	2.0701	.3843	1.0329	.9283
.4	1.4630	2.0874	.3803	1.0406	.9311
.5	1.5510	2.1047	.3763	1.0480	.9335
.6	1.6362	2.1220	.3724	1.0552	.9355
.7	1.7191	2.1395	.3685	1.0622	.9372
.8	1.8000	2.1574	.3665	1.0690	.9387
.9	1.8796	2.1756	.3606	1.0758	.9398
1.0	1.9579	2.1944	.3567	1.0825	.9407

TABLE XXIV

EFFECT OF THE REYNOLDS NUMBER

$H(0) = 0.30$, $M_0 = 2.0$, $C = 0.033$, $R\delta_0 = 2.0$

x/L	Δ_1	Δ	H	P/P_∞	$\frac{\tau_0 \delta_1}{\mu_1 U_e}$
0.0	1.1510	2.0306	.2942	1.0139	.6082
.2	1.4204	2.0839	.2837	.0386	.5905
.4	1.6836	2.1380	.2725	1.0631	.5719
.6	1.9689	2.1979	.2596	1.0900	.5506
.8	2.3373	2.2748	.2425	1.1251	.5231
1.0	5.1044	2.7965	.1218	1.3700	.3854
1.2	4.8941	2.7916	.1221	1.3835	.3077
1.4	4.6632	2.7813	.1246	1.3837	.3066
1.6	3.7561	2.6762	.1641	1.3899	.3528
1.8			SEPARATION		
2.0					

TABLE XXV

EFFECT OF THE REYNOLDS NUMBER

$H(0) = 0.30$, $M_0 = 2.0$, $C = 0.033$, $R\delta_0 = 4.0$

x/L	Δ_1	Δ	H	P/P_∞	$\frac{\tau_0 \delta_1}{\mu_1 U_e}$
0.0	1.0734	2.0134	.2973	1.0068	.6113
.1	1.2124	2.0387	.2921	1.0194	.6028
.2	1,3458	2.0630	.2868	1.0316	.5940
.3	1.4769	2.0876	.2814	1.0438	.4850
.4	1.6089	2.1109	.2757	1.0561	.5755
.5	1.7451	2.1350	.2696	1.0688	.5654
.6	1.8901	2.1598	.2630	1.0825	.5543
.7	2.0515	2.1860	.2555	1.0977	.5418
.8	2.2465	2.2152	.2464	1.1162	.5269
.9	2.5387	2.2527	.2329	1.1439	.5058
1.0	2.5961	2.2710	.2290	1.1496	.4859

TABLE XXVI

EFFECT OF THE REYNOLDS NUMBER

$H(0) = 0.30$, $M_0 = 2.0$, $C = 0.033$, $R\delta_0 = 5.0$

x/L	Δ_1	Δ	H	P/P_∞	$\frac{\tau_0 \delta_1}{\mu_1 U_e}$
0.0	1.0579	2.0099	.2979	10052	.6119
.1	1.1700	2.0297	.2937	1.0155	.6052
.2	1.2780	2.0486	.2895	1.0254	.5983
.3	1.3836	2.0671	.2853	1.0351	.5912
.4	1.4885	2.0851	.2809	1.0448	.5838
.5	1.5943	2.1029	.2763	1.0547	.5762
.6	1.7026	2.1205	.2715	1.0648	.5681
.7	1.8158	2.1381	.2664	1.0754	.5595
.8	1.9369	2.1559	.2608	1.0868	.5502
.9	2.0713	2.1741	.2545	1.0995	.5397
1.0	2.2303	2.1931	.2470	1.1145	.5274

TABLE XXVII

EFFECT OF THE REYNOLDS NUMBER

$H(0) = 0.30$, $M_0 = 2.0$, $C = 0.332$, $R\delta_0 = 2.0$

x/L	Δ_1	Δ	H	P/P_∞	$\frac{\tau_0 \delta_1}{\mu_1 U_e}$
0.0	1.1584	2.0364	.2922	1.0143	.7322
.1	1.4372	2.1010	.2777	1.0394	.7525
.2	1.7098	2.1725	.2616	1.0644	.7466
.3	2.0131	2.2648	.2416	1.0927	.7443
.4	2.5193	2.4547	.2037	1.1418	.7237
.5	2.2364	2.2897	.2299	1.1110	.7519
.6	2.3264	2.3916	.2095	1.1443	.7403
.7	2.4919	2.6568	.1365	1.6736	.5924
.8	2.8628	2.7564	.0539	1.9674	.5164
.9			SEPARATION		
1.0					

TABLE XXVIII

EFFECT OF THE INITIAL BOUNDARY LAYER THICKNESS

$H(0) = 0.5$, $M_0 = 2.0$, $C = 0.01$, $\delta_0 = 0.001$, $\Delta(0) = 1.0$

x/L	Δ_1	Δ	H	P/P_∞	$\frac{\tau_0 \delta_1}{\mu_1 U_e}$
0.0	1.0635	1.0075	.4978	1.0102	1.0028
.1	1.3421	1.0401	.4879	1.0534	.9842
.2	1.5775	1.0656	.4797	1.0870	.9685
.3	1.7848	1.0863	.4726	1.1140	.9549
.4	1.9727	1.1033	.4661	1.1367	.9428
.5	2.1467	1.1176	.4601	1.1564	.9315
.6	2.3109	1.1300	.4544	1.1744	.9209
.7	2.4684	1.1411	.4488	1.1913	.9105
.8	2.6216	1.1512	.4434	1.2075	.9004
.9	2.7721	1.1604	.4380	1.2235	.8904
1.0	2.9214	1.1689	.4327	1.2394	.8804

TABLE XXIX

EFFECT OF THE INITIAL BOUNDARY LAYER THICKNESS

$H(0) = 0.5$, $M_0 = 2.0$, $C = 0.01$, $\delta_0 = 0.001$, $\Delta(0) = 1.50$

x/L	Δ_1	Δ	H	P/P_∞	$\frac{\tau_0 \delta_1}{\mu_1 U_e}$
0.0	1.0635	1.5107	.4982	1.0098	1.0015
.1	1.3416	1.5568	.4905	1.0514	.9866
.2	1.5759	1.5932	.4842	1.0837	.9746
.3	1.7816	1.6226	.4789	1.1099	.9645
.4	1.9673	1.6768	.4744	1.1319	.9558
.5	2.1386	1.6676	.4703	1.1510	.9481
.6	2.2993	1.6859	.4665	1.1685	.9409
.7	2.4523	1.7019	.4628	1.1846	.9341
.8	2.5997	1.7167	.4594	1.2000	.9275
.9	2.7431	1.7305	.4559	1.2149	.9211
1.0	2.8835	1.7432	.4525	1.2296	.9148

TABLE XXX

EFFECT OF THE INITIAL BOUNDARY LAYER THICKNESS

$H(0) = 0.5$, $M_0 = 2.0$, $C = 0.01$, $\delta_0 = 0.001$, $\Delta(0) = 2.0$

x/L	Δ_1	Δ	H	P/P_∞	$\frac{\tau_0 \delta_1}{\mu_1 U_e}$
0.0	1.0639	2.0139	.4984	1.0096	1.0008
.1	1.3436	2.0735	.4913	1.0501	.9872
.2	1.5786	2.1207	.4858	1.0818	.9764
.3	1.7849	2.1589	.4812	1.1075	.9675
.4	1.9711	2.1909	.4772	1.1292	.9599
.5	2.1427	2.2183	.4737	1.1483	.9531
.6	2.3037	2.2426	.4705	1.1656	.9470
.7	2.4569	2.2646	.4675	1.1817	.9412
.8	2.6043	2.2849	.4645	1.1970	.9357
.9	2.7474	2.3039	.4617	1.2119	.9303
1.0	2.8874	2.3217	.4589	1.2264	.9251

TABLE XXXI

EFFECT OF THE INITIAL BOUNDARY LAYER THICKNESS

$H(0) = 0.5$, $M_0 = 2.0$, $C = 0.332$, $\delta_0 = 0.001$, $\Delta(0) = 3.0$

x/L	Δ_1	Δ	H	P/P_∞	$\frac{\tau_0 \delta_1}{\mu_1 U_e}$
0.0	1.1690	3.0553	.4926	1.0194	1.0592
.1	1.4528	3.1482	.4805	1.0512	1.0540
.2	1.6925	3.2239	.4709	1.0762	1.0501
.3	1.9032	3.2872	.4629	1.0967	1.0476
.4	2.0932	3.3417	.4561	1.1140	1.0459
.5	2.2686	3.3905	.4499	1.1292	1.0448
.6	2.4333	3.4361	.4443	1.1430	1.0438
.7	2.5906	3.4799	.4390	1.1561	1.0429
.8	2.7424	3.5233	.4313	1.1747	1.0419
.9	2.8904	3.5668	.4287	1.1808	1.0408
1.0	3.0355	3.6109	.4238	1.1928	1.0395

TABLE XXXII

EFFECT OF THE INITIAL BOUNDARY LAYER THICKNESS

$H(0) = 0.4$, $M_0 = 2.0$, $C = 0.332$, $\delta_0 = 0.001$, $\Delta(0) = 2.0$

x/L	Δ_1	Δ	H	P/P_∞	$\frac{\tau_0 \delta_1}{\mu_1 U_e}$
0.0	1.1748	1.0285	.3797	1.0184	1.0197
.1	1.4854	1.0848	.3399	1.0475	1.0231
.2	1.7937	1.1543	.2951	1.0757	1.0131
.3	2.2370	1.2945	.2241	1.1189	.9715
.4		SEPARATION			
.5					
.6					
.7					
.8					
.9					
1.0					

TABLE XXXIII

EFFECT OF THE INITIAL BOUNDARY LAYER THICKNESS

$H(0) = 0.5$, $M_0 = 2.0$, $C = 0.332$, $\delta_0 = 0.001$, $\Delta(0) = 4.0$

x/L	Δ_1	Δ	H	P/P_∞	$\frac{\zeta_0 \delta_1}{\mu_1 U_e}$
0.0	1.1717	4.0704	.4932	1.0190	1.0432
.1	1.4592	4.1882	.4823	1.0500	1.0355
.2	1.7017	4.2839	.4737	1.0747	1.0297
.3	1.9151	4.3640	.4666	1.0952	1.0254
.4	2.1079	4.4330	.4605	1.1127	1.0222
.5	2.2861	4.4946	.4551	1.1283	1.0197
.6	2.4538	4.5515	.4503	1.1426	1.0174
.7	2.6141	4.6056	.4454	1.156	1.0154
.8	2.7689	4.6582	.4408	1.1691	1.0134
.9	2.9200	4.7100	.4364	1.1818	1.0114
1.0	3.0683	4.7617	.4321	1.1943	1.0094

TABLE XXXIV

EFFECT OF THE INITIAL BOUNDAY LAYER THICKNESS

$H(0) = 0.4$, $M_0 = 2.0$, $C = 0.332$, $\delta_0 = 0.001$, $\Delta(0) = 3.0$

x/L	Δ_1	Δ	H	P/P_∞	$\frac{\zeta_0 \delta_1}{\mu_1 U_e}$
0.0	1.1544	3.0438	.3948	1.0150	.8748
.1	1.4154	3.1150	.3863	1.0392	.8788
.2	1.6390	3.1739	.3791	1.0589	.8819
.3	1.8415	3.2269	.3725	1.0763	.8842
.4	2.0315	3.2776	.3662	1.0927	.8859
.5	2.2137	3.3278	.3600	1.1084	.8869
.6	2.3913	3.3783	.3538	1.1237	.8873
.7	2.5666	3.4302	.3475	1.1390	.8873
.8	2.7417	3.4841	.3411	1.1543	.8867
.9	2.9189	3.5411	.3344	1.1699	.8857
1.0	3.1007	3.6025	.3275	1.1860	.8840

TABLE XXXV

EFFECT OF THE INITIAL BOUNDARY LAYER THICKNESS

$H(0) = 0.4$, $M_0 = 2.0$, $C = 0.332$, $\delta_0 = 0.001$, $\Delta(0) = 4.0$

x/L	Δ_1	Δ	H	P/P_∞	$\frac{\rho_0 \delta_1}{\mu_1 U_e}$
0.0	1.1581	4.0565	.3953	1.0151	.8553
.1	1.4248	4.1486	.3876	1.0395	.8558
.2	1.6536	4.2251	.3811	1.0598	.8561
.3	1.8615	4.2940	.3752	1.0779	.8561
.4	2.0569	4.3594	.3696	1.0950	.8558
.5	2.2447	4.4232	.3641	1.1115	.8551
.6	2.4283	4.4866	.3586	1.1276	.8541
.7	2.6101	4.5504	.3531	1.1437	.8527
.8	2.7925	4.6156	.3475	1.1598	.8510
.9	2.9780	4.6831	.3417	1.1763	.8490
1.0	3.1697	4.7543	.3356	1.1935	.8465

TABLE XXXVI

EFFECT OF THE INJECTION VELOCITY

$H(0) = 0.38$, $M_0 = 2.0$, $C = 0.332$, $\delta_0 = 0.001$, $\Delta(0) = 2.0$

x/L	Δ_1	Δ	H	P/P_∞	$\frac{\tau_0 \delta_1}{\mu_1 U_e}$
0.0	1.1533	2.0324	.3732	1.0150	.8772
.1	1.4143	2.0861	.3615	1.0388	.8870
.2	1.6417	2.1330	.3509	1.0586	.8939
.3	1.8525	2.1789	.3405	1.0768	.8984
.4	2.0560	2.2268	.3298	1.0945	.9011
.5	2.2581	2.2788	.3188	1.1122	.9020
.6	2.3603	2.3070	.3130	1.1213	.9018
.7	2.6828	2.4060	.2940	1.1503	.8982
.8	2.9272	2.4931	.2789	1.1728	.8923
.9	3.238	2.6213	.2592	1.2021	.8808
1.0	4.2088	3.1302	.1959	1.2977	.8243

TABLE XXXVII

EFFECT OF THE INJECTION VELOCITY

$H(0) = 0.36$, $M_0 = 2.0$, $C = 0.332$, $\delta_0 = 0.001$, $\Delta(0) = 2.0$

x/L	Δ_1	Δ	H	P/P_∞	$\frac{\tau_0 \delta_1}{\mu_1 U_e}$
0.0	1.1528	2.0325	.3532	1.0146	.8412
.1	1.4139	2.0866	.3413	1.0380	.8518
.2	1.6446	2.1355	.3302	1.0581	.8588
.3	1.8624	2.1854	.3190	1.0772	.8631
.4	2.0770	2.2392	.3072	1.0962	.8651
.5	2.2964	2.3000	.2945	1.1159	.8649
.6	2.5317	2.3730	.2802	1.1373	.8621
.7	2.8070	2.4706	.2626	1.1629	.8552
.8	3.2319	2.6508	.2342	1.2037	.8369
.9	4.6775	3.3777	.1342	1.3468	.7457
1.0	4.6311	3.322	.1374	1.3408	.7538

TABLE XXXVIII

EFFECT OF THE INJECTION VELOCITY

$H(0) = 0.34$, $M_0 = 2.0$, $C = 0.332$, $\delta_0 = 0.001$, $\Delta(0) = 2.0$

x/L	Δ_1	Δ	H	P/P_∞	$\frac{\tau_0 \delta_1}{\mu_1 U_e}$
0.0	1.1533	2.0331	.3330	1.0143	.8056
.1	1.4165	2.0887	.3207	1.0377	.8160
.2	1.6538	2.1415	.3088	1.0586	.8228
.3	1.8836	2.1978	.2962	1.0791	.8264
.4	2.1181	2.2617	.2825	1.1003	.8270
.5	2.3735	2.3402	.2665	1.1238	.8243
.6	2.6933	2.4544	.2451	1.1540	.8154
.7	4.2415	3.1791	.13329	1.3070	.7162
.8	4.1924	3.1258	.1370	1.3010	.7349
.9	4.1387	3.0695	.1414	1.2948	.7436
1.0	4.0764	3.0084	.1466	1.2909	.7534

TABLE XXXIX

EFFECT OF THE INJECTION VELOCITY

$H(0) = 0.33$, $M_0 = 2.0$, $C = 0.332$, $\delta_0 = 0.001$, $\Delta(0) = 2.0$

x/L	Δ_1	Δ	H	P/P_∞	$\frac{\tau_0 \delta_1}{\mu_1 U_e}$
0.0	1.1539	2.0336	.3229	1.0142	.7869
.1	1.4192	2.0905	.3103	1.0378	.7979
.2	1.6617	2.1463	.2977	1.0594	.8044
.3	1.9007	2.2073	.2841	1.0809	.8073
.4	2.1509	2.2794	.2687	1.1039	.8067
.5	2.4464	2.3766	.2493	1.1314	.8011
.6	2.9732	2.589	.2117	1.1624	.7771
.7	2.8015	2.4703	.2262	1.1837	.7961
.8	3.7862	2.9115	.1518	1.2555	.7426
.9	3.8237	2.8874	.1451	1.2752	.7453
1.0	4.0794	3.0045	.0218	1.2950	.6208

TABLE XXXX

EFFECT OF THE INJECTION VELOCITY

$H(0) = 0.32$, $M_0 = 2.0$, $C = 0.332$, $\delta_0 = 0.001$, $\Delta(0) = 2.0$

x/L	Δ_1	Δ	H	P/P_∞	$\frac{\tau_0 \delta_1}{\mu_1 U_e}$
0.0	1.1549	2.0343	.3127	1.0142	.7687
.1	1.4233	2.0931	.2996	1.0381	.7797
.2	1.6728	2.1526	.2862	1.0605	.7856
.3	1.9247	2.2201	.2713	1.0834	.7875
.4	2.2033	2.3053	.2533	1.1093	.7849
.5	2.5927	2.4471	.2260	1.1464	.7721
.6	3.0862	2.6443	.1895	1.1943	.7560
.7	2.7868	2.4700	.2143	1.1605	.7833
.8	1.3993	1.7571	.3312	1.0483	.8914
.9	2.3072	2.1837	.2459	1.1371	.7987
1.0	3.1197	2.5314	.1778	1.1782	.7391

TABLE XXXXI

EFFECT OF THE INJECTION VELOCITY

$H(0) = 0.31$, $M_0 = 2.0$, $C = 0.332$, $\delta_0 = 0.001$, $\Delta(0) = 2.0$

x/L	Δ_1	Δ	H	P/P_∞	$\frac{\tau_0 \delta_1}{\mu_1 U_e}$
0.0	1.1564	2.0352	.3025	1.0142	.7505
.1	1.4291	2.0964	.2888	1.0386	.7612
.2	1.6887	2.1611	.2742	1.0621	.7664
.3	1.9593	2.2380	.2574	1.0871	.7668
.4	2.2911	2.3481	.2346	1.1184	.7600
.5		SEPARATION			
.6					
.7					
.8					
.9					
1.0					

TABLE XXXXII

EFFECT OF THE SIZE OF $\Delta x/L$

$H(0) = 0.5$, $M_0 = 2.0$, $C = 0.01$, $\delta_0 = 0.001$, $\Delta(0) = 1.50$

$\Delta x/L = 0.01$

x/L	Δ_1	Δ	H	P/P_∞	$\frac{\tau_0 \delta_1}{\mu_1 U_e}$
0.0	1.0410	1.5127	.4980	1.0117	1.0014
.1	1.3953	1.6150	.4826	1.1030	.9709
.2	1.6857	1.6880	.4718	1.1673	.9498
.3	1.9502	1.7494	.4627	1.2220	.9321
.4	2.2129	1.8084	.4538	1.2757	.9152
.5	2.4922	1.8694	.4447	1.3328	.8976
.5	2.8148	1.9360	.4344	1.3988	.8781
.7	3.2709	2.0202	.4208	1.4913	.8526
.8	2.5790	1.9572	.4364	1.3614	.8540
.9	2.9585	2.0392	.4246	1.4397	.8587
1.0	4.7450	2.3153	.3771	1.7934	.7928

TABLE XXXXIII

EFFECT OF THE SIZE OF $\Delta x/L$

$H(0) = 0.5$, $M_0 = 2.0$, $C = 0.01$, $\delta_0 = 0.001$, $\Delta(0) = 1.50$

$\Delta x/L = 0.04$

x/L	Δ_1	Δ	H	P/P_∞	$\frac{\tau_0 \delta_1}{\mu_1 U_e}$
0.00	1.1127	1.5099	.4981	1.0091	1.0014
.08	1.3102	1.5279	.4946	1.0252	.9949
.16	1.4830	1.5436	.4914	1.0393	.9889
.24	1.6391	1.5577	.4884	1.0518	.9833
.32	1.7824	1.5703	.4855	1.0629	.9781
.40	1.9159	1.5816	.4929	1.0730	.9732
.48	2.0411	1.5918	.4804	1.0822	.9685
.56	2.1596	1.6010	.4780	1.0905	.9641
.64	2.2722	1.6094	.4757	1.0982	.9598
.72	2.3798	1.6170	.4735	1.1053	.9558
.80	2.4829	1.6239	.4714	1.1119	.9518
.88	2.5823	1.6303	.4697	1.1180	.9480
.96	2.6783	1.6361	.4674	1.1239	.9443
1.00	2.7251	1.6388	.4664	1.1266	.9425

TABLE XXXXIV

THE VELOCITIES q_1 AND q_2 FOR DIFFERENT VALUES OF H, C AND δ_1 / δ

C = 0.01, δ_1 / δ = 1.0, H = 0.50

η_1	q_1	η_1	q_1	η_2	q_2	η_2	q_2
0.0	.0000	.6	.4188	1.0	.5000	.4	.9167
.1	.0945	.7	.4539	.9	.5381	.3	.9612
.2	.1792	.8	.4792	.8	.6072	.2	.9874
.3	.2539	.9	.4945	.7	.6911	.1	.9982
.4	.3188	1.0	.5000	.6	.7766	0.0	1.0000
.5	.3737			.5	.8540		

C = 0.01, δ_1 / δ = 1.0, H = 0.40

0.0	.0000	.6	.3345	1.0	.4000	.4	.9000
.1	.0754	.7	.3627	.9	.4458	.3	.9535
.2	.1430	.8	.3830	.8	.5287	.2	.9849
.3	.2027	.9	.3954	.7	.6293	.1	.9979
.4	.2545	1.0	.4000	.6	.7319	0.0	1.0000
.5	.2985			.5	.8248		

TABLE XXXXV

THE VELOCITIES q_1 AND q_2 FOR DIFFERENT VALUES OF H, C AND δ_1/δ

C = 0.01, δ_1/δ = 1.0, H = 0.30

η_1	q_1	η_1	q_1	η_2	q_2	η_2	q_2
0.0	.0000	.6	.2503	1.0	.3000	.4	.8834
.1	.0563	.7	.2715	.9	.3534	.3	.9457
.2	.1068	.8	.2868	.8	.4502	.2	.9824
.3	.1515	.9	.2963	.7	.5675	.1	.9976
.4	.1903	1.0	.3000	.6	.6873	0.0	1.0000
.5	.22325			.5	.7956		

C = 0.01, δ_1/δ = 1.0, H = 0.20

0.0	.0000	.6	.1660	1.0	.2000	.4	.8667
.1	.6372	.7	.1803	.9	.2610	.3	.9380
.2	.0707	.8	.1907	.8	.3716	.2	.9799
.3	.1003	.9	.1972	.7	.5058	.1	.9972
.4	.1260	1.0	.2000	.6	.6426	0.0	1.0000
.5	.1480			.5	.7665		

TABLE XXXXVI

THE VELOCITIES q_1 AND q_2 FOR DIFFERENT VALUES OF H, C AND δ_1/δ

C = 0.01, δ_1/δ = 1.0, H = 0.10

η_1	q_1	η_1	q_1	η_2	q_2	η_2	q_2
0.0	.0000	.6	.0818	1.0	.1000	.4	.8501
.1	.0181	.7	.0891	.9	.1687	.3	.9302
.2	.0345	.8	.0945	.8	.2931	.2	.9774
.3	.0491	.9	.0981	.7	.4440	.1	.9969
.4	.0618	1.0	.1000	.6	.5979	0.0	1.0000
.5	.0727			.5	.7373		

C = 0.01, δ_1/δ = 1.0, H = 0.05

0.0	.0000	.6	.0397	1.0	.0500	.4	.8417
.1	.60864	.7	.0435	.9	.1225	.3	.9264
.2	.0164	.8	.0464	.8	.2538	.2	.9761
.3	.0235	.9	.4864	.7	.4131	.1	.9969
.4	.02972	1.0	.0500	.6	.5756	0.0	1.0000
.5	.0351			.5	.7227		

TABLE XXXXVII

THE VELOCITIES q_1 AND q_2 FOR DIFFERENT VALUES OF H, C AND δ_1/δ

C = 0.01, δ_1/δ = 1.0, H = 0.0

η_1	q_1	η_1	q_1	η_2	q_2	η_2	q_2
0.0	.0000	.6	− .0024	1.0	.0000	.4	.83347
.1	− .0009	.7	− .0021	.9	.0763	.3	.9225
.2	− .0016	.8	− .0016	.8	.2145	.2	.9749
.3	− .0021	.9	− .0009	.7	.3822	.1	.9965
.4	− .0024	1.0	0.0000	.6	.5533	0.0	1.0000
.5	− .0015			.5	.7081		

C = 0.01, δ_1/δ = 1.0, H = − .050

0.0	.0000	.6	− .0445	1.0	− .0500	.4	.8251
.1	− .0104	.7	− .0477	.9	.0301	.3	.9186
.2	− .0196	.8	− .0496	.8	.1753	.2	.9736
.3	− .0277	.9	− .0504	.7	.3513	.1	.9964
.4	− .0345	1.0	− .0500	.6	.5309	0.0	1.0000
.5	− .0401			.5	.6935		

TABLE XXXXVIII

THE VELOCITIES q_1 AND q_2 FOR DIFFERENT VALUES OF H, C AND δ_1/δ

C = 0.01, δ_1/δ = 1.0, H = − .1000

η_1	q_1	η_1	q_1	η_2	q_2	η_2	q_2
0.0	.0000	.6	− .0866	1.0	− .1000	.4	.8168
.1	− .0199	.7	− .0933	.9	− .0160	.3	.9147
.2	− .0377	.8	− .0977	.8	.1360	.2	.9724
.3	− .0533	.9	− .0999	.7	.3204	.1	.9962
.4	− .0666	1.0	− .1000	.6	.5086	0.0	1.0000
.5	− .0777			.5	.6789		

C = 0.01, δ_1/δ = 1.0, H = − .200

0.0	.0000	.6	− .1708	1.0	− .2000	.4	.8001
.1	− .0390	.7	− .1845	.9	− .1083	.3	.9070
.2	− .6739	.8	− .1939	.8	.0575	.2	.9698
.3	− .1045	.9	− .1990	.7	.2587	.1	.9959
.4	− .1308	1.0	− .2000	.6	.4639	0.0	1.0000
.5	− .1530			.5	.6497		

TABLE XXXXIX

THE VELOCITIES q_1 AND q_2 FOR DIFFERENT VALUES OF H, C AND δ_1/δ

C = 0.01, δ_1/δ = 2.0, H = .500

η_1	q_1	η_1	q_1	η_2	q_2	η_2	q_2
0.0	.0000	.6	.4176	1.0	.5000	.4	.9167
.1	.0941	.7	.4529	.9	.5381	.3	.9612
.2	.1784	.8	.4784	.8	.6072	.2	.9874
.3	.2529	.9	.4941	.7	.6911	.1	.9982
.4	.3176	1.0	.5000	.6	.7766	0.0	1.0000
.5	.3725			.5	.8540		

C = 0.01, δ_1/δ = 3.0, H = .500

0.0	.0000	.6	.4164	1.0	.5000	.4	.9167
.1	.9365	.7	.4518	.9	.5381	.3	.9612
.2	.1776	.8	.4776	.8	.6072	.2	.9874
.3	.2518	.9	.4936	.7	.6911	.1	.99829
.4	.3164	1.0	.5000	.6	.7766	0.0	1.0000
.5	.3712			.5	.8540		

TABLE L

THE VELOCITIES q_1 AND q_2 FOR DIFFERENT VALUES OF H, C AND δ_1/δ

C = .030, δ_1/δ = 1.0, H = .500

η_1	q_1	η_1	q_1	η_2	q_2	η_2	q_2
0.0	.0000	.6	.4164	1.0	.5000	.4	.9167
.1	.0936	.7	.4518	.9	.5381	.3	.9612
.2	.1776	.8	.4776	.8	.6072	.2	.9874
.3	.2518	.9	.4936	.7	.6911	.1	.9982
.4	.3164	1.0	.5000	.6	.7766	0.0	1.0000
.5	.3712			.5	.8540		

C = .110, δ_1/δ = 1.0, H = .500

0.0	.0000	.6	.4068	1.0	.5000	.4	.9167
.1	.0900	.7	.4434	.9	.5381	.3	.9612
.2	.1712	.8	.4712	.8	.6072	.2	.9874
.3	.2434	.9	.4900	.7	.6911	.1	.9982
.4	.3068	1.0	.5000	.6	.7766	0.0	1.0000
.5	.3612			.5	.8540		

TABLE LI

THE VELOCITIES q_1 AND q_2 FOR DIFFERENT VALUES OF H, C AND δ_1/δ

C = .220, δ_1/δ = 1.0, H = .500

η_1	q_1	η_1	q_1	η_2	q_2	η_2	q_2
0.0	.0000	.6	.3936	1.0	.5000	.4	.9167
.1	.0851	.7	.4319	.9	.5381	.3	.9612
.2	.1624	.8	.4624	.8	.6072	.2	.9874
.3	.2319	.9	.4851	.7	.6911	.1	.4982
.4	.2936	1.0	.5000	.6	.7766	0.0	1.0000
.5	.3475			.5	.8540		

C = .330, δ_1/δ = 1.0, H = .500

0.0	.0000	.6	.3804	1.0	.5000	.4	.9167
.1	.0801	.7	.4203	.9	.5381	.3	.9612
.2	.1536	.8	.4536	.8	.6072	.2	.9874
.3	.2203	.9	.4801	.7	.6911	.1	.9982
.4	.2804	1.0	.5000	.6	.7766	0.0	1.0000
.5	.3337			.5	.8540		

TABLE LII

THE VELOCITIES q_1 AND q_2 FOR DIFFERENT VALUES OF H, C AND δ_1/δ

C = .010, δ_1/δ = .800, H = .500

η_1	q_1	η_1	q_1	η_2	q_2	η_2	q_2
0.0	.0000	.6	.4190	1.0	.5000	.4	.9167
.1	.0946	.7	.4541	.9	.5381	.3	.9612
.2	.1793	.8	.4793	.8	.6072	.2	.9874
.3	.2541	.9	.4946	.7	.6911	.1	.9982
.4	.3190	1.0	.5000	.6	.7766	0.0	1.0000
.5	.3746			.5	.8540		

APPENDIX E

NOMENCLATURE

NOMENCLATURE

A	Speed of Sound
C	Viscosity Ratio = $0.332\ \mu_2/\mu_1$
F	A Parameter Proportional to the Pohlhausen Parameter
H(x)	Interface Velocity Ratio
H(0)	Injection Velocity Ratio
L	Characteristic Length
M	Mach Number
P(x)	Pressure
P_s	Pressure at Shock Impingement Point
PR	Shock Strength
$R_{\delta 0}$	Reduced Reynolds Number
u	Velocity Component, in the Boundary Layer, Parallel to the Flow
U	Velocity at the Boundary Layer Edge
v	Velocity Component, in the Boundary Layer, Normal to the Flow
VR	A Parameter Proportional to the Pressure Gradient
x	Dimension along the Wall
y	Dimension Perpendicular to the Wall
α	Angle of Deflection
γ	Ratio of Specific Heats
δ	Boundary Layer Thickness
δ_*	Displacement Thickness
Δ	Thickness Ratio

η	Dimensionless Distance
θ	Momentum Thickness
θ	Energy Thickness
θ^*	Moment of Momentum Thickness
θ^{**}	
Θ	Thickness Ratio
μ	Viscosity
ν	Kinematic Viscosity
ρ	Density
τ_o	Shear Stress
ψ	Stream Function

SUBSCRIPTS

c	Compressible
e	Boundary Layer Edge
0	At the Injection Slot
x	First Derivative with Respect to x
y	First Derivative with Respect to y
1	Fluid Layer
2	Gas Layer
∞	Upstream

VITA

Essam M. M. Mitwally

Candidate for the Degree of

Doctor of Philosophy

Thesis: SHOCK WAVE-BOUNDARY LAYER INTERACTION WITH TANGENTIAL INJECTION

Major Field: Mechanical Engineering

Biographical:

Personal Data: Born in Cairo, Egypt, U. A. R., November 14, 1936, the son of Mohamed Mokhtar and Nabiha Mitwally.

Education: Attended primary school (1944-48), secondary school (1948-53), Faculty of Engineering, Cairo University (1953-58). Received the Bachelor of Science Degree in 1958, with a major in Mechanical Engineering; attended Oklahoma State University (1960-61), completed the requirements for the Master of Science Degree in January 1961, attended the University of Michigan (1961-62), the University of California, Berkeley (1962-64), then Oklahoma State University (1964-65). Completed the requirements for the Doctor of Philosophy Degree in August 1965.

Professional Experience: Worked as a steam power plant designer at the General Petroleum Authority, Suez, Egypt, U. A. R., (September 1958-December 1959), Research Assistant at the University of California, Berkeley, (June 1962-December 1963), Research Assistant at Oklahoma State University, (July 1964-July 1965).